Luminescence spectroscopy of Eu(III) in lanthanum magnesium aluminate, a solid state laser host

by

Madjid Michael W. Nafi

A Thesis Submitted to the Faculty of Graduate Studies and Research in Partial Fulfillment of the Requirements for the Degree of Doctor of Philosophy

McGill University
Department of Chemsitry
Montréal, Québec, Canada
© March 1992

"... Beatus ille qui pro delendis culpis suis,
asininos tritus nafioni (*) patienter leget (**),
quia post mortem aeternae gaudia vitae gustabit,
et nectareos angelorum concentus in fonte voluptatis potabit".
After M.A. Charpentier's (1643-1704) "Epitaphium Carpentarii.

In original text: (*): capronini, (**): audiet.

ABSTRACT

Laser induced luminescence of Eu(III) in La $_{1-x}$ Eu $_x$ MgAI $_{11}$ O $_{19}$ (LMA) was studied for three different concentrations (x=0.1, 0.01 and <0.01) at various temperatures between 6K and 300K. The polarization of this luminescence was investigated in the highest concentration sample. Results show that Eu(III) occupies three distinct substitutional sites associated respectively with: the Beevers-Ross position (BR, D $_{3h}$), the mid-Oxygen position (mO, C $_{2v}$) and a third "intermediate energy" position. The BR site was identified for the first time in these samples. Luminescence peaks of the 5 D $_0$ — 7 F $_{0,1}$ were assigned for the first time and the orientation of the principal axis of the three sites with respect to c was determined. Excitation spectra recorded at low temperature for the three concentrations show that Eu(III) is forced into the BR site as its concentration increases. An analysis of the phenomenological crystal-field parameters suggests that the "intermediate energy site" is mid-way between the BR and the mO sites.

RESUME

Les spectres de luminescence induite par laser de l'ion europium trivalent La Eu MgAl Q (LMA) ont été étudiés matériau pour trois concentrations differentes (x=0.1, 0.01 et <0.01) et à diverses temperatures entre 6K et 300K. La polarisation de cette luminescence fut examinée à basse temperature dans l'échantillon de plus haute concentration. Les résultats trois sites distincts aue l'Eu(III) occupe correspondant respectivement à: la position dite de Beevers-Ross (BR, symétrie $Q_{\rm h}$), la position dite mid-oxygen (mO, symétrie C_{2v}) et une troisième position intermédiaire. Le site BR a été mis en évidence pour la première fois dans ces échantillons. Une attribution de toutes les transitions ${}^5D_0 \longrightarrow {}^7F_0$, est avancée pour la première fois et l'orientation des axes principaux des sites par rapport à l'axe cristallin c est determinée. Les spectres d'excitation à basse température enregistrés pour les trois concentrations mentionnées plus haut montrent que l'Eu(III) est forcé d'occuper la position BR lorsque sa concentration dans cette matrice augmente. Une analyse des paramètres phénoménologiques de champ cristallin suggère que le site "intermédiare" se trouverait dans une position mitoyenne entre le site BR et le site mO.

ACKNOWLEDGMENTS

I would like to thank Professor D.J. Simkin for accepting me in his group, for his financial support for the major part of my studies at McGill and for covering the transportation costs incurred during my visit to Professor G. Boulon's Laboratory in Lyon (France).

My thanks also go to the members of my Ph.D research committee:

Professors D. Gilson, I. Butler and A. Shaver.

I thank Professors A-M Lejus and D. Vivien (Ecole Nationale Supérieure de Chimie de Paris) for making the Eu-doped LMA samples available to me, for extremely helpful discussions on the structural problem in LMA as well as for

their hospitality during my brief visit of their laboratory.

I am indebted to Professor G. Boulon Director of the French CNRS laboratory where I carried out the major part of the experimental work of my thesis. I thank him for inviting me to his laboratory, for arranging some financial support from the CNRS during my two-months stay in France and for helping me solve a major technical problem related to my samples. While I was in Lyon I had the opportunity to have interesting discussions with a number of researchers of this group on various topics, particularly with Dr. B. Jacquier, Dr. J. Linarès and Dr. M. Pedrini. A special word of thanks to Dr. R. Moncorgé for allowing me to use his laser equipment for a full two weeks period. I am most grateful to Yannick Guyot for spending the time to teach me how to use this equipment and for helping me set up my experiments. I also thank Dr. P. Nelson, who was visiting professor Boulon's group, for teaching me a special polishing technique for thin crystalline samples and for suggesting I apply a polarization technique she used in her Ph.D work. The modification of her technique to fit the special characteristics of my system represents a very important part of my work. I will never forget the friendliness of Anne-Marie Briançon, Hassan Manaa, Mohammed Mouzaoui and Alain Mermet. I would also like to mention that I was particularly touched by the farewell party organized by Aline and Christophe Dujardin.

This trip would have not been possible without the help of McGill University's financial aid department, in the form of a loan, and the

understanding of Ms C. Pissimisi (accounting department).

I also thank my family and personal friends for their continued moral support throughout my studies. I would like to express a special word of thanks to fellow members of the "Choir of the Church of St. Andrew & St. Paul" and their successive directors Patrick Wedd and James Wells for giving me opportunities in a field that helped relief the stress of graduate studies.

Last but not least I would like to thank Allan Bruce for my computer education and Monique Laberge (compagne de misère!) for more things than this

limited space allows (y compris les chicanes!).

TABLE OF CONTENTS

Abstract	ii
Résumé	iii
Acknowledgments	. iv
Table of Contents	
Introduction	
1. Review of the literature	I
2. Critical discussion of literature work	4
References	9
Table I	IO
Experimental	
1. Sample preparation	12
2. Luminescence detection	13
Results and discussions	
Notes to the Reader	16
Part A: "Site-selective spectroscopy in Eu3+: lanthanum	magnesium
aluminate"	•
Statement of contributions	18
Abstract	19
1. Introduction	19
2. Experimental	20
3. Nomenclature and structural differences	21
of hexa-aluminates	
4. Results and discussions	23
5. Conclusion	27
Acknowledg ments	28
References	29
Figure Captions	30
Figures	31-36

Part	B: "Polarization of the ⁵ D ₀ → ⁷ F _J Eu ⁺³ luminescence	in
La	Eu _x MgAl ₁₁ O ₁₉ : The nature of the substitutional sites"	
	Statement of contributions	38
	Abstract	39
1. Introduction		
	2. Experimental	43
	3. Selection rules for the ⁵ D ₀ → ⁷ F _J transitions	
	a) J selection rules	45
	b) Site-symmetry slection rules	45
	4. Results and discussion	
	 a) Non-polarized luminescence results 	49
	b) Polarization of the ${}^5D_0 \longrightarrow {}^7F_{0,1,2,3}$ luminescence	52
	14	
	5. Conclusion	58
	Acknowledgments	59
٠.	Figure captions	60
	Figures	62-68
	Tables	69-72
	References	73
Part (C: "Luminescence of the Eu(III) in lanthanum magnesium alumin	ate:
	ull picture"	
	Abstract	76
	1. Introduction	77
	2. Experimental	77
	3. Results and discussions	
	3.1 Excitation spectra	78
	3.2 Emission spectra	81
	3.2.1 Temperature dependence	81
	3.2.2 Concentration dependence	82
	3.3 Lifetimes	84
	4. Crystal-field parameters	85
	Acknowledgments	88

Figure captions	89
Figures	90-93
Table I	94
Table II	95
References	96
Conclusions	98
1. Contribution to knowledge	99
2. Suggestions for further work	100
Appendices I: Energy levels of Eu ⁴³	102
II to VII additional spectra	105-132

INTRODUCTION

1. Review of the literature

Since the development of the first solid state laser intense research efforts have been devoted to the synthesis of crystalline and glassy materials to serve as laser hosts to a variety of transition metal and rare earth ions. In this context, β -alumina or β "-alumina-type materials [1] have received a particular attention. The structure of these matrices is such that they can easily accommodate a wide variety of metal ions. The crystalline compound LaMgAl₁₁O₁₉ (LMA) belongs to this category of materials [2,3] .

A fine analysis of the composition of LMA using microprobe techniques shows that this compound is "non-stoichiometric"; its formula is in fact La_{0.90}Mg_{0.50}Al_{11.43}O₁₉. According to Professor Anne-Marie Lejus [4] from Professor Vivien's group (Ecole Nationale Supérieure de Chimie de Paris) "stoichiometric LMA" can be synthesized but crystals of a manageable size are very difficult to grow.

Mel'nik et al. [5] reported some Raman spectroscopic data on single crystals of LMA as well as Nd(III)-doped LMA, at room temperature, between 50 and 1000 cm⁻¹, under laser excitation of wavelengths: 488.0, 514.5 and 457.9 nm. They assigned the lowest frequency phonons (62 and 71 cm⁻¹) to vibrations involving the lanthanum ions. The rest of their Raman spectra exhibited a large number of fairly broad phonons. These authors also noted that the spectra of undoped and doped LMA were practically identical.

X-ray studies [6] have shown that the unit cell of LMA,

which belongs to the space group P63/mmc, is composed of spinel blocks separated by mirror planes. The backbone of this structure is made up of layers of oxygen ions stacked along the c-direction. Al+3 and Mg+2 occupy the octahedral and tetrahedral holes in this structure; Mg+2 is present exclusively in the spinel blocks whereas Al+3 is found both in the spinel blocks and the corners of the mirror plane of a unit cell (so-called anti-Beevers-Ross (aBR) positions). The mirror plane also contains the lanthanum ion in the 2d position (so-called Beevers-Ross (BR) position of symmetry D_{3h} with a C₃ axis along c, and three O⁻² ions in three equivalent 6h positions, which is characteristic of the magnetoplumbite structure [7]. A detailed discussion of the structural similarities and differences between different types of spinel-stacked materials is presented in chapter III. However, at this stage, we should emphasize a major difference between lanthanide-doped Na B alumina and Na B" alumina, on one hand, and lanthanide doped LMA, on the other. The dopant, Eu(III) in the case of this study, is introduced in the LMA matrix in the form of a metal oxide mixed with the starting materials. In the case of Na β and β'' -aluminas the dopant ion is introduced in the mirror plane by ion exchange methods and substitutes for monovalent sodium ions. Because of the defect nature of lanthanide doped-LMA's it is very difficult to analyze their X-ray diffraction patterns. In this context, the study of the luminescence of the dopant ion can be very useful. Furthermore, from a purely fundamental point of view, these

materials offer a good example to further our understanding of the influence of structure on the luminescent properties of rareearth ions.

A number of studies have reported site-selective luminescence results in La_{1-x}Eu_xAl₁₁O₁₉. Saber et al. [8] who carried out such a study in crystalline samples with x=0.02 and x=0.05 reported the presence of two substitutional sites for Eu⁺³ (referred to as sites A and B) which they believed to correspond to the so-called mid-oxygen or mO positions. These positions are close to the BR (2d) crystallographic site, have their main axis perpendicular to c and are of C2 symmetry. On the other hand, Buijs et al. [9], who studied energy transfer processes in fully substituted powdered samples of La_{1-x}Eu_xMgAl₁₁O₁₉, identified four different Eu+3 substitutional sites but did not discuss their exact nature. Finally, in a paper on the luminescence of La_{1-x}Gd_xMgAl₁₁O₁₉, Salem et al. [10] reported the polarization of the ⁵D_o← ⁷F₁ transitions at 295K in La_{1-x}Eu_xMgAl₁₁O₁₉ for the Eu+3 sites previously identified by Saber et al. conclusions were that both of these sites, of C_{∞} symmetry, were derived from the ideal D_{3h} site, which they did not observe, and that site A is less distorted than site B.

In order to put the present spectroscopic study in the context of the ones mentioned above the following section presents a critical discussion of the three most relevant papers: references [8,9 and 10].

2- Critical discussion of literature work:

Let us begin with Saber et als paper. These authors first generated what they believe to be "nonselectively-excited" luminescence spectra to locate the different ${}^5D_0 \longrightarrow {}^7F_J$ emission peaks. Then, they excited into the ⁵D₀ — ⁷F₀ region and recorded the ${}^5D_0 \longrightarrow {}^7F_J$ luminescence (with $J \ge 1$). They did not record the resonance fluorescence (i.e. the ${}^5D_0 \longrightarrow {}^7F_0$ luminescence). Therefore, in their work, it is unclear whether the luminescence they observed is the result of direct excitation into the nondegenerate ${}^5D_0 \leftarrow {}^7F_0$ transition of a single site or follows the indirect excitation of other sites via energy transfer from the initially excited site. Furthermore, the luminescence they attributed to the site they called A is clearly the result of simultaneous emission from at least two different sites since the number of peaks in all regions exceeds the maximum number of peaks expected under the lowest possible site-symmetry. Although these authors did point to the presence of these extra peaks they offered no explanation for this experimental fact. Another experimental observation on which they did not comment is the fact that the ratio of intensities in their "non-selectively" excited spectra varied greatly with the Eu(III) content of their samples. The ${}^5D_0 \longrightarrow {}^7F_0$ luminescence appears to be much weaker in the most concentrated sample. On the basis of the number of Stark components of the different ${}^5D_0 \longrightarrow {}^7F_J$ transitions (J \geq 1) these authors concluded that the symmetry of the Eu(III) substitutional sites is C_{2v} or distorted C_{2v} and probably results from the

distortion of the ideal BR site of symmetry D_{3h}. They fail to point out in this paper that such lowering of symmetry may result from either one of the following situations:

- (i) A displacement along the <1120> direction of the Eu⁺³ ion from the ideal 2d or BR position of symmetry D_{3h} to one of the three equivalent 6h or mO positions.
- (ii) A displacement of the 12 first neighbours of the Eu⁺³ ion while the Eu⁺³ ion remains in the BR site.

Depending on the extent and the nature of the distortion the principal axis of the site either remains along the main crystallographic axis c or becomes perpendicular to it. This point was indeed made in Saber's doctoral thesis [11] but this author offers no suggestion of the use of spectroscopic data to distinguish between these possibilities. Besides laser-induced luminescence data, these authors presented the results of crystal-field calculations as well as some experimental EPR results on Eu(II)-doped LMA. Unfortunately, they did not examine these results according to the two possible choices of orientation of the principal axes of the distorted sites with respect to c.

In their paper on Gd(III)-doped LMA Y. Salem et al. [10] re-examined the crystal-field calculations carried out by Saber and presented some polarization experimental results on Saber's samples of Eu(III)-doped LMA. They assumed that Saber's assignment of the observed luminescence was correct and concluded, from their crystal-field calculations, that Saber's

sites A and B represented different degrees of distortions of the ideal BR site. More specifically, they stated that site B being the more distorted one should correspond to a location in the unit cell very near the ideal mO (C_{2v}) position. Two points remain unclear in their paper:

- (i) Although they do conclude that site B is for all practical purposes the mO site, it is clear that the correlation diagramme they drew between the $|^7F_1\rangle$ states of the ideal D_{3h} site and the distorted C_{2v} sites corresponds to the case where the principal axis remains parallel to the **c** direction.
- (ii) They do not report the polarization of the "extra" peaks observed by Saber. This would have been an important point to verify especially in view of the fact that the luminescence attributed to site A might have contained some peaks related to Eu(III) ions in site B. In this perspective, one wonders whether their peak at 585.9 nm in site A (Euc polarized) originates from the same ${}^5D_0 \leftarrow {}^7F_1$ transition as the peak at 585.7 nm in site B (same polarization), at room-temperature.

We would like to conclude this discussion with the examination of the results included in Buijs *et al.*'s paper [9]. These authors studied the Eu(III) laser induced luminescence in powdered samples of EuMgAl₁₁O₁₉. Their main conclusions were the following:

(i) Eu(III) is present in four different substitutional sites. Table I presents the positions of the Eu(III) ${}^5D_0 \longrightarrow {}^7F_0$ transitions for these sites in comparison to those reported by

Saber et al.

- (ii) There is some dynamic evidence (life-time studies) for the existence of energy transfer between these sites,
- (iii) These energy transfer processes occur via the 5D_0 level with a rise time of 100 μs .

The first conclusion was based on two experimental results. The first one was a low-temperature luminescence spectrum obtained under excitation into the ${}^5D_2 \leftarrow {}^7F_0$ transition, with the 464 nm argon ion laser line. In this spectrum the ${}^5D_0 \longrightarrow {}^7F_0$ region seems to be composed of four overlapping peaks. Since the intensity in this region is very weak (less than 10% of the peak of highest intensity), it is extremely hard to judge whether these four very close peaks are not artifacts. Furthermore, an important criticism can be made against the use of this technique to draw this type of conclusion. Indeed, laser excitation into the ${}^5D_2 \leftarrow {}^7F_0$ is not entirely "non-selective". For instance, the following scenario can easily be imagined:

- (i) Suppose there are only two inhomogeneously broadened site distributions I and II.
- (ii) Accidental degeneracies between different Stark components of the ⁵D₂ multiplet for these two site distributions are expected to be quite common.
- (iii) Suppose that there is downward energy transfer between the two site distributions via the ⁵D₂ levels.

Under these very reasonable assumptions, when we excite into the 5D_9 \leftarrow 7F_0 region, at a given wavelength, we could be selecting a

given component of two given sites within site distributions I and II. If this direct excitation is transferred to other sites within these two distributions we would have effectively selected four sites within the inhomogeneous site distributions I and II. The ${}^5D_0 \longrightarrow {}^7F_0$ region will show four peaks.

To strengthen their argument these authors present two series of excitation and related emission spectra. Their excitation spectra were obtained by tuning the excitation wavelength in the $^5D_2 \leftarrow ^7F_0$ region while monitoring the $^5D_0 \rightarrow ^7F_0$ luminescence. The corresponding emission spectra show the $^5D_0 \rightarrow ^7F_0$ luminescence generated by pumping into the peaks seen in the excitation spectra. Besides the fact that these authors should have shown the entire emission spectra to allow a better comparison of the luminescence of their four sites, it is clear to us that these results support the existence of two site distributions coupled by energy transfer processes; their site 1 and 2 belonging to site distribution I and their site 3 and 4 to site distribution II.

An important question then remains concerning their dynamic study: were the rise times observed due to energy transfer via the 5D_2 or the 5D_0 levels?

The study undertaken within the framework of this doctoral thesis was an attempt to answer all of these questions and carry out other experiments to draw more conclusions concerning the nature of the Eu(III) substitutional sites in LMA.

1]. R.Collongues, D. Gourier, A. Kahn-Harari, A.M. Lejus, J. Thery and D. Vivien, Ann. Rev. Mater. Sci. 20, 51 (1990)

[2]. A. Kahn, A.M. Lejus, J. Théry and D. Vivien, French Patent No.80-15171. July 1980 (Patents pending in Europe, USA and

Japan).

[3]. Kh. S. Bagdasarov, L. M. Dorozhkin, L.A. Ermakova, A.M. Kevokov, Yu. I. Krasilov, N. T. Kuznetsov, I. I. Kuratev, A. V. Potemkin, L. N. Raiskaya, P.A. Tseltlin and A. V. Shestakov, Sov. J. Quantum Electron. 13(8), 1082 (1983).

[4]. A-M Lejus, private communication

5]. N.N. Mel'nik, M.N. Popova, I.T. Makhmudov and P. A. Arsen'ev, Sov. Phys. Solid State 26(9), 1659 (1984).

[6]. A. Kahn, A.M Lejus, M. Madsac, J.Théry, D. Vivien, J.C. Bernier, J. Appl. Phys. 52, 6864 (1981).

[7]. R. Collongues, D. Gourier, A. Kahn-Harari, A.M. Lejus, J.Théry and D. Vivien, Ann. Rev. Mater. Sci. 20, 51 (1990).

[8]. D. Saber, J. Dexpert-Ghys, P.Caro, A.M. Lejus, J. Chem.

Phys. 82, 5648 (1985).

[9]. M Buijs and G. Blasse, J. Solid State Chem. 71, 296 (1987). [10]. Y. Salem, C. Linares, B. Jacquier, M.C. Saine, M. Gasperin, A.M. Lejus and D. Vivien, J. Chem. Phys 93, 7076 (1990)

[11]. D. Saber, Thèse de Troisième cycle, Université P. et M. Curie, Paris, France (1983).

Table I: Positions of the ${}^5D_0 \longrightarrow {}^7F_0$ transitions for different Eu(III) substitutional sites reported by Buijs *et al.* and Saber *et al.*

Buijs et al.'s results	Saber et al.'s results
site 1: 577.19 nm site 2: 577.75 nm site 2: 578.43 nm site 3: 578.92 nm	site A: 577.9 nm site B: 578.6 nm

EXPERIMENTAL

The data acquisition and sample preparation techniques applied in this thesis work are described in each experimental section of the three manuscripts to follow. This chapter intends to clarify and complete those descriptions.

1. Sample preparation:

The highly reducing atmosphere of the Verneuil flame favours the lower oxidation state of europium. Some of the samples made available to us displayed a very low luminescence efficiency in the region of interest. When illuminated with a UV lamp they showed very little of the characteristic red emission of Eu(III) but gave off an intense blue luminescence indicative of the presence of Eu(II). These samples had to be treated in an oven with a constant circulation of oxygen at 1200°C. The UV lamp test was used to verify the degree of oxidation. It was clear that these samples were not homogeneous. Therefore, the concentrations given in the three manuscripts to follow are only nominal. We avoided for this reason any quantitative discussion of concentration effects. Despite this fact it is clear that the main three samples which we focused provide a wide enough range of concentrations to allow qualitative descriptions of concentration effects. The highly concentrated samples (20%, and 30% europium contents) had a milky aspect and scattered a considerable amount of light. One sample of apparent good quality (nominal concentration of 10%) was used for the polarization study. This sample was cast into a polymer matrix ("Fast acrylic kit #441 from from Buehler) and held with a plastic roll (provided with the epoxy kit) to maintain it in any chosen direction and then polished. The cast was then removed by soaking it in acetone for about an hour. The freed sample was then

cleaned with methanol and dried.

2. Luminescence detection:

An important point is not mentioned in the experimental sections of the manuscripts to follow. In the first manuscript, a chopper equipped with a photo diode was used to trigger the acquisition of signal a few micro seconds after the laser pulse. When the laser pulse was on, the entrance slits to the monochromator were blocked. In the last two manuscripts (experiments carried out in Lyon, France), the monochromator was scanned right through the laser line; therefore, a large number of photons from the scattered laser beam do reach the detector during the duration of the pulse. This effect was practically eliminated from the averaged luminescence signal the following way:

- (i) first of all since the detection was always carried out at 90° from the direction of excitation, only a small percentage of the laser beam reached the detector.
- (ii) secondly, the signal from the photo tube detector was fed into a photon counter. This device was set to count photons for at least 1 minute (in some experiments the dwell time was longer). The number of photons due to luminescence that are counted by this device over a period of 1 minute far exceeds the number of photons due to direct laser scattering which takes place during the duration of a laser pulse (10 ns). In the practice, because the detector actually receives a large number of photons during the first nanoseconds following the triggering of the laser, the related electronics recovers this transient regime after about 10μs. This time of recovery was actually measured using the Stanford multi channel scaler and represents our

lower limit for the detection of lifetimes and rise times.

RESULTS AND DISCUSSIONS

NOTES TO THE READER

The following section is composed of three manuscripts.

The first manuscript was published in the Journal of Luminescence (J. Lumin. 50, 339 (1992)). It represents a preliminary study in which the viability of the project was tested and an ambiguity concerning the number of Eu(III) substitutional sites was lifted.

A version of the second manuscript was accepted for publication in the same journal in February 1992, with minor corrections. It concentrates on the investigation of the polarization of the luminescence lines observed in the preliminary study. This manuscript was intended to answer the basic question of the crystallographic nature of the Eu(III) substitutional sites.

A version of the last manuscript is to be submitted soon to the Journal of Physical Chemistry. It intends to answer some questions left unanswered in the previous two manuscripts. In particular it addresses the question of concentration dependence of the occupation ratios of the three sites observed in the previous manuscript, draws further conclusions concerning the nature of the intermediate site and explains why some of the polarization data in the second manuscript where more difficult to interpret.

PART A

STATEMENT OF CONTRIBUTIONS

The data discussed in the following manuscript were acquired jointly with M. Laberge (Ph.D candidate, same research group). The results were interpreted entirely by M.M. NAFI and the manuscript was prepared by this same author.

SITE-SELECTIVE SPECTROSCOPY IN EU³⁺:LANTHANUM MAGNESIUM ALUMINATE

M.M NAFI, M. LABERGE and D.J SIMKIN Department of Chemistry, McGill University, Montreal, Quebec, Canada H3A 2K6

ABSTRACT:

Pulsed resonance emission spectra for La_{1-x}Eu_xMgAl₁₁O₁₉ are reported under excitation into the non-degenerate $^5D_0 < --- ^7F_0$ transition of Eu³⁺ at 77K. Emission spectra recorded under continuous-wave excitation into the same transition at liquid helium temperature were also examined. These results show clear evidence for the existence of only two distinct substitutional site distributions for Eu³⁺, with their $^5D_0 < --- ^7F_0$ transitions between 577 and 579 nm. The suggestion of a third site distribution ca. 576 nm is also reported. Discrepancies concerning the number of Eu³⁺ substitutional sites and the positions of their corresponding $^5D_0 --- > ^7F_0$ peaks reported in other studies are addressed in the light of our results.

1. Introduction

Lanthanum magnesium hexa-aluminate (LMA), which has a magnetoplumbite-type structure, is a particularly interesting material. It has been extensively studied for its potential as a solid-state laser host for transition metal and rare earth ions [1-4] and within the broad spectrum of the influence of structure on the optical properties of luminescent materials. In this context, Eu^{3+} is a particularly useful dopant because of the simple dependence of its luminescence on local symmetry variations. Saber et al. have identified two different substitutional sites for Eu^{3+} in crystalline samples of $La_{1-x}Eu_xMgAl_{11}O_{19}$ (x = 0.02, 0.05) [5]. Their site-selective spectroscopic results were obtained under continuous-wave dye laser excitation into the non-degenerate $^5D_0 < --- ^7F_0$ transition, at 77K. Buijs et al., on the other hand, studied the

luminescence of powdered samples of $La_{1-x}Eu_xMgAl_{11}O_{19}$ (x = 1) under excitation into the multi Stark-component $^5D_2 < ^{---} ^7F_0$ transition, at liquid helium temperature [6]. They identified four different Eu^{3+} substitutional sites and found evidence for energy transfer between europium ions in different sites. The present paper addresses this discrepancy showing that it can be accounted for by the differences in the experimental approaches and that emission spectra assigned to two distinct sites can be assigned otherwise. Furthermore, it suggests that a site distribution on the high energy side of the $^5D_0 < ^{---} ^7F_0$ region may have been missed in both studies.

2. Experimental

The single crystals synthesized by A.M. Lejus (ENSCP, Paris) using the Verneuil method were used without further treatment. The formula of the compound is La_{1-x}Eu_xMgAl₁₁O₁₉, the samples used in this study had a nominal concentration of x=0.1 and x=0.02. The resonance fluorescence measurements were performed using a grazing incidence pulsed dye laser [7] pumped with a Lumonics TE-861M-3 excimer laser. The dye used was rhodamine 590 (Exciton) and the excimer gas was XeCl. The resonance emission spectra were recorded using a Spex 1702 single monochromator (focal length 3/4 m and 1200 grooves/mm grating, slits at 150 μm, giving a spectral bandpass of 0.16 nm at 570 nm), a Hamamatsu R928 photomultiplier tube as a detector, a mechanical chopper placed between the sample and the entrance slit of the monochromator, and an EG&G model 4400 boxcar averager. The laser was triggered by a pulse derived from the chopper blade. This allowed us to introduce a delay between the laser pulse and the mechanical chopper which was adjusted to eliminate direct laser radiation while the resonance emission which occurs on a much longer time-scale was let through. The continuous-wave experiments were carried out using a Spectra physics 375 dye laser pumped with a Spectra Physics 164 argon ion laser, a Ramanor U-1000 spectrometer (ISA instruments) equipped with a Jobin Yvon double monochromator (slits

at 150 μ m, giving a spectral bandpass of 0.1 nm at 570 nm), a Pelletier-cooled photon counter and the ISA Prism software package.

In all of these experiments the sample was mounted in a CF204 Oxford Instruments continuous flow cryostat. Low temperatures down to 69K were achieved with liquid nitrogen while liquid helium was used for temperatures below 69K.

3. Nomenclature and structural differences of hexa-aluminates

LMA of formula LaMgAl₁₁O₁₉ belongs to a large group of closely related aluminates. The fact that the structural differences between these compounds are very subtle is a source of confusion in the literature. In addition, these materials are often non-stoichiometric and quite different from their idealized structure because of the presence of a large number of defects. This makes their classification and the study of their X-ray crystallographic patterns difficult. This section attempts to summarize the nomenclature usage for these compounds and the structural relationships between them.

All of the aluminates that belong to this family consist of ordered densely-packed spinel blocks separated by a mirror plane. If a given aluminate is an electrolyte its mirror plane is referred to as the conduction plane. The unit cell of the idealized structure of hexa-aluminates or hexagonal aluminates (space group P63/mmc) is characterized by a two-fold screw axis. This category of aluminates includes such compounds as the solid-state electrolyte Na B alumina [8]. They are to be distinguished from the parent rhombohedral aluminates (space group R3m) in which the spinel blocks are related by a three-fold screw axis. Na B" alumina, for instance, is a rhombohedral aluminate [9]. Hexa-aluminates are further divided into those which adopt the magnetoplumbite structure and those which are related to Na B alumina. It would seem simple to put in the first category all compounds isomorphous to the mineral magnetoplumbite PbFe7.5Mn3.5Al0.5O19, i.e those of general formula AB12O19, and in the second category those of general formula AB11O17 [10]. In fact, the nomenclature cannot be

this restrictive because of the diversity in the stoichiometry of these compounds. To take this diversity into account these two categories can be differentiated by the differences in the structure of their mirror plane. Fig. 1 shows these differences. The mirror plane of the magnetoplumbite is characterized by the presence of Al³⁺ ions at the so-called anti-Beevers-Ross positions (plane corners or 2b Wyckoff position) and the presence of oxygen atoms at the three equivalent 6h positions [11]. The mirror plane of Na B alumina is much less compact; it contains only one O²- ion located near or at the center of the triangle formed by the three empty 6h positions (2c Wyckoff position) and there are no Al3+ ions in the anti-Beevers-Ross positions [12]. Hexa-aluminates containing monovalent cations adopt the B structure. The distribution of the monovalent ions within the mirror plane depends largely on the size of this ion: this leads some authors to further distinguish between, for instance, Na B alumina and Ag B alumina structures [13]. On the other hand, hexa-aluminates containing large divalent cations adopt the magnetoplumbite structure (except in the case of Ba²⁺); they are referred to as magnetoplumbite-type hexa-aluminates [14]. Lanthanum hexa-aluminates, which were first recognized by Roth and Hasko [15] and named lanthanum B-alumina, were studied by several groups. Dexpert-Ghys et al. proposed a model in which these compounds would in fact be composed of B-type and magnetoplumbite-type microdomains; this model explains particularly well the stoichiometry range of lanthanum hexa-aluminates (10.3-14.7 Al₂O₂/1 La₂O₃) [16]. In a more recent publication, Iyi et al. reported that the Fourier maps at the different stages of the refinement of the X-ray crystal structure of La_{0.827}Al_{11.9}O_{19.09} did not show any increase of electronic density at the 2c position (which, as previously noted, would be characteristic of a \(\mathbb{B}\)-type unit cell), they therefore concluded that this compound has a magnetoplumbite structure and proposed a different model for the stoichiometry of lanthanum hexa-aluminates [17]. The introduction of a divalent ion in the crystalline lattice of lanthanum hexa-aluminates (in the form of a metal oxide mixed with the starting materials) yields a series of compounds which are

more stable [18]. The most common one is lanthanum magnesium hexa-alumina (LMA) of formula LaMgAl₁₁O₁₉. This material is easily doped with luminescent trivalent lanthanide ions to give compounds of general formula La_{1-x}Ln_xMgAl₁₁O₁₉ where Ln=Pr, Nd, Sm, Eu, Gd (also introduced in the form of metal oxides mixed with the starting materials). Although there is an agreement in the literature that the mirror plane of La_{1-x}Ln_xMgAl₁₁O₁₉ resembles that of magnetoplumbite there are some discrepancies on the nature and the number of substitutional sites for the dopant rare earth ion. This provided the motivation for this work. In the next sections we will examine the particular case of La_{1-x}Eu_xMgAl₁₁O₁₉ also denoted Eu³⁺:LMA.

4. Results and discussion

Before we present our luminescence results for Eu³⁺:LMA we would like to emphasize a few important points. Even though we are dealing with a crystalline material the electronic transitions of the dopant ion are inhomogeneously-broadened by the presence of strain, defects and vacancies. In other words, the number of actual substitutional sites is virtually infinite. However, within this large number of sites there should be a limited number of distinct site distributions. Structural differences within the same site distribution are of very little relevance; therefore, in a site-selective spectroscopic study, one should exercise extreme caution in deciding to assign two different luminescence spectra to two "relevantly" distinct sites or to two sites belonging to the same inhomogeneously-broadened site distribution. Fig. 2 shows a series of emission spectra for La_{1-x}Eu_xMgAl₁₁O₁₉ (nominal concentration x=0.1). The bottom spectrum was acquired under excitation with the 457 nm Ar⁺ laser line. This spectrum is only used to identify the approximate limits of the different ${}^5D_0 \longrightarrow {}^7F_{0.1.2}$ regions in the pulsed resonant emission experiments. The result of these experiments is shown in the same figure, the corresponding excitation wavelength is indicated for each spectrum. This series clearly shows two prominent Eu³⁺ site distributions with ${}^5D_0 \longrightarrow {}^7F_0$

transitions around 578.0 (site distribution I) and 577.2 nm (site distribution II). The site distribution around 578.0 nm is characterized by an intense ${}^{5}D_{0} \longrightarrow {}^{7}F_{2}$ emission, with a prominent peak around 625 nm, and a relatively large Stark splitting in the ⁷F₁ region while the distribution around 577.2 nm is characterized by a weaker ⁷F₂ emission, the absence of a peak around 625 nm and a smaller Stark splitting in the ${}^7\!F_1$ region. The spectrum under 577.7 nm excitation cannot be the result of an emission from a single site since there are more than 3 peaks in the ${}^5D_0 \longrightarrow {}^7F_1$ region. Furthermore, since this spectrum exhibits features that are common to site distributions I and II we interpret it as simultaneous emission from these same distributions. The previous conclusions are further supported by the examination of the weaker ${}^5D_0 \longrightarrow {}^7F_{3,4}$ regions. The sharp peak around 652 nm and the very weak ${}^{5}D_{0} \longrightarrow {}^{7}F_{4}$ emission are clearly characteristic of site distribution I while the peak around 708 nm and the broad emission above 680 nm can easily be ascribed to site distribution II. The ${}^5D_0 \longrightarrow {}^7F_{3,4}$ emission obtained under 577.7 nm excitation can easily be interpreted as simultaneous emission from site distributions I and II. These results also lead us to think that the emission from Saber et al.'s site A[5] under excitation ca. 577.9 nm was in fact simultaneous emission from sites belonging to distributions I and II. This explains why these authors observed additional lines which they could not assign. In particular, we clearly showed here that the additional line they observed around 652 nm is a characteristic emission line of the lowest-energy site distribution (our site I, Saber et al's site B). As we tuned the excitation wavelength to the limit of our pulsed dye laser (576.3 nm) some interesting results were observed; these are summarized in fig. 3 and 4. These spectra reveal the existence of a third site distribution with a ${}^5D_0 < --- {}^7F_0$ transition on the high energy side of this spectral region. Indeed, if we were simply tuning out of site distribution II we would expect the emission to decrease in intensity in all regions. This is not the case: the peak ca. 610 nm in the ${}^5D_0 \longrightarrow {}^7F_2$ region (fig. 3) is more intense under 576.3 excitation than under 577.2 excitation. The examination of the ${}^5D_0 \longrightarrow {}^7F_{3,4}$ region (fig. 4)

further supports this conclusion: the peaks ca. 647 nm and 708 nm are characteristic of site distribution III and grow as we tune the excitation wavelength into the $^5D_0 < --- ^7F_0$ absorption band of this distribution.

This high energy site distribution was not reported in the spectroscopic studies performed independently on Eu³⁺:LMA by Saber et al. (x=0.02 and x=0.05) [5] and by Buijs et al.(x=1) [6]. On the other hand, Buijs et al. reported the existence of 4 different Eu³⁺ substitutional sites in the region between 577.19 nm and 578.92 nm at a temperature of 4K for their powdered samples. We decided to investigate this region more systematically for a crystalline sample of a concentration comparable to that of Saber et al. (x=0.02) at liquid helium temperature. Contrary to Buijs' work, our spectra were recorded under excitation into the non-degenerate ${}^{5}D_{0} < --- {}^{7}F_{0}$ transition. Fig. 5 shows the ${}^5D_0 \longrightarrow {}^7F_{1,2,3}$ emission recorded with a continuous-wave dye laser tuning the excitation between 579.0 and 577.3 nm at a temperature of 4.2 K. inhomogeneously-broadened site distributions can easily be identified in this series of spectra. Their ${}^5D_0 < --- {}^7F_0$ transitions occur respectively ca. 578.6 nm (low-energy site distribution I) and ca. 577.6 nm (mid-energy site distribution II). The low-energy site distribution is characterized by a peak ca. 625 nm in the ⁷F₂ region and a peak ca. 645 nm in the ⁷F₃ region. The mid-energy site distribution is characterized by the absence of the two previous peaks and the presence of other peaks in the ⁷F₃ region. This figure clearly shows that sites ca. 579.0 nm and 578.3 nm also belong to site distributions I and II respectively since their emission does not exhibit any new features when compared to the spectra that were labelled with the same site distribution numbers. The shortest wavelength component of the ${}^5D_0 \longrightarrow {}^7F_1$ multiplet ca. 585 nm is very narrow and relatively intense. Fig. 6 shows the dependence of the position of this peak with the excitation wavelength. Within the same site distribution (spectra previously labelled I or II), this peak clearly appears to be shifting in the same direction as the excitation wavelength. The break that occurs in this trend at an excitation wavelength of about 578 nm is another indication of the fact that spectra acquired under excitation wavelengths on either side of this value belong to two distinct site distributions. In fig. 6 we also included the first two ${}^5D_0 \longrightarrow {}^7F_1$ peaks from the emission spectrum acquired under 578.3 nm excitation (diamond points). The narrow peak around 585 nm clearly follows the trend attributed to site distribution I while the second peak around 587 nm fits the line corresponding to site distribution II. Similar conclusions can be drawn for the emission spectrum recorded under an excitation wavelength of 577.3 nm. The facts that this spectrum shows more than three peaks in the ${}^5D_0 \longrightarrow {}^7F_1$ region, that the position of the peak around 584 nm follows the trend attributed to site distribution II (star point in fig. 6) and that this spectrum presents some additional new features all point to the following conclusions:

- (i) There are no other distinct site distributions between 577.3 and 579 nm besides site distributions I and II.
- (ii) There exists another less luminescent site distribution with a ${}^{5}D_{0} < --- {}^{7}F_{0}$ absorption below 577.3 nm.

As pointed out before, the maximum number of peaks per site in the $^5D_0 \longrightarrow ^7F_1$ region is 3 but an additional broad band is seen in the entire series, very close to the excitation wavelength. This band was not observed by Saber et al. because under their experimental conditions stray light from the laser line was still quite noticeable in this range. The fact that this band is very broad, that its maximum is always approximately 150 cm $^{-1}$ away from the excitation wavelength and that it must be short-lived since it was not observed in our pulsed experiments (which use a delay between the excitation and the detection) leads us to reject the possibilities of this being either a $^5D_0 \longrightarrow ^7F_0$ band or the short wavelength Stark component of the $^5D_0 \longrightarrow ^7F_1$ multiplet. We postulate that this is a Raman band. This is consistent with the fact that this band is most intense in the spectra that show the weakest emission and is weakest around the maximum of the absorption band of a given site distribution. Raman bands were

observed in this range by N.N. Mel'nik et al. [19]. We should also point out that this band cannot be due to emission from higher levels that might be expected to be populated via two-photon absorption at this level of excitation power. If this were the case, one would expect to see other emission from these higher levels in the anti-Stoke's region. When we recorded spectra in this region under the same conditions we did not observe any emission.

5.. Conclusions

Our results show clear evidence for only two distinct Eu³⁺ site distributions with $^{5}D_{0} \longrightarrow ^{7}F_{0}$ transitions between 577 and 579 nm. Although the position of the maximum of the ${}^5D_0 < --- {}^7F_0$ absorption bands of these two distributions seem to depend on the concentration, the corresponding emission spectra are easily characterized by the absence or the presence of a peak around 625 nm and, to a lesser degree, by the magnitude of the ⁷F₁ Stark splitting. This allows us to easily compare our results with the ones obtained in other studies. The emission from Saber et al.'s site A (excited at 577.9 nm) is in fact due to simultaneous emission from their site B and a site with a $^{5}D_{0} < ---^{7}F_{0}$ absorption band located at a shorter wavelength. We also found evidence for the existence of a third site at an even shorter wavelength around 576 nm which was not reported by Saber et al. or Buijs et al. Lower temperature does not show the existence of any additional distinct site distribution besides the previous three observed at liquid nitrogen temperature. We do not believe that the discrepancy in the reported number of sites in the two previous studies is simply the result of the different europium concentrations. Rather, we suggest two possible alternate explanations for Buijs et al. having observed four sites (very close together) between 577 and 579 nm:

(i) Powdered samples are usually inhomogeneous. Since, as shown in this work, the position of the maximum of the ${}^5D_0 < --- {}^7F_0$ absorption bands of these site distributions depend, to different degrees, on concentration, one can easily be mislead

into thinking that there are more site distributions than there actually are. However, with a random Eu³⁺ concentration distribution this would lead only to increased inhomogeneous-broadening.

(ii) Site-selective spectroscopic studies performed under excitation into the multi-component ${}^5D_2 < ---- {}^7F_0$ transition can lead to simultaneous excitation of more than one site at a time (because of the usual occurrence of accidental degeneracies in this region). We avoided this problem by excitating into the non-degenerate ${}^5D_0 < ---- {}^7F_0$ transition.

A systematic study of this system at different temperatures and for different compositions is now under way using time-resolved site-selective spectroscopy and polarization studies. This should allow us to draw definite conclusions concerning the exact nature of these substitutional site distributions and to determine whether the reported simultaneous emission is due to energy transfer or simultaneous excitation.

Acknowledements

We would like to thank Professors A. M. Lejus and D. Vivien, E. N. S. C. P., Paris for making these samples available to us. This work was supported by the Natural Sciences and Engineering Research Council of Canada. One of the authors (ML) gratefully acknowledges the same agency for their support in the form of a graduate scholarship.

References

- [1] V. M. Garmash, A. A. Kaminskii, M. I. Polyakov, S. E. Sarkov and A. A. Filimonov, Phys. Status Solidi A75, K111 (1983).
- [2] Kh. S. Bagdasarov, L. M. Dorozhkin, L. A. Ermakova, A. M. Kevokov, Yu. I. Krasilov, N. T. Kuznetsov, I. I. Kuratev, A. V. Potemkin, L. N. Raiskaya, P. A. Tseltlin and A. V. Shestakov, Sov. J. Quantum Electron. 13(8), 1082 (1983).
- [3] C. Wyon, J. J. Aubert, D. Vivien, A. M. Lejus and R. Moncorge, Topical Meeting on Tunable Solid State Lasers, Williamsburg, Virginia (USA), Technical Digest, 63 (1987).
- [4] R. Moncorge, J. Thery and D. Vivien, J. Lumin. 43(3), 167 (1989).

- [5] D. Saber, J. Dexpert-Ghys, P. Caro, A. M. Lejus and D. Vivien, J. Chem. Phys. 82(12), 5648 (1985).
- [6] M. Buijs and G. Blasse, J. Solid State Chem. 71, 296 (1987).
- [7] M. G. Littman and H. J. Metcalf, Appl. Opt. 17, 2224 (1978).
- [8] C. A. Beevers and M. A. S. Ross, Z. Krist. 97, 59 (1937).
- [9] J. P. Boilot, G. Collin, Ph. Colomban and R. Comes, Phys. Rev. **B22**, 5912 (1980).
- [10] J. M. P. J. Verstegen and A. L. N. Stevels, J. Lumin. 9, 406 (1974).
- [11] R. Collongues, D. Gourier, A. Kahn-Harari, A. M. Lejus, J. Thery and D. Vivien, Ann. Rev. Mater. Sci. 20, 51 (1990).
- [12] G. R. Peters, M. Bettman, J. W. Moore and M. D. Glick, Acta Crystallogr. B27, 1826 (1971).
- [13] J. Dexpert-Ghys, M. Faucher and P. Caro, J. Solid State Chem. 19, 193 (1976).
- [14] P. I. Bykovskii, V. A. Lebedev, V. F. Pisarenko and V. V. Popov, translation from Zhurnal Prikladnoi Spectroscopii 44(5), 711 (1986).
- [15] R. S. Roth and S. Hasko, J. Amer. Ceram. Soc. 41, 146 (1958).
- [16] J. Dexpert-Ghys, M. Faucher and P. Caro, J. Solid State Chem. 41, 27 (1982).
- [17] N. Iyi, Z. Inoue, S. Takekawa and S. Kimura, J. Solid State Chem. 54, 70 (1984).
- [18] M. Gasperin, M. C. Saine, A. Kahn, F. Laville and A. M. Lejus, J. Solid State Chem. 54, 61 (1984).
- [19] N. N. Melnik, M. N. Popova, I. T. Makhmudov and P. A. Arsen'ev, Sov. Phys. Solid State 26(9), 1659 (1984).

FIGURE CAPTIONS:

Fig. 1: Position of Al³⁺ and O²⁻ ions in the mirror plane of hexaaluminates: a) magnetoplumbite-type structure; b) Na β alumina-type structure.

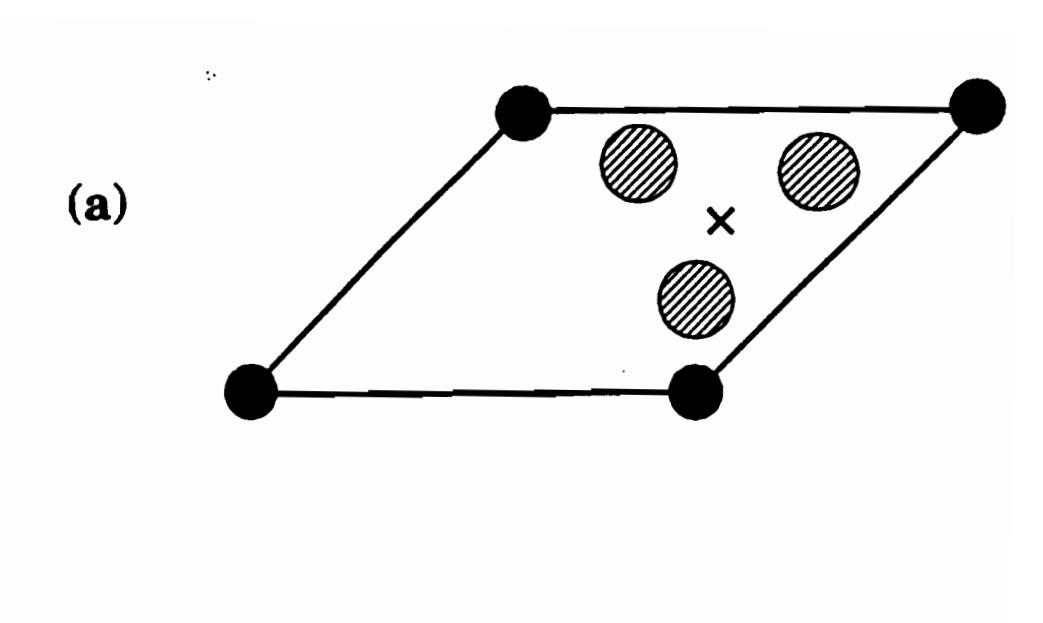
Fig. 2: ${}^5D_0 \longrightarrow {}^7F_{0,1,2,3,4,5}$ emission spectra for $La_{1-x}Eu_xMgAl_{11}O_{19}$ (x=0.1) under pulsed dye laser excitation. Temperature 70K. Bottom spectrum acquired under excitation with Ar^+ 457nm laser line. Intensities normalized to most intense peak in each spectrum.

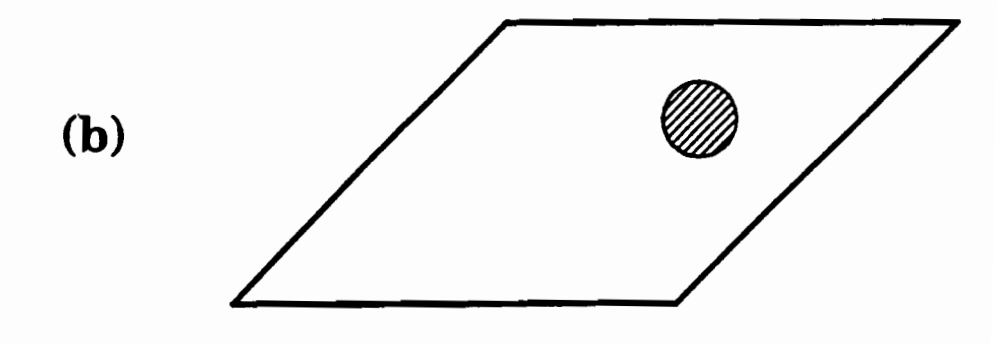
Fig. 3: ${}^5D_0 \longrightarrow {}^7F_{0,1,2}$ emission spectra for excitations between 577.2 and 576.3 nm. Temperature 70K. Intensities normalized to most intense peak in each spectrum.

Fig. 4: Emission spectra for excitations between 577.2 and 576.3. Temperature 70K. Details of ${}^5D_0 \longrightarrow {}^7F_{2,3,4}$. Intensities normalized to most intense peak in each spectrum.

Fig. 5: ${}^5D_0 \longrightarrow {}^7F_{1,2,3}$ emission under continuous-wave dye laser excitation for La_{1-x}Eu_xMgAl₁₁O₁₉ (x=0.02). Excitation wavelength shown for each spectrum. I: site distribution I, II: site distribution II and III: site distribution III. Temperature 4K. Intensities normalized to most intense peak in each spectrum.

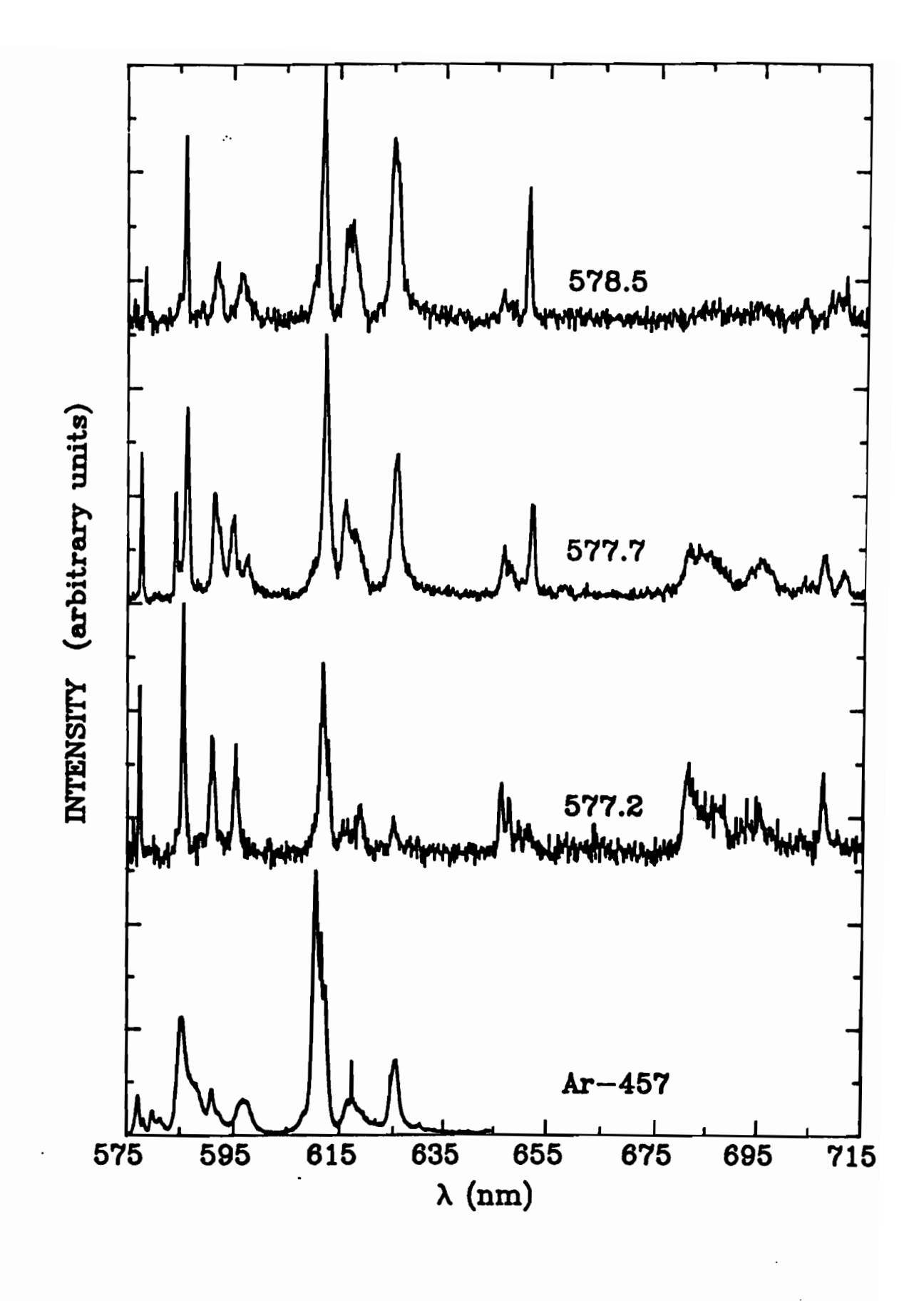
Fig. 6: Dependence between the position λ (em) of the shortest wavelength component of the $^5D_0 \longrightarrow ^7F_1$ multiplet vs excitation wavelength. +: site distribution I, ×: site distribution II. Other points as described in text.

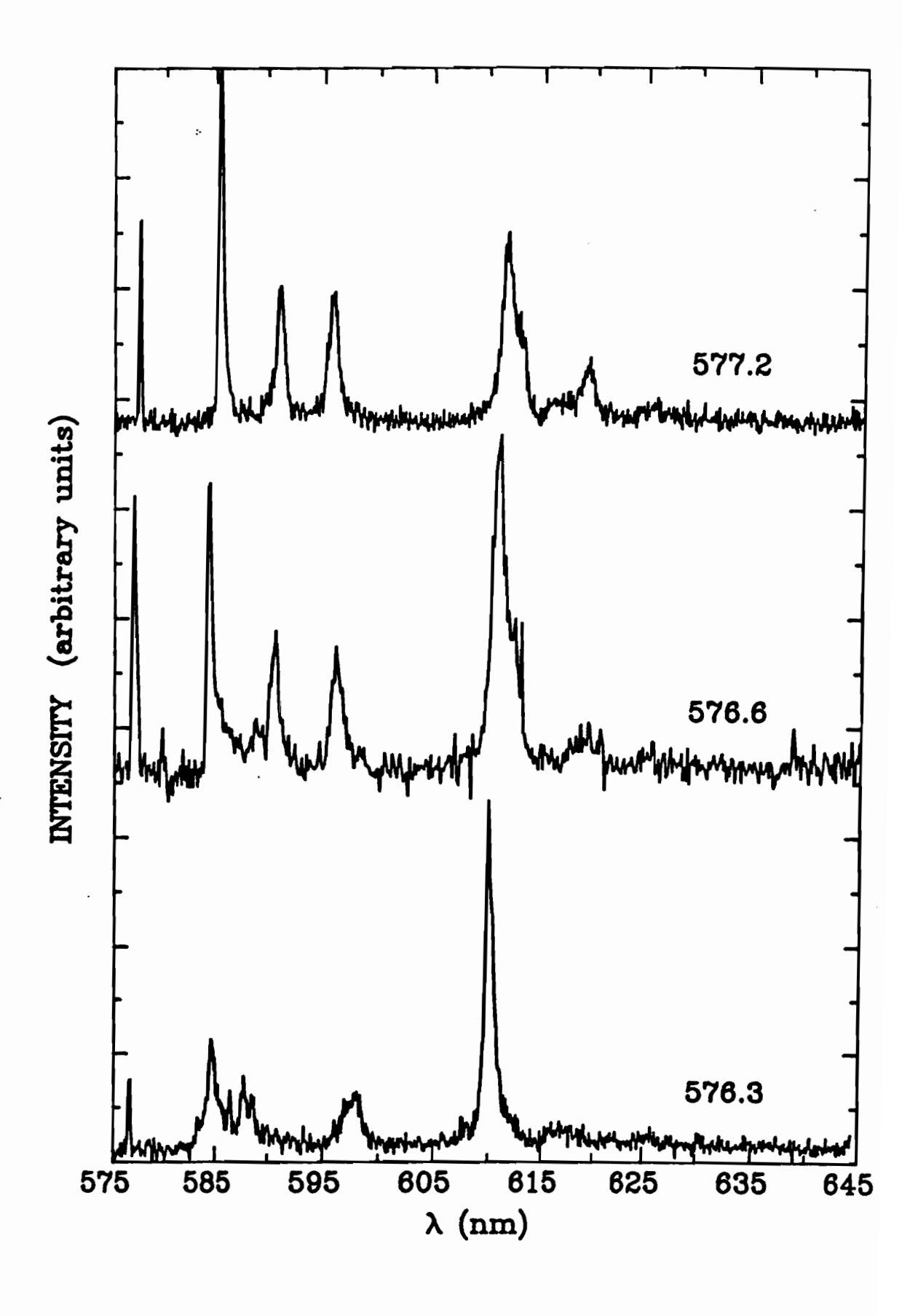


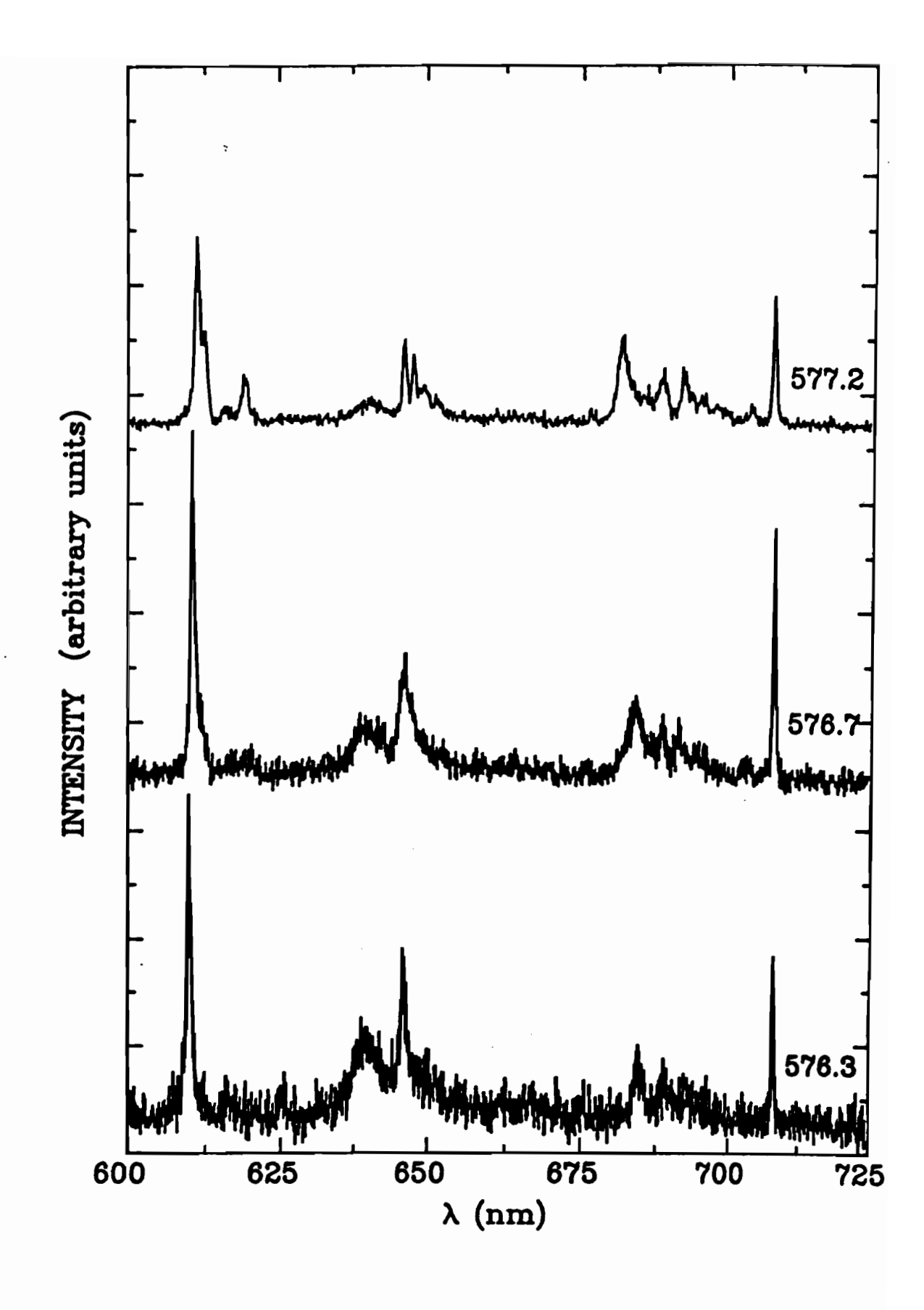


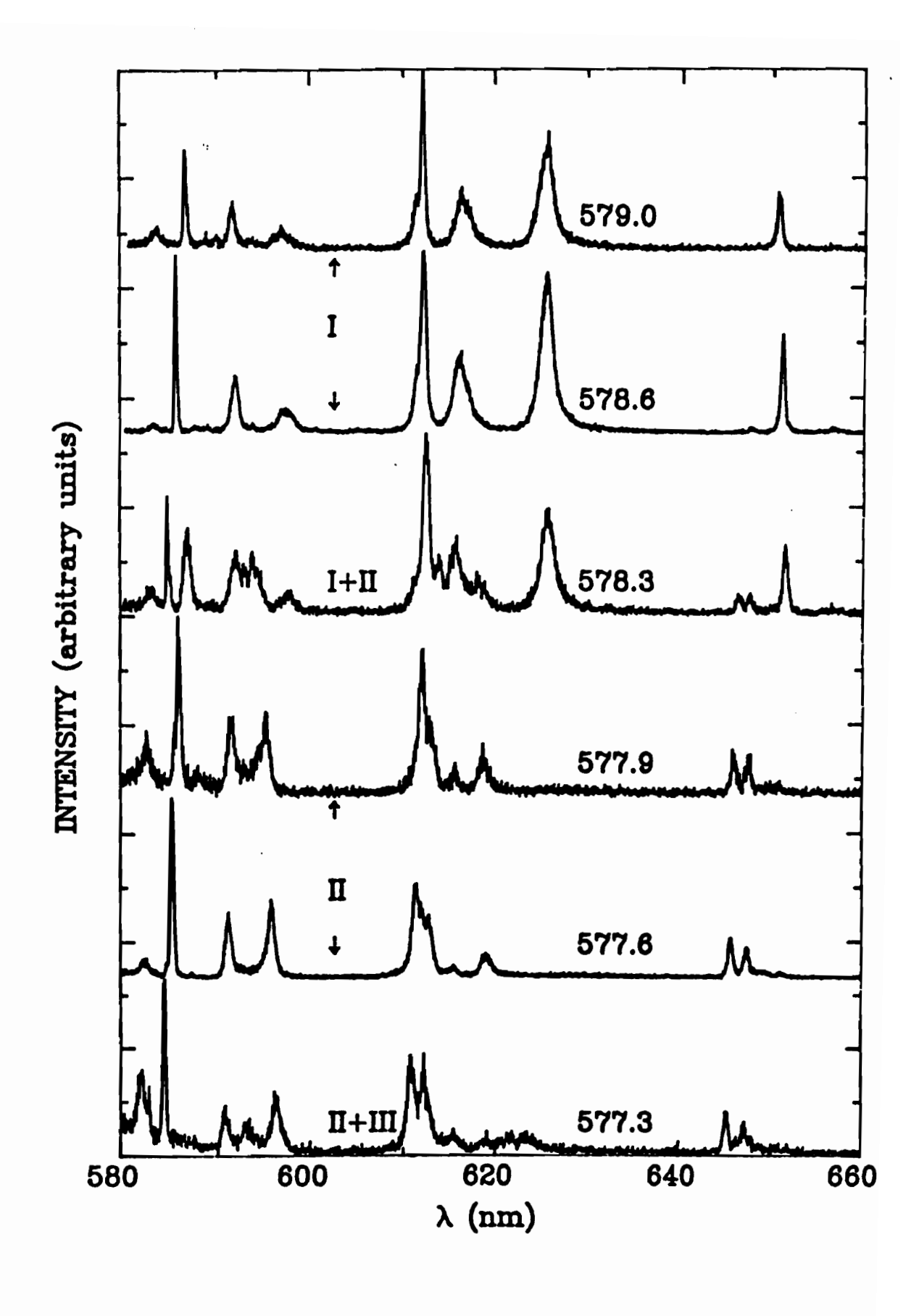


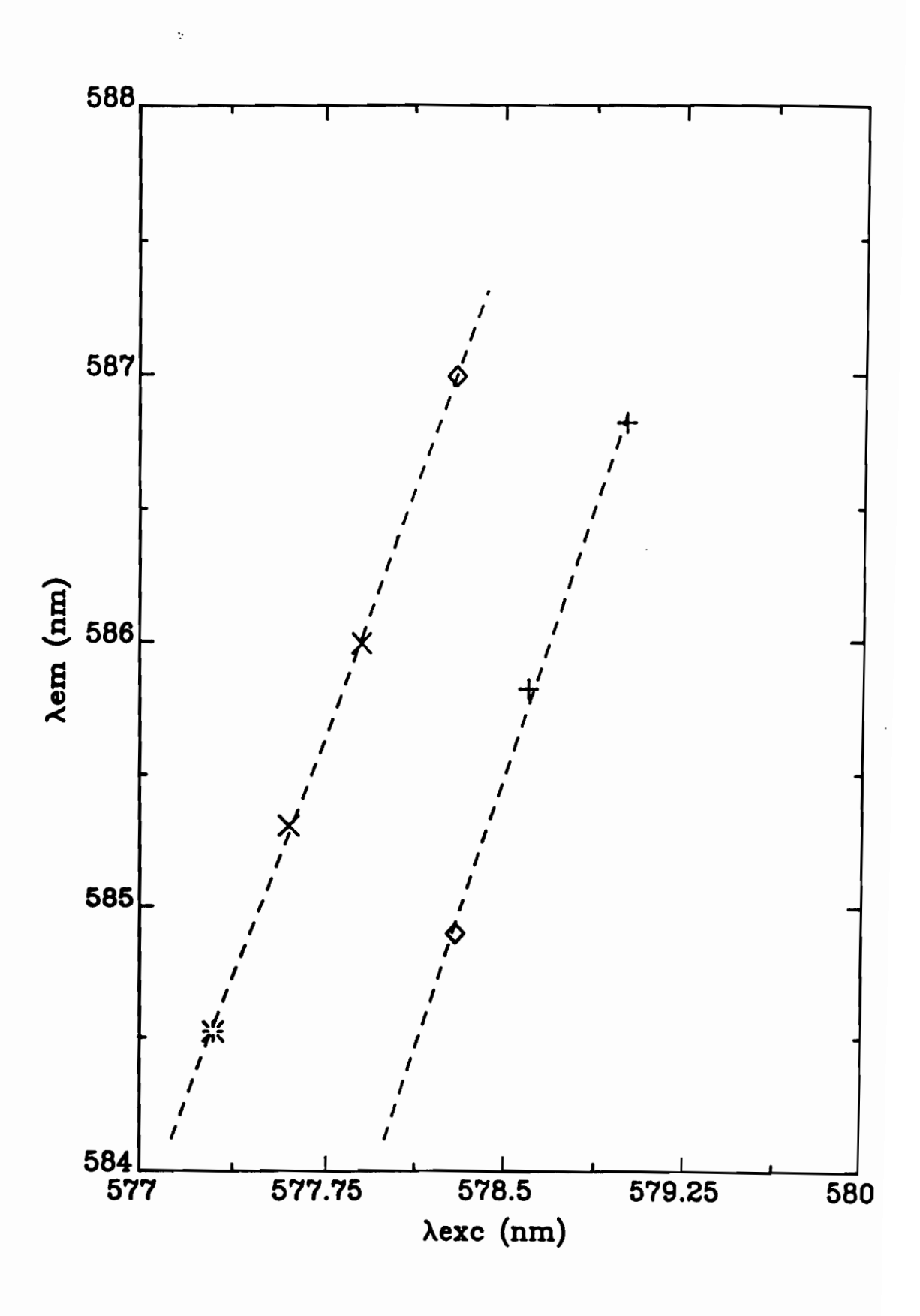
× 2 c position











PART B

STATEMENT OF CONTRIBUTIONS

The data reported and discussed in the following manuscript were acquired using Professor R. Moncorgé's equipment. M.M. NAFI planned these experiments, acquired the data with some assistance from Y. Guyot, interpreted all the results and prepared this manuscript. Dr. P. Nelson is acknowledged for suggesting the polarization work. It is important to emphasize that the first author decided to carry out a polarization study that is very different from the technique used in Dr. Nelson's Ph.D work. Dr. Nelson used the polarization for site-selection purposes while we used the polarization to assign the luminescence peaks of a site-selected spectrum. We believe this techniques is more powerful and allows us to draw more conclusions on the crystallographic nature of the substitutional sites.

POLARIZATION OF THE $^5D_0^{-7}F_J$ Eu $^{+3}$ LUMINESCENCE IN La $_{1-x}$ Eu $_x$ MgAl $_{11}$ O $_{19}$: THE NATURE OF THE Eu $^{+3}$ SUBSTITUTIONAL SITES

M.M. NAFI, D.J. SIMKIN,
Department of Chemistry, McGill University, Montreal, Quebec, Canada H3A 2K6.

R. MONCORGE

Laboratoire de Physico-Chimie des Materiaux Luminescents, Université de Lyon I, U.A. CNRS rP 442, 69622 Villeurbanne Cedex, France.

ABSTRACT:

Low temperature site-selected luminescence spectra of Eu^{+3} in $La_{1-x}Eu_xMgAl_{11}O_{19}$ were assigned on the basis of intensity ratios and number of components in the ${}^5D_0 \rightarrow {}^7F_{0,1,2}$ Stark-multiplets. The luminescence from the high energy site (${}^5D_0 \leftarrow {}^7F_0$ ca. 575 nm) was found to be consistent with D_{3h} symmetry (Beevers-Ross (BR) site) while that from the low energy site (ca. 579 nm) was attributed to Eu^{+3} ions very near one of the three equivalent mid-oxygen (mO) positions of symmetry C_{2v} . The assignment was verified with a polarization study of the ${}^5D_0 \rightarrow {}^7F_{0,1,2}$ luminescence. These results shed some new light on the crystallographic nature of the Eu^{+3} sites.

1. Introduction:

The crystalline host LaMgAl₁₁O₁₉ of magnetoplumbite structure has been studied for its potential as a solid state laser host [1,2] and its structural similarities with two solid state electrolytes Na \(\beta\)-alumina and Na \(\beta^*\)-alumina (3). X-ray studies on this material [4] have shown that its unit cell which belongs to the space group P6₃/mmc is composed of spinel blocks separated by mirror planes. Fig.1 shows that such a structure arises from the stacking along the c-direction of layers of oxygen ions with Al+3 and Mg+2 occupying octahedral and tetrahedral holes. The mirror plane contains the lanthanum ion in the 2d position (so-called Beevers-Ross (BR) position of symmetry D_{3b}) with a C₃ axis along c, three O⁻² ions in three equivalent 6h positions, which is characteristic of the magnetoplumbite structure [5] and Al+3 ions in the 2b positions also called anti-Beevers-Ross (aBR) positions. Trivalent lanthanide ions can be introduced in such a host in the form of oxides mixed with the starting materials. This generally results in a number of structural defects and distortions which makes any X-ray structural determination extremely tedious if not impossible. In this context, the study of the luminescence of the dopant ion can be very useful.

A number of studies have reported site-selective luminescence results in $La_{1-x}Eu_xAl_{11}O_{19}$. Saber *et al.* [6] who carried out such a study in crystalline samples with x=0.02 and

x=0.05 reported the presence of two substitutional sites for Eu+3 (referred to as sites A and B) which they believed to correspond to the mid-Oxygen (mO) positions. These positions are close to the BR (2d) crystallographic site, have their main axis perpendicular to c and are of C_{∞} symmetry. On the other hand, Buijs et al. [7], who studied energy transfer processes in fully substituted powdered samples of La_{1-x}Eu_xMgAl₁₁O₁₉, identified four different Eu+3 substitutional sites but did not discuss their exact nature. In a recent paper Nafi et al. [8] addressed the discrepancies between the positions and the number of sites reported in these studies. This paper showed that a site distribution with its ${}^5D_0 \leftarrow {}^7F_0$ ca. 575 nm was in fact missed in previous studies and that the emission from Saber et als site A was actually due to simultaneous emission from their site B and a site with a ${}^5D_0 \leftarrow {}^7F_0$ transition ca. 577 nm. Finally, in a paper on the luminescence of La_{1-x}Gd_xMgAl₁₁O₁₉, Salem et al. [9] reported the polarization of the ⁵D₀← ⁷F₁ transitions at 295K in La_{1.x}Eu_xMgAl₁₁O₁₉ for the Eu⁺³ sites identified by Saber et al. Their conclusions were that both of these sites, of C₂ symmetry, were derived from the ideal D_{3h} site, which they did not observe, and that site A is less distorted than site B.

The present paper presents the results of a polarization study of the ${}^5D_0 \rightarrow {}^7F_{0,1,2,3}$ luminescence under site-selective excitation into the non-degenerate ${}^5D_0 \leftarrow {}^7F_0$ transition, at liquid helium temperature. These results are discussed in the context of the determination of the nature of the Eu⁺³

substitutional sites.

2. Experimental

The single crystal of $La_{1-x}Eu_xMgAl_{11}O_{19}$ (x=0.1) was synthesized by A.M. Lejus (ENSCP, Paris) using the Verneuil method. The sample was subjected to heat treatment (1200°C for 48 hrs) with a constant circulation of oxygen gas to oxidize the residua! Eu(II), which forms in the highly reducing atmosphere of the Verneuil flame, into Eu(III). It was then mounted in a He closed-cycle refrigerator (T=6K for all experiments), the excitation beam was parallel to the main crystallographic axis c and the luminescence signal was collected at 90° with respect to this direction. Excitation into the ⁵D₀← ⁷F₀ Eu+3 transition was achieved with a pulsed dye laser (Rhodamine 590) pumped with a frequency-doubled Quantel YAG laser (model TDL-50) (excitation power level, measured before the focal point on the sample, was kept ca. 100 µJ/pulse). The luminescence signal was recorded using a Jobin-Yvon monochromator with a slitwidth of 250µ (model HRS1 resolution 12Å/mm slitwidth), an RCA photomultiplier tube and an Ortec 9315 photon counter interfaced with an IBM PC computer.

In the polarization study a polaroid sheet was placed close to the cryostat window with its axis parallel or perpendicular to the main crystallographic axis c. The EIIc and ELc luminescence was passed through a $\lambda/2$ retardation plate, with a properly adjusted axis, before it was focused on the entrance slits of the monochromator. Note that in this geometrical arrangement only the kLc luminescence is detected. In this paper

we refer to the EIIc and ELC polarizations respectively as σ and $\pi.$

3. Selection rules for the ${}^5D_0 \rightarrow {}^7F_J$ transitions:

a) J selection rules:

The selection rules on the total quantum number J in the Russel-Saunders coupling limit have been derived by Judd and Ofelt [10,11]. The electric dipole operator allows transitions $|\Delta J| \le 6$ unless $J_{initial}$ or $J_{final} = 0$ in which case the condition $|\Delta J| = 2,4,6$ has to hold. The magnetic dipole operator, on the other hand, forbids 0↔0 transitions but allows any other transitions fulfilling the condition: △J=0±1. Electric dipole f→f transitions which obey the previous selection rules are still forbidden by the Laporte rule. This rule, however, is relaxed in non-centro-symmetric crystals where the odd components of the crystal field allow the mixing of even fⁿ configuration wave functions with odd wave functions corresponding to other configurations of higher energies. In a centro-symmetric crystal where such odd components are all equal to zero, the Laporte rule can be lifted only through the second order dynamic terms of the crystal-field.

b)Site-symmetry selection rules:

In the free lanthanide ion with an even number of electrons, the Hamiltonian of an f^n electron is invariant with respect to the operations of the single-valued K_h group (also referred to as the three dimensional rotation-inversion group). As a result its eigenvectors in Russel-Saunders coupling, the

 $|^{(2S+1)}L_{J}\rangle$ states, belong to the $D_{q}^{(J)}$ representations, in Wigner's notation, or, in atomic species notation, to the S_a , P_a , D_a ...species for J=0,1,2,3 ... respectively. When the ion is introduced in a solid on a site of a given point group G, these states are split into Stark-multiplets. Since the only additional term in the Hamiltonian, the crystal-field perturbation which causes this splitting, is invariant with respect to the elements of G, each component of this multiplet will belong to an irreducible representation of G. Consequently, in addition to the J selection rules which are generally relaxed through "J-mixing", there are selection rules which are specifically related to the symmetry of the substitutional site on which the dopant ion is located. For a given Eu⁺³ ⁵D₀→⁷F₁ transition, these rules will determine the intensities and the polarization of the emission peaks within the corresponding Stark-multiplet. Although the determination of the characters of the D(J) representations for the purposes of their reduction in G is a tedious process [12]. the detailed calculations are unnecessary because any group G is a sub-group of K_h and correlation tables between K_h and its subgroups are widely available [13]. Such correlation tables help to quickly establish the number and the symmetry species of the components in a given | (2S+1)L₁) Stark-multiplet under any symmetry G. In a second step, a simple examination of the character table of G provides us with the selection rules for the different transitions. their electric or magnetic dipole character as well as their polarization.

c) Predictions for the ${}^5D_0 \rightarrow {}^7F_J$ Eu $^{+3}$ transition in D_{3h} and C_{2v} symmetries:

The application of the general procedure outlined in the previous paragraph to the $|^{7}F_{0,1,2,3}\rangle$ multiplets in the pertinent case of D_{3h} site-symmetry yields the results summarized in table I and table II.

Saber et al. [6] suggested that the Eu^{+3} ions may be occupying a site of symmetry C_{2v} . Such a site may result from either one of the following situations:

- (i) A displacement along the <11 20 > direction of the Eu $^{+3}$ ion from the ideal 2d or BR position of symmetry D_{3h} to one of the three equivalent 6h or mO positions.
- (ii) A displacement of the 12 first neighbours of the Eu⁺³ ion while the Eu⁺³ ion remains in the BR site.

Clearly these two scenarios should be viewed as limiting theoretical cases, the actual situation is probably a combination of both. In the first limit-case the main axis of the site is perpendicular to \mathbf{c} , while it remains parallel to \mathbf{c} in the second. Table III shows the correlation between the D_{3h} and C_{2v} groups for these two possibilities [13]. Saber *et al.* [6] did not explain, in the context of the previous scenario, whether their two distinct C_{2v} site distributions arise from:

- (i) the occurrence of the two limit cases, or
- (ii) the occurrence of only one of the two previous limit-cases. In this context two distinct site distributions could still be observed if, for instance, the three equivalent ideal mO sites are rendered inequivalent by some special distribution of the defects.

could still be observed if, for instance, the three equivalent ideal mO sites are rendered inequivalent by some special distribution of the defects.

Table IV shows the selection rules for the ${}^5D_0 \rightarrow {}^7F_{0,1,2}$ transitions and the predicted polarization for C_{2v} symmetry in both limit-cases.

4. Results and discussion:

a) Non-polarized luminescence results:

Fig. 2 shows the three types of luminescence spectra that were obtained under selective laser excitation into the $^5D_0 \leftarrow ^7F_0$ transitions at 575, 577 and 579 nm at 6K. These correspond to the three sites we identified in our previous paper [8].

A close examination of the spectrum in fig. 2a shows that under 575 nm laser excitation there are two peaks in the ${}^5D_0 \rightarrow {}^7F_0$ region: the resonance and a broader peak at lower energies. Since this transition has only one Stark component under any site-symmetry we believe that this observation is evidence for the occurrence of energy transfer from the high-energy site distribution to the distributions located at lower energy. We interpret the spectrum in this figure as luminescence mainly due to Eu^{+3} located on or very near the ideal BR (2d) position of symmetry D_{3h} . The detailed spectral features in fig. 2a are interpreted as follows:

- (i) This is the spectrum that shows the weakest $^5D_0 \rightarrow ^7F_0$ emission which is expected to be forbidden by both J and D_{3h} site-symmetry selection rules.
- (ii) The broad peak ca. 585 nm is assigned to the

 $^5D_0(A_1') \rightarrow ^7F_1(E'')$ transition. The fact that this peak is broad can be attributed to a slight deviation from D_{sh} symmetry which would cause this doubly-degenerate transition to yield two very close peaks.

- (iii) The peak ca. 597 nm is ascribed to the ${}^5D_0(A_1') \rightarrow {}^7F_1(A_2')$ transition.
- (iv) The strong emission ca. 610 nm is assigned to the $^5D_0(A_1') \rightarrow ^7F_2(E')$ transition.
- (v) The weaker ${}^5D_0(A_1') {\to} {}^7F_2(E'')$ (magnetic dipole allowed in D_{3h} more difficult to assign. Indeed, weak emission peaks due to energy transfer to lower energy sites could easily be mistaken for these emissions. This assignment will be discussed further below.

Fig. 2c shows the spectrum obtained under laser excitation ca. 579. The number of peaks and the intensity ratios within the 7F_0 and 7F_1 regions are clearly consistent with C_{2v} sitesymmetry:

- (i) The ${}^5D_0(A_1) \rightarrow {}^7F_0(A_1)$ transition, which is allowed in C_{2v} symmetry (electric dipole) but forbidden by J selection rules, is expected to yield a less intense emission peak than the ${}^5D_0 \rightarrow {}^7F_1$ and the ${}^5D_0 \rightarrow {}^7F_2$ transitions (respectively magnetic and electric dipole allowed by J selection rules).
- (ii) The ${}^5D_0 \rightarrow {}^7F_1$ region is fully split.
- (iii) The weakest peak in the ${}^5D_0 \rightarrow {}^7F_1$ region ca. 595 nm is assigned to the ${}^5D_0(A_1) \rightarrow {}^7F_1(A_2)$ since this is the

only magnetic dipole allowed component of the ${}^5D_0 \rightarrow {}^7F_1$ multiplet (according to C_{2v} site-symmetry selection rules).

The spectrum in fig. 2b is clearly intermediate between the two other spectra. This supports the idea that the three sites observed are all derived from the ideal BR (D_{3h}) site. The spectral features in fig. 2b which lead to this conclusion are:

- (i) The ${}^5D_0 \rightarrow {}^7F_0$ transition which is forbidden in D_{3h} symmetry and electric dipole allowed in C_{2v} symmetry is expected to acquire considerable intensity as the site symmetry evolves from D_{3h} to C_{2v} . Furthermore, since the ${}^5D_0 \rightarrow {}^7F_0$ emission intensity is known to be more sensitive to the environment than the ${}^5D_0 \rightarrow {}^7F_1$ emission intensity [14], one can easily understand the observation that the emission ca. 577 is stronger than any emission in the ${}^5D_0 \rightarrow {}^7F_1$ region, in fig.2b.
- (ii) Fig. 2b shows that the crystal-field in the "intermediate site" is strong enough to fully split the ${}^5D_0 \rightarrow {}^7F_1$ region but not strong enough to have the same effect on the ${}^5D_0 \rightarrow {}^7F_2$ or ${}^5D_0 \rightarrow {}^7F_3$ regions. This conclusion is further supported by the observation that the two peaks on the high-energy side of the ${}^5D_0 \rightarrow {}^7F_1$ region are very close. Indeed, this is consistent with our assignment in the D_{3h} site of the degenerate ${}^5D_0(A_1') \rightarrow {}^7F_1(E'')$, which splits up in C_{2v} symmetry, to the

"highest-energy-peak" in the ${}^5D_0 \rightarrow {}^7F_1$ region.

Fig. 3 (a and b) summarizes the assignments of this section and show the correlation diagrams between the D_{3h} and C_{2h} sites, in the ${}^{7}F_{0}$ and ${}^{7}F_{1}$ regions, for the two limit cases discussed above. In fig.3a, the levels arising from the $|^{7}F_{1}(E'')\rangle$ and $|^{7}F_{1}(A'_{2})\rangle$ states were intentionally not crossed for this diagram to be consistent with the luminescence results above. This is the only way to ensure that the magnetic dipole $^5\mathrm{D_n}(\mathrm{A_1}){\to}^7\mathrm{F_1}(\mathrm{A_2})$ is assigned to the peak ca.595 nm (highest energy in ${}^5D_0 \longrightarrow {}^7F_1$ spectral region) in fig.2c. For the same reason, these levels should cross in fig. 3b. To verify and further clarify these assignments we measured the polarization of the ${}^5D_0 \rightarrow {}^7F_{0,1,2,3}$ emissions with respect to the crystallographic axis. For the purposes of the discussion of these results we have included in the same figure the predicted polarizations of the ${}^5D_0 \rightarrow {}^7F_1$ and ${}^5D_0 \rightarrow {}^7F_0$ transitions next to the corresponding terminating level.

a) Polarization of the ${}^5\mathrm{D_0}{\to}^7\mathrm{F}_{0,1,2,3}$ luminescence:

Fig. 4 shows our polarization results for the high-energy site. It is important to note that the polarization effects are not complete. Therefore, in the ensuing discussion " σ or π -polarized emission" simply means that for a given transition the intensity in one direction of observation is greater than the one in the direction perpendicular to it. These observations are not unusual for a

defect system. In this perspective, it is clear that the results presented in fig. 4 are consistent with the assignments in fig. 3 and table II for a Eu+3 located on or very near the BR position of symmetry D_{sh} . For instance, the observation that the ${}^5D_0(A_1') \rightarrow {}^7F_1(A_2')$ emission peak is indeed π -polarized is consistent with the prediction that the (z) principal axis of this site is along c. Furthermore, the fact that the ${}^5D_0(A_1'){\rightarrow}^7F_1(E'')$ is $\sigma\text{-polarized}$ is certainly inconsistent with an orientation of the principal axis in the direction perpendicular while it is at least compatible with z being along c (depending on the orientation of the a and b crystallographic axes with repect to the direction of detection this transition could appear to be σ -polarized). The apparent absence of polarization effects in the ${}^5D_0 \rightarrow {}^7F_2$ region can be explained by a combination of the following factors:

- (i) incomplete polarization effects due to defects,
- (ii) contributions to the intensity of the ${}^5D_0 \rightarrow {}^7F_2$ emission from other sites, via energy transfer,
- (iii) the possibility that the three levels E', E" and A'₁ are very close so that the intensity of the peak ca. 610 nm results from the corresponding three $^5D_0 \rightarrow ^7F_2$ transitions.

In fig. 5, the polarization of the ${}^5D_0 \rightarrow {}^7F_0$ transition (π) establishes that if the low-energy site is of C_{2v} symmetry, which is consistent with the results reported in the previous

section, its principal axis (z) is perpendicular to the main crystallographic axis **c** (see table IV and fig. 3). The other arguments in favour of this conclusion are very strong:

- (i) There is only one π -polarized emission peak in the $^5D_0 {\to}^7F_1$ region, two are expected in the case where zero for the C_∞ site (see table IV).
- (ii) More specifically, since the highest energy ${}^5D_0 \rightarrow {}^7F_1$ component in the D_{3h} site was ascribed to the $|{}^7F_1(E'')\rangle$ level, the highest energy component in the same region for the C_{2v} site should correspond to a level which correlates to $|{}^7F_1(E'')\rangle$. The fact that the corresponding emission peak in fig. 5 (ca. 585 nm) is σ -polarized is fully consistent with the predictions of fig. 3b (C_{2v} with $z \perp c$) and inconsistent with those of fig. 3a (C_{2v} with $z \parallel c$).

Fig. 6 shows the results obtained for the "intermediate site". It is clear that this luminescence spectrum retains all of the polarization characteristics of the high-energy site. For instance, the two peaks arising from the splitting of the σ -polarized $^5D_0(A') \rightarrow ^7F_1(E'')$ (in D_{3h} symmetry) are also σ -polarized. These are indications that beyond the effects discussed above, the distortions of the BR site leading to the "intermediate site" are not very strong. This is further supported by the observation that the splittings in the $^5D_0 \rightarrow ^7F_3$ are too small to be observed.

The observations in the ⁷F₂ and ⁷F₃ regions reveal more

subtle aspects of the nature of the substitutional sites which we would like to discuss in this section. At this point, there is enough evidence to conclude that Eu+3 is present on or very near the BR site and that all other sites result from a gradual displacement of this ion towards the nearby mO position of symmetry C_{2v}. As the site symmetry is gradually modified from D_{sh} to C2 we expect the main axis of the site to change from being parallel to c to become perpendicular to c. Fortunately, the splittings within the ${}^{7}F_{1}$, ${}^{7}F_{2}$ and ${}^{7}F_{3}$ regions are not sensitive to the same degree to changes of the crystal field (this is because these splittings are determined by a different set of B_{α}^{K} parameters in these three regions). The extent to which these regions split provide a qualitative measure of the degree of variations of the crystal field strength and symmetry. From the discussion above it is clear that in our case these variations are never large enough for any of these sites to lead to a full the ⁷F₃ multiplet. We believe that even in the lowest-energy site (Fig. 5) these variations are barely large enough to lift the degeneracies of the $|^{7}F_{2}(E')\rangle$ and $|^{7}F_{2}(E'')\rangle$ states when we move from D_{3h} to C_{2v} since we do not observe five well-resolved peaks in this region (between 610 and 630 nm). This leads us to think that although the Eu+3 ions may be located very near the mO positions they are never on them. In other words, except for the high-energy site the other sites correspond to "intermediate positions" between the BR and the mO sites. Whether their main axis will appear to be parallel or perpendular to c

will depend on the spectral region that we choose to examine. As we tune the excitation wavelength within the ${}^5D_0 \leftarrow {}^7F_0$ inhomogeneous absorption profile, the most sensitive region (7F_0 and 7F_1) will display a "zlc character" sooner than the less sensitive regions (7F_2 , 7F_3). In the light of this discussion the results in the 7F_2 become very clear. In fig. 5 they are consistent with the predictions of table IV in the "z||c" case:

- (i) Out of the most intense peaks between 610 and 630 nm two are σ -polarized and two are π -polarized (three π and one σ expected for the zLc case).
- (ii) If the splittings are not very large we expect no level crossings in the correlation diagram between D_{3h} and C_{2v} in the 7F_2 region. In this perspective any "doublet" in this region in fig. 5 should correspond to two levels correlating to a degenerate 7F_2 level in D_{3h} symmetry. It is interesting to see that the weak shoulder ca. 610 (magnetic dipole transition) is associated with a σ -polarized intense peak (electric dipole transition). According to table IV this is indeed expected as a result of the lifting of the degeneracy of the $|^7F_2(E')\rangle$ state.
- (iii)Along the same line of reasoning the two intense π -polarized peaks ca. 615 nm should correspond to the lifting of the degeneracy of the $|^7F_2(E'')\rangle$ state (cf. fig 5 and table IV).
- (iv) The last relatively broad and intense peak ca. 625 nm is assigned to the ${}^5D_0(A_1) {\longrightarrow} {}^7F_2(A_1)$ transition in C_∞

(zic case) (table IV).

If we assume a correlation between the levels of the three site distributions the assignments of the ${}^5D_0 \rightarrow {}^7F_2$ peaks for the low-energy site lead to the following conclusions for the peaks between 610 and 630 nm in fig. 4:

- (i) The broad peak ca. 615 nm correspond to the $^5\mathrm{D_0(A_1')} {\longrightarrow}^7\mathrm{F_2(E'')}$ magnetic dipole transition in $\mathrm{D_{3h}}$ symmetry.
- (ii) The weak peak ca. 625 nm corresponds to the $^5D_0(A_1^\prime) \longrightarrow ^7F_2(A_1^\prime)$ forbidden transition.
- (iii) The two previous assignments are further supported by the fact that the peak ca. 615 nm grows as we move from the high-energy site (fig. 4) to the intermediate-energy site (fig. 6).

The small splittings of the ${}^5D_0 \rightarrow {}^7F_3$ region prevent us from discussing the polarization results of the emission peaks located beyond 630 nm. However, we should point out the presence of a broad emission ca. 640 nm which is σ -polarized and present in the luminescence from all the identified sites.

5. Conclusion:

Our results show that Eu+3 ions occupy or are very near the crystallographic site which corresponds to the ideal BR (Dab). They also occupy positions which are intermediate between the BR position and one of the equivalent mO ($C_{2\nu}$) positions in $\text{La}_{1,1}\text{Eu}_{1}\text{MgAl}_{11}\text{O}_{19}$. The major source of inhomogeneous broadening appears to be the gradual displacement of the Eu+3 ions from the BR position towards the nearby mO position along the <1120> In this context, it is important to distinguish direction. distributions" between "spectroscopic site and "relevantly distinct" crystallographic sites. This is particularly true for the intermediate site with a ${}^5D_0 \leftarrow {}^7F_0$ ca. 577 nm. Clearly, a large enough displacement from the $D_{\rm sh}$ site will have the following effects on the Eu⁺³ luminescence:

- (i) A full splitting of the ${}^5D_0 \rightarrow {}^7F_1$ region
- (ii) A sudden increase of the intensity of the ${}^5D_0 \rightarrow {}^7F_0$ emission which acquires an electric dipole character and ceases to be forbidden by all selection rules.

These effects are so salient that one can easily be misled into thinking that the corresponding spectrum is due to a Eu^{+3} located on a "distinct" site. The consequence of the second effect, in particular, is a "non-monotonous" inhomogeneous profile for the ${}^5D_0 \rightarrow {}^7F_0$ emission of the " D_{3h} " site distribution. This work clearly shows the danger in using broad band spectra or even excitation spectra to determine the number of distinct substitutional site distributions in Eu^{+3} doped

crystals. It also shows that polarization studies should always examine several spectral regions at the same time.

A study of the concentration and temperature dependence of the luminescence and the lifetimes of the different transitions is now underway. This will allow us to draw more conclusions on the dynamics of the system, the nature of the distortions of the Eu⁺³ substitutional sites and the assignment of the broad emission ca. 640 nm.

Acknowledgments

We would like to thank Professors A.M. Lejus and D. Vivien, E.N.S.C.P, Paris, for making these samples available to us. This work was supported by grants from the Natural Sciences and Engineering Research Council of Canada and the Centre National de la Recherche Scientifique. We also acknowledge Dr. P. Nelson for suggesting the polarization study, Y. Guyot for technical assistance and Professors G. Boulon and B. Jacquier for helpful discussions. Finally we wish to thank Prof. Cohen-Haddad and her group (Department of Chemistry, Université de Lyon, France) for the use of their furnace to treat our samples.

Figure captions

Fig. 1: Unit cell of LaMgAl₁₁O₁₉. Eu⁺³ is introduced in this matrix in the form of an oxide mixed with the starting materials.

Fig. 2: The three different ${}^5D_0 \rightarrow {}^7F_J$ luminescence spectra for $La_{1-x}Eu_xMgAl_{11}O_{19}$ obtained under pulsed dye laser excitation into the ${}^5D_0 \leftarrow {}^7F_0$ Eu^{+3} transition. Temperature 6K. Intensities normalized to most intense peak in each spectrum. a) High energy site excited at 575 nm b) Intermediate site excited at 577 nm c) Low energy site excited at 579 nm. Arrows show position of laser excitation in each spectrum.

Fig. 3: Correlation diagram for the 7F_0 and 7F_1 levels of the high energy (D_{3h}) and the low energy (C_{2v}) sites. if:

(a) principal axis remains along c,

(b) principal axis is perpendicular to \mathbf{c} . Selection rules and polarization of the ${}^5D_0 {\rightarrow}^7F_{0,1}$ are shown next to the corresponding terminating level.

MD: magnetic dipole, ED: electric dipole, F: forbidden.

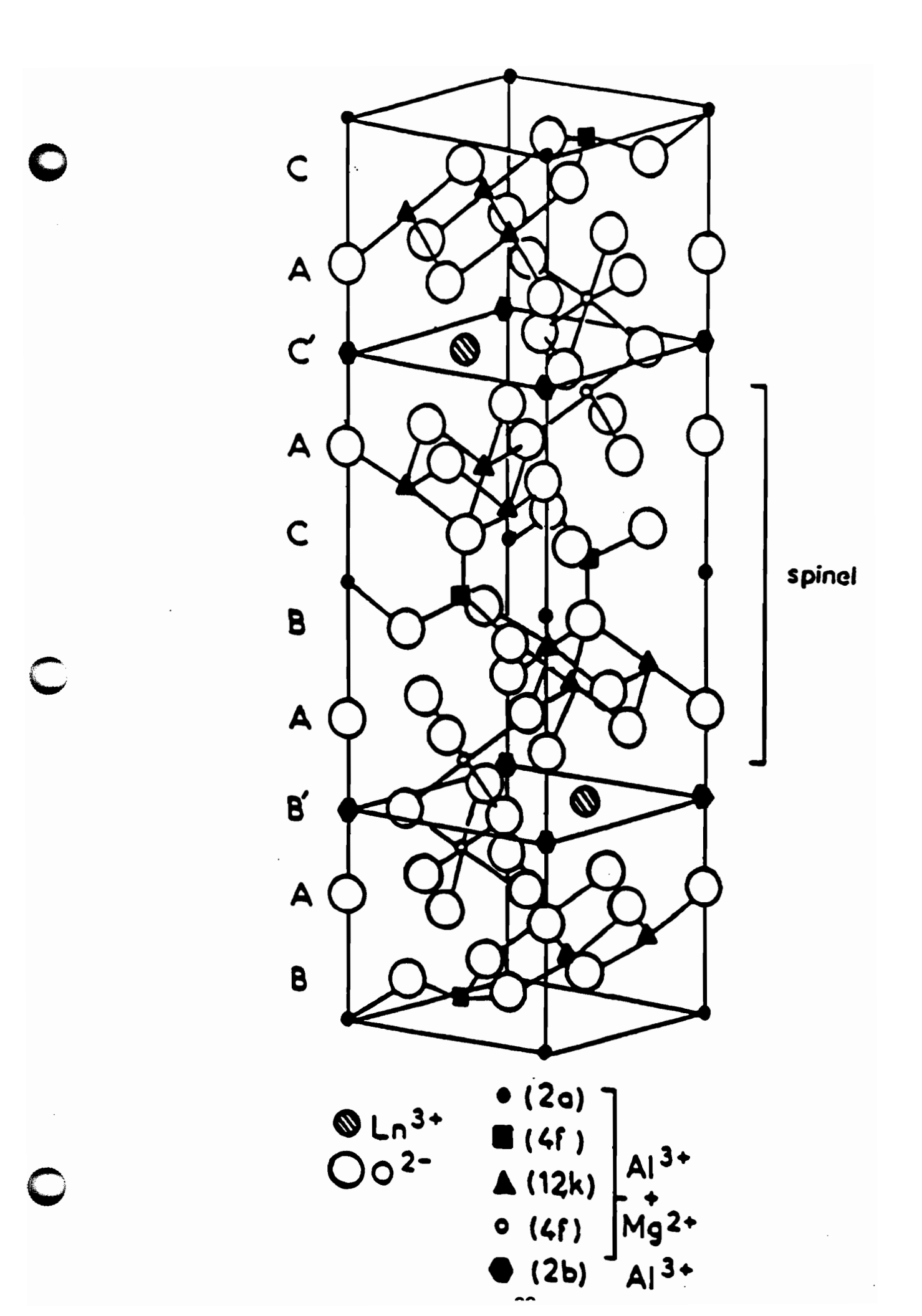
Polarizations:

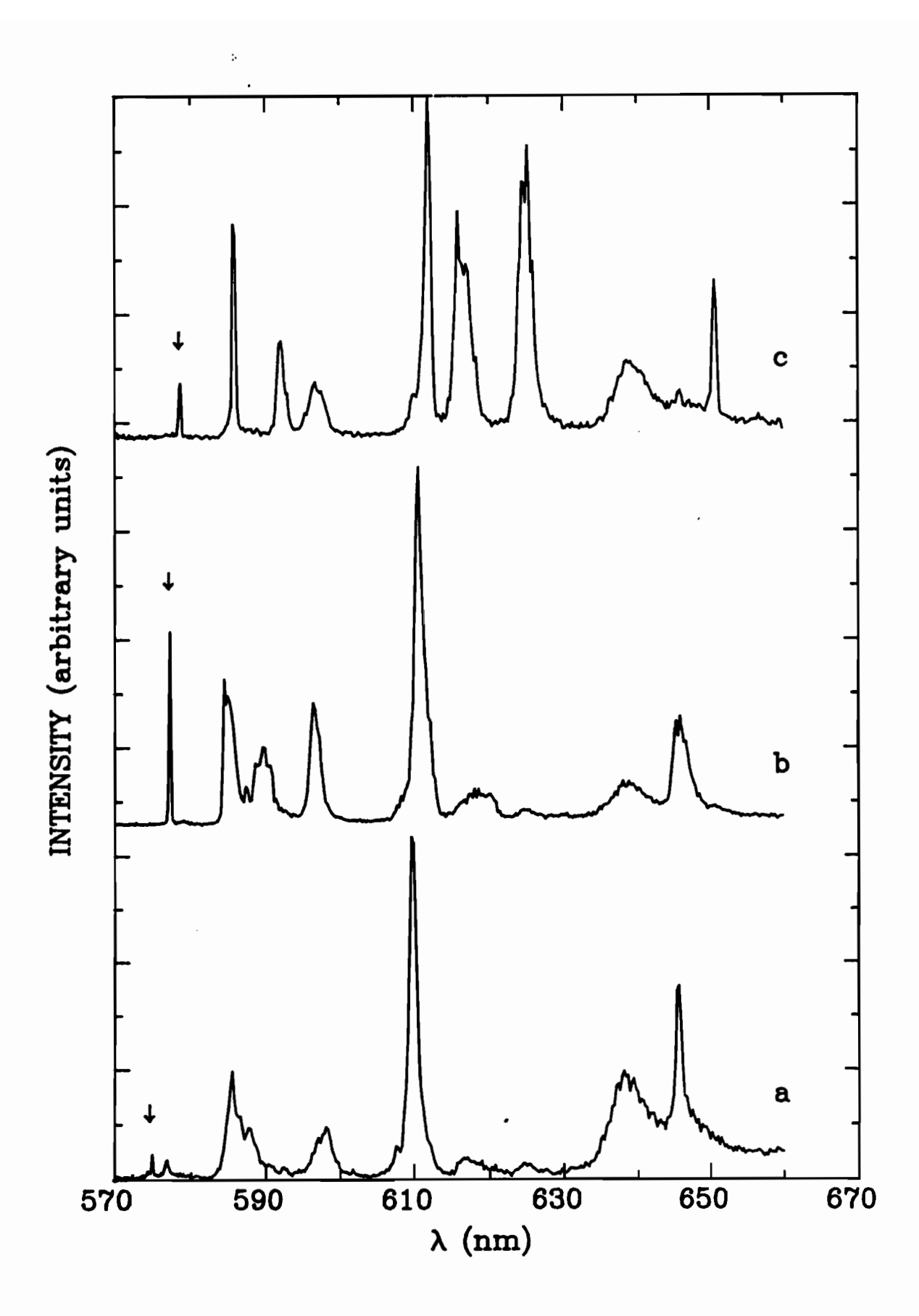
Undet.:undetermined, σ : Ellc and π : E \perp c.

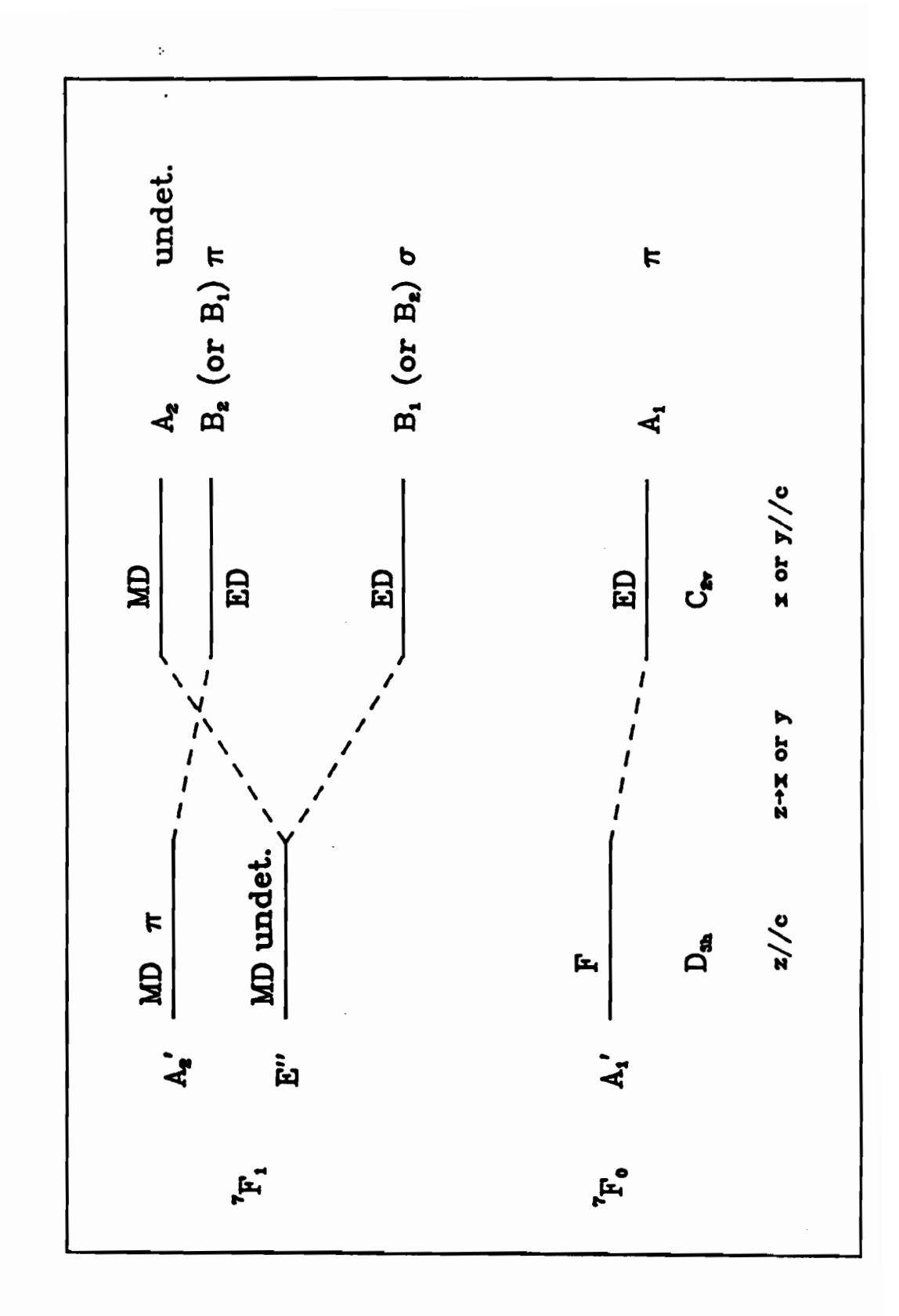
Fig. 4: Polarization of the $^5D_0 \rightarrow ^7F_{0,1,2,3}$ emissions from the high energy D_{3h} site (excitation at 575 nm). σ :EIIC, π :ELC.

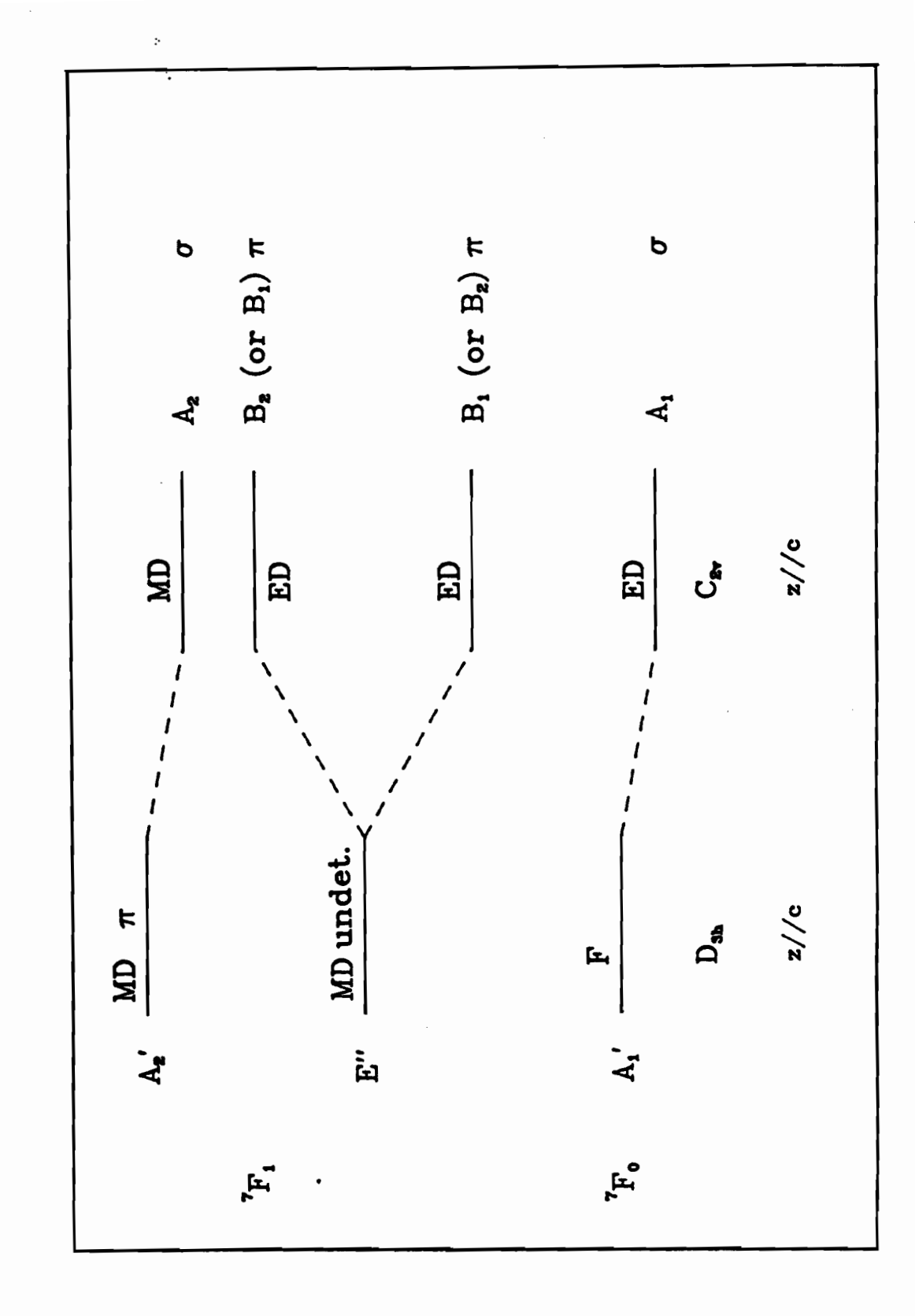
Fig. 5: Polarization of the ${}^5D_0 \rightarrow {}^7F_{0,1,2,3}$ emissions from the low energy " C_{2v} " site (excitation at 579 nm). Insert shows ${}^5D_0 \rightarrow {}^7F_0$ region. σ : EIIC; π :ELC.

Fig. 6: Polarization of the $^5D_0 \rightarrow ^7F_{0,1,2,3}$ emissions from the "intermediate site" (excitation ca. 577 nm). σ : EIC, π : ELC.

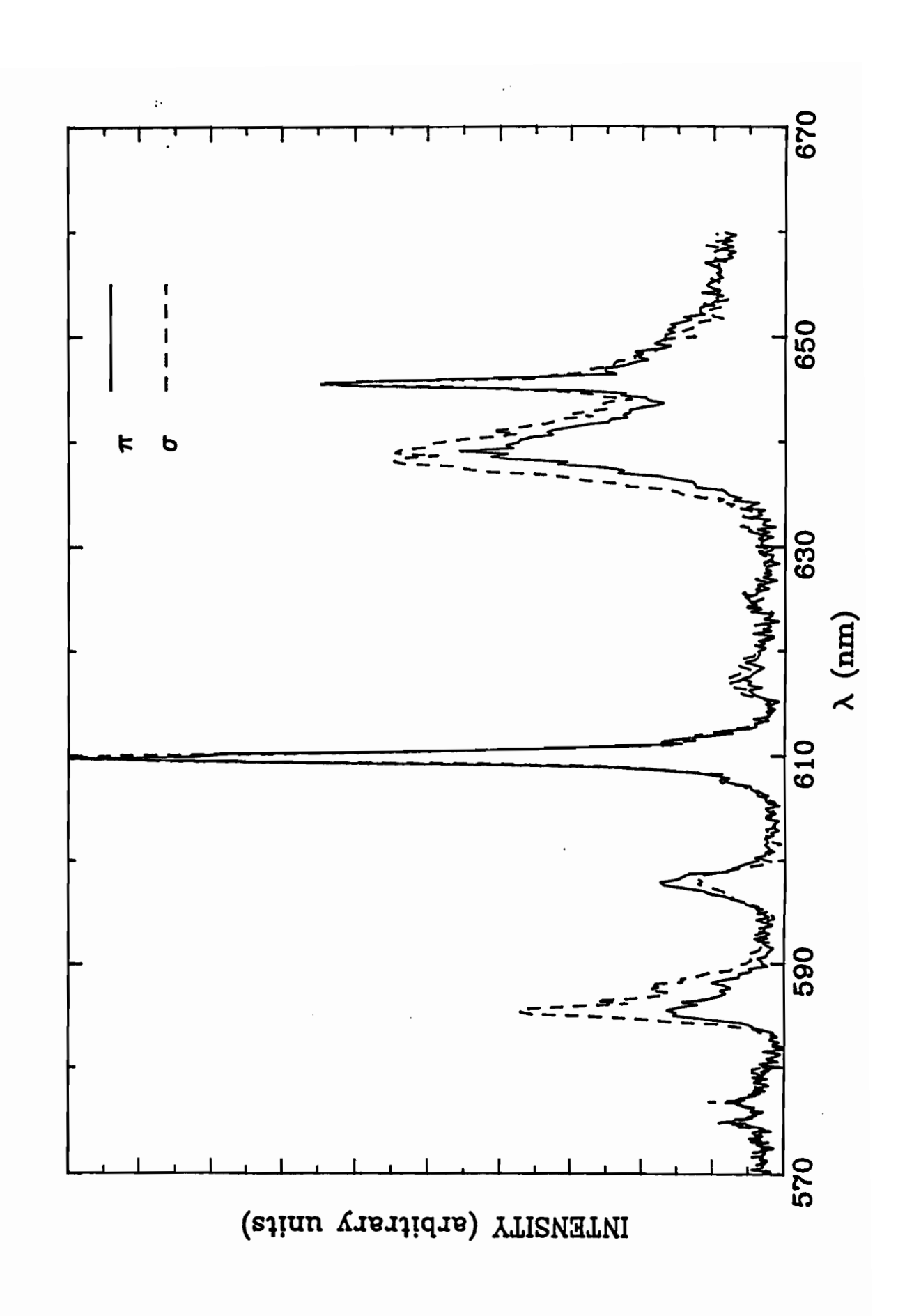


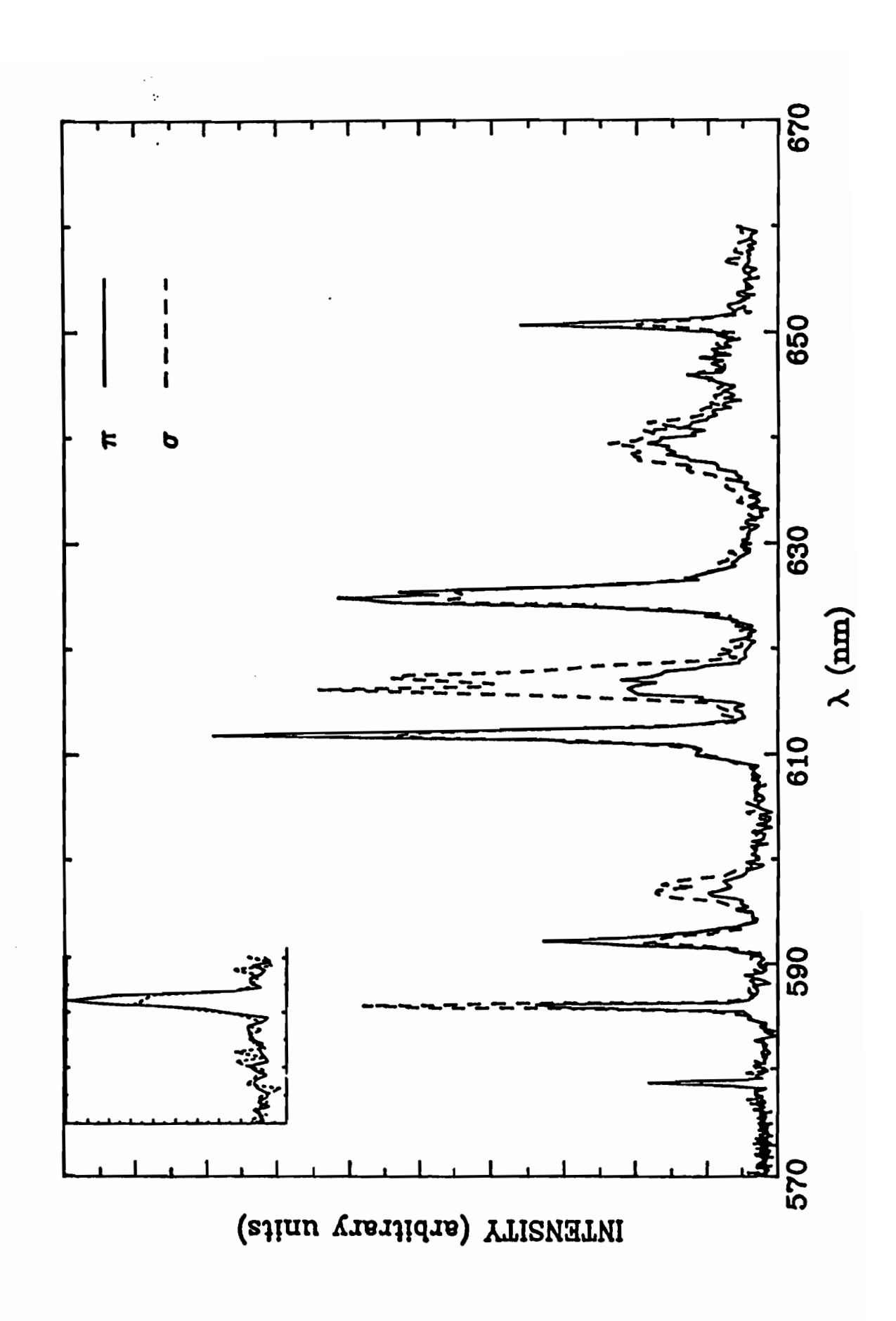






_-





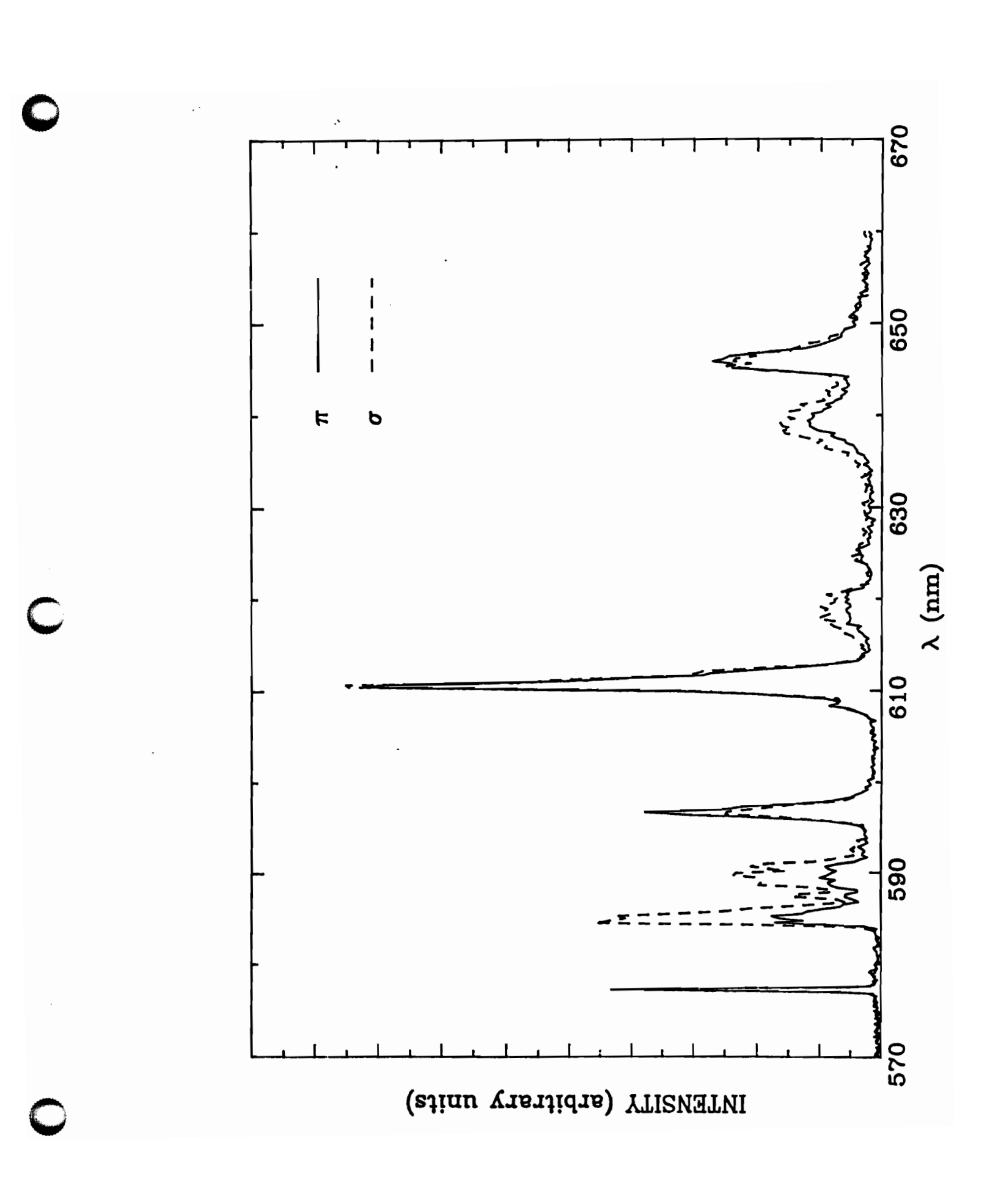


Table I: Correlation table between the K_h and the D_{3h} groups.

Multiplet	K _h	D _{3h}
⁷ F ₀ (⁵ D ₀)	$S_g \equiv D_g^{(0)}$	A ₁
⁷ F ₁	$P_{g} \equiv D_{g}^{(1)}$	A' ₂ + E"
⁷ F ₂	$D_g \equiv D_g^{(2)}$	$A'_1 + E' + E''$
⁷ F ₃	$F_g \equiv D_g^{(3)}$	$A_1'' + A_2' + A_2'' + E' + E''$

Table II: D_{3h} site symmetry selection rules for ${}^5D_0 \longrightarrow {}^7F_J$ transitions.

⁷ F _J	Selection rule	Polarization
⁷ F ₀ (A' ₁)	Forbidden	•••••
⁷ F ₁ (A ₂ ')	MD	E ⊥ z (π)
⁷ F ₁ (E")	MD	E ⊥ x,y (undet.)
⁷ F ₂ (A' ₁)	Forbidden	
⁷ F ₂ (E')	ED	E x , y (π)
⁷ F ₂ (E")	MD	E ⊥ x,y (undet.)

MD: Magnetic dipole allowed, ED: electric dipole allowed. Polarization shown in bracket when z_{||}c: σ : E_{||}c, π : E_{||}c, undet.: undetermined (depends on the orientation of the **a** and **b** axes with repect to the direction of observation)

STATEMENT OF CONTRIBUTIONS

The data reported and discussed in the present manuscript were acquired using Professor R. Moncorgé's equipment. M.M. NAFI planned the experiments, carried them out and prepared this manuscript.

LUMINESCENCE OF EU(III) IN LANTHANUM MAGNESIUM ALUMINATE: THE FULL PICTURE

M.M. NAFI, D.J. SIMKIN,

Department of Chemistry, McGill University, Montréal, Québec, Canada H3A 2K6.

R. MONCORGE

Laboratoire de Physico-Chimie des Matériaux Luminescents, Université de Lyon I, U.A. CNRS rP 442, 69622 Villeurbanne Cedex, France.

ABSTRACT:

Laser excitation spectra of $La_{1-x}Eu_xMgAl_{11}O_{19}$ for x=0.1, 0.01 and x<0.01 were recorded at 10K. The temperature dependence of the selectively excited emission spectra was examined in the range 6K to room-temperature for these concentration and the corresponding lifetimes were measured. The results show that Eu(III) ions are forced to occupy Beevers-Ross (BR) sites when the concentration is above x=0.01. Crystal-field calculations for the three observed sites: BR (D_{3h}), intermediate energy site and mid-Oxygen (mO, C_{2v}) support the proposition that the intermediate energy site is in fact mid-way between the BR and the mO sites.

1. Introduction:

LaMgAl, O, (LMA) a stacked spinel-type material has received some attention for its potential use as an optical material when doped with rare-earth or transition metal ions. For instance, it has been shown that Nd(III)-doped LMA yields a larger laser output than Nd:YAG, for a given pumping power, in continuous mode [1]. In an early preliminary work [2] we suggested that spectroscopic studies by other authors [3,4] might have failed to identify a high symmetry Eu(III) in $La_{1-x}Eu_xMgAl_{11}O_{19}$. This was substitutional site confirmed by us [5] upon the study of the polarization of the $^{5}D_{0} \longrightarrow ^{7}F_{J}$ luminescence under laser excitation into the nondegenerate ⁵D₀← ⁷F₀ transition, in a sample of composition x=0.1. In the same paper we also showed that for this composition, two other Eu(III) substitutional sites of symmetry C_{2v} or near-C_{2v} symmetry can be identified. One with its axis nearly parallel to c the other with its axis nearly perpendicular to c. We proposed that the high symmetry site corresponded to the Beevers-Ross (BR) site of symmetry D_{3h}. The present paper addresses some of the questions left unanswered in the previous papers.

2. Experimental

The single crystals of $La_{1-x}Eu_xMgAl_{11}O_{19}$ (nominal concentrations x=0.1, 0.01 and less than 0.01) were synthesized by A.M. Lejus (ENSCP, Paris) using the Verneuil method. The

samples were subjected to heat treatment (1200°C for 48 hrs) with a constant circulation of oxygen gas to oxidize the residual Eu(II), which forms in the highly reducing atmosphere of the Verneuil flame, into Eu(III). The sample under consideration was then mounted in a He closed-cycle refrigerator (T varied from room temperature to 6K). The excitation beam was propagated along the main crystallographic axis c and the luminescence signal was collected at 90° with respect to this direction. Excitation into the ⁵D₀← ⁷F₀ Eu+3 transition was achieved with a pulsed dye laser (Rhodamine 590) pumped with a frequency-doubled Quantel YAG laser (model TDL-50) (excitation power level, measured before the focal point on the sample, was kept ca. 100 µJ/pulse). The luminescence signal was recorded using a Jobin-Yvon monochromator with a slit width of 250µ (model HRS1 dispersion 12Å/mm at a wavelength of 650 nm), an RCA photo multiplier tube and an Ortec 9315 photon counter interfaced with an IBM PC computer. Lifetime measurements were carried out using a Stanford Research multi channel scaler.

3. Results and Discussion:

3.1. Excitation spectra:

The determination of the position of the ${}^5D_0 \leftarrow {}^7F_0$ absorption band is obviously very important in any Eu(III) site-selective spectroscopic study. Unfortunately, in most matrices it is not very easy to obtain an absorption profile of this spectral region, since this transition is forbidden by J-selection rules.

Laser induced excitation spectra are very often used to mimic absorption spectra in Eu(III)-doped materials. In all of the previous spectroscopic studies of Eu(III)-doped LMA such spectra were recorded by monitoring the emission in the ${}^5D_0 \longrightarrow {}^7F_0$ region following an excitation into the stronger ${}^5D_2 \longleftarrow {}^7F_0$ hypersensitive transition. Although, pumping efficiency argues in favour of such a method, it is important to point out the following disadvantages:

- (i) This procedure does not entirely solve the low throughput problem since the detected emission is still the weak $^5D_0 \longrightarrow ^7F_0$ emission.
- In this procedure, several spectra have to be recorded by small modifications of the monitoring position to ensure the identification of the ⁵D_o← ⁷F_o bands of the different site distributions. The identification of these site distribution is based on the comparison of these spectra: similar spectra are associated with the same site distributions while those with more ascribed important differences are to different site cases it is not very difficult to distributions. In most distinguish between site distributions with ⁵D_o← ⁷F_o transitions occurring on the opposite edges of the $^5D_o \leftarrow ^7F_o$ region. This may not be the case for intermediate site distributions. The ⁵D₂ transition has more than one Stark component per site and accidental degeneracies are not uncommon in this region (coincidence of ${}^5D_2 \leftarrow {}^7F_0$ transitions associated with different sites). If we add the possibility of energy transfer from site to

site, it is clear that it will be very difficult to distinguish between excitation spectra of intermediate site distributions.

We prefer another method which can be justified as follows:

- (i) A relatively broad and generally intense ${}^5D_0 \longrightarrow {}^7F_2$ emission band occurs ca. 610 nm for all sites even when the corresponding ${}^5D_0 \longleftarrow {}^7F_0$ bands do not overlap considerably. Therefore, this is the best monitoring position. Indeed, a Eu(III) located on any site in a given matrix will yield a relatively intense luminescence around this position. This procedure ensures that the ${}^5D_0 \longleftarrow {}^7F_0$ of all the sites are identified in a single excitation spectrum.
- (ii) The only instance where a site maybe missed in this procedure is when this particular site transfers all of its energy to another site.

Fig. 1 presents excitation spectra recorded according to the above method in Eu(III)-doped LMA samples of three different compositions (x=0.1, 0.01, <0.01). The three site distributions which we previous identified in a sample of composition x=0.1 are all evident in this figure. These excitation spectra show that Eu^{+3} ions are forced into the high energy BR site distribution (${}^5D_0 \leftarrow {}^7F_0$ ca. 575 nm) when the europium content is increased. This explains a seemingly unusual result reported by Saber *et al.*. These authors recorded emission spectra under argon ion excitation at 300K. They observed that when the europium content is increased (x=0.02 to x=0.05) the intensity of the ${}^5D_0 \rightarrow {}^7F_0$

emission band decreases. We believe that this is a direct consequence of the increased occupation ratio of the Beevers-Ross site distribution. Indeed, since this site is of symmetry D_{3h} , its ${}^5D_0 \longrightarrow {}^7F_0$ is forbidden by both J and site-symmetry selection rules; therefore, as the occupation ratio of this site increases at the expense of the other sites the ${}^5D_0 \longrightarrow {}^7F_0$ emission from the entire Eu(III) population decreases. For low europium content, when the concentration is increased it seems that the excess europium is divided almost equally between the intermediate and low energy site distributions. Another concentration effect on these excitation spectra is the shifting of the position of the ⁵D_o←−⁷F_o bands for the three site distribution to higher energies. We intentionally exercise extreme caution in the use of the relative intensities of the three excitation bands to determine occupation ratios for a given europium content, since the oscillator strength of the ${}^5\mathrm{D_0} {\longrightarrow}^7\mathrm{F_2}$ transition depends on the symmetry of the corresponding site.

3.2. Emission spectra:

We recorded site-selected luminescence for the three site distributions for temperatures of 10, 70, 200, 300K for the three europium concentrations x=0.1, 0.01, <0.01. The following section discusses the most prominent changes observed in these experiments.

3.2.1. Temperature dependence:

It is remarkable that although generally speaking the

luminescence from any site decreases when the temperature increases, Eu(III) emission lines are much narrower than expected at room-temperature in this matrix..

Fig. 2 shows the ${}^5D_0 \longrightarrow {}^7F_{0.1}$ luminescence (excited at 575.4 nm) from an Eu(III) located on the BR site, for temperatures of 10K, 70K and 300K. It is clear that energy transfer from the BR site distribution to the intermediate site distribution, which is present at low temperature, is not notably more efficient as the temperature increases (top to bottom). Energy transfer from the BR site distribution to the low energy site distribution also appears as the temperature increases. Fig. 3 clearly shows that these two effects combined do not preclude site-selection. The spectra presented in this figure are excited at 579.2 nm (low-energy mO site) at temperature of 10K (top spectrum) and 300K (bottom spectrum). Despite the increase in homogeneous line widths and the efficiency of energy transfer processes it is clear that is not significantly more difficult to selectively excite a single site. Another interesting feature of this last figure is the fact that the broad peak ca. 640 nm which we reported in another paper and which is present in all three site distributions at low temperature completely disappears as the temperature increases.

3.2.2. Concentration dependence:

Our results show that it is practically impossible to obtain a laser induced luminescence spectrum from Eu+3 ions

located on the BR site for Eu(III) concentrations lower than x=0.01. Such spectra can be obtained for a concentration of x=0.01 but they are very noisy. For all practical purposes, we conclude that significant occupation of the BR site occurs only for Eu(III) contents higher than x=0.01.

Fig. 4 presents the ${}^5D_0 \longrightarrow {}^7F_{123}$ luminescence from the intermediate site distribution at room-temperature, for a composition x=0.01. This spectrum illustrates the absence of manifestation spectral diffusion, or the of Anderson's localization in this sample at room-temperature. Excitation into the intermediate energy site distribution does not lead to indirect excitation of other sites (via site-to-site energy transfer or through the overlap of absorption bands), the emission that follows can be attributed almost entirely to the excited site. Furthermore, it is important to note that the emission lines are very narrow for this sample at 300K. In fact, we suggest that Eu(III)-doped LMA for a composition around x=0.01 could be an ideal candidate for room-temperature optical data storage and it might be interesting to explore this possibility by an application of the technique used by M.Mitsunaga et al. [6].

Besides the trends discussed here, the examination of the spectra of this series of experiments shows that the broad peak ca. 640 nm is much weaker for the samples with the lowest europium concentrations, at a given temperature.

3.3. Lifetimes:

We measured the lifetimes of the ${}^5D_0 \leftarrow {}^7F_J$ emission peaks for the three site distributions at the above temperature and concentrations. The broad emission ca. 640 nm which, as we pointed out in a previous paper occurs in all sites, has a very short lifetime (450 μs) it cannot be due to any of the Eu(III) ${}^5D_0 \leftarrow {}^7F_J$ emission. We suggest that it might be related to singly excited Cr(III)-Eu(III) pairs, since Cr(III) is a natural impurity of alumina. Van der Ziel *et al.* [7] as well as L.V. Haley *et al.* [8] have observed evidence for the existence of such pairs in other matrices. The emission bands from such pairs are expected to disappear as the temperature is increased and fast de-excitation processes become available.

All the other peaks have lifetimes which reasonably fit single exponentials with lifetimes varying between 1.2 and 1.5 ms. For a given site, differences observed between the lifetimes of different ${}^5D_0 \longrightarrow {}^7F_J$ emission peaks are of the same order of magnitude as the ones observed for a given peak when the temperature and the concentration are varied.

We also recorded these lifetimes on very short time scales to look for rise-times, especially under laser excitation into the high-energy BR site. No rise-times were observed including in the ${}^5D_0 \longrightarrow {}^7F_0$ emission peak of the possible acceptor sites. Since the spectra clearly showed evidence for such phonon-assisted energy transfers, we conclude that these processes must be very fast (because of electronic noise our lower limit for the

detection of such rise-times is $10\mu s$ for peaks very near the excitation wavelength). Our experiment show that the $100\mu s$ rise-times observed by Buijs *et al.* [4] could not have been due to energy transfers via the 5D_0 levels.

4. Crystal-field parameters:

In the following section we will discuss the size of the Eu(III) site crystal-field parameters for the three distributions. We purposely chose a simple approach to keep a physical sense of these parameters. J-mixing was ignored here because it is known to have a minor effect on the splittings of the Stark-multiplets even if it does affect the barycenters of the levels [9] and the intensities of the peaks [10] to a significant degree. We will concentrate on those parameters that are directly calculated from such splittings and exercise more caution on those that depend on the absolute positions of some of these levels.

Table I lists the positions of the 7F_1 levels from the ground 7F_0 level for the three site distributions in a high concentration sample. Table II shows the theoretical expressions of these energy levels in D_{3h} and C_{2v} symmetries. In table II, the H_{ij} 's represent the matrix elements of the crystal-field Hamiltonian. The equations relating these terms to the B_{kq} crystal-field parameters are listed in reference [9]. The B_{22} parameter which vanishes in D_{3h} symmetry happens to be directly related to the splitting between two of the 7F_1 levels in C_{2v}

symmetry. It is given by:

$$B_{22} = \frac{1}{\alpha_1} H_{-1,1} = \frac{1}{2\alpha_1} \Delta[^7 F_1(E'')]$$
 Eq.1

Where $\Delta[^7F_1(E'')]$ is the splitting corresponding to the lifting of the degeneracy of $|^7F_1(E'')\rangle$ state as the site symmetry is lowered from D_{3h} to C_{2v} . Note that according to the assignment made in the previous paper [5], the relevant levels are at the following positions: 224.7 and 389.5 cm⁻¹ for the intermediate site (site 2 in table I), and 222.6 and 531.0 cm⁻¹ for the mO site (site 3 in the same table).

This expression yields values of 0, \pm 412 and \pm 771 cm⁻¹, respectively for the BR site, the intermediate site and the mO site. Wherever comparisons are possible these results are in good agreement with the ones reported by Y.Salem *et al.* [11]. It is interesting to note that the B₂₂ for the intermediate site is approximately 50% smaller than the one for the mO site. Since it is reasonable to assume a gradual variation of this parameter with the distance from the BR position. These calculations suggest that the intermediate site is in mid-position between the mO site and the BR site.

At this point, let us consider the lifting of the degeneracies of the 7F_2 multiplet as me move from D_{3h} symmetry to C_{2v} symmetry. The first question we would like to address is whether a large splitting of the ${}^7F_1(E'')$ level as we move from D_{3h} to C_{2v} can be compatible with a small splitting of the ${}^7F_2(E'')$ level. The latter is given by:

2 (3 $\alpha_2^{}$ B₂₂ - 12 $\beta_2^{}$ B₄₂) Eq. 2

if such a splitting is assumed to be very small (zero for all practical purposes) the ratio between the two parameters of involved is 0.825. Since B_{42} is zero in D_{3h} and becomes non-zero as we move towards C_{2v} symmetry, we expect this parameter to behave the same way as B_{22} . We therefore conclude that a large splitting of the $^7F_1(E'')$ level is indeed compatible with a very small splitting of the $^7F_2(E'')$ level. The situation for the lifting of the degeneracy of $^7F_2(E')$ level is very different. Indeed, since this state corresponds to values of M_J of ± 2 in D_{3h} symmetry (in Russell-Saunders treatment), it is coupled to the $^7F_2(A_1)$ state as the degeneracy is lifted. There 3! possible assignments of the 3 new states that are obtained after diagonalization of the corresponding 3 x 3 matrix. These last points explain why we had more difficulty interpreting the polarization results in the 7F_2 region [5].

Acknowledgments

We would like to thank Professors A.M. Lejus and D. Vivien, E.N.S.C.P, Paris, for making these samples available to us. This work was supported by grants from the Natural Sciences and Engineering Research Council of Canada. The first author acknowledges the support of the Centre National de la Recherche Scientifique. We also acknowledge Y. Guyot for technical assistance and Professors G. Boulon and B. Jacquier for helpful discussions.

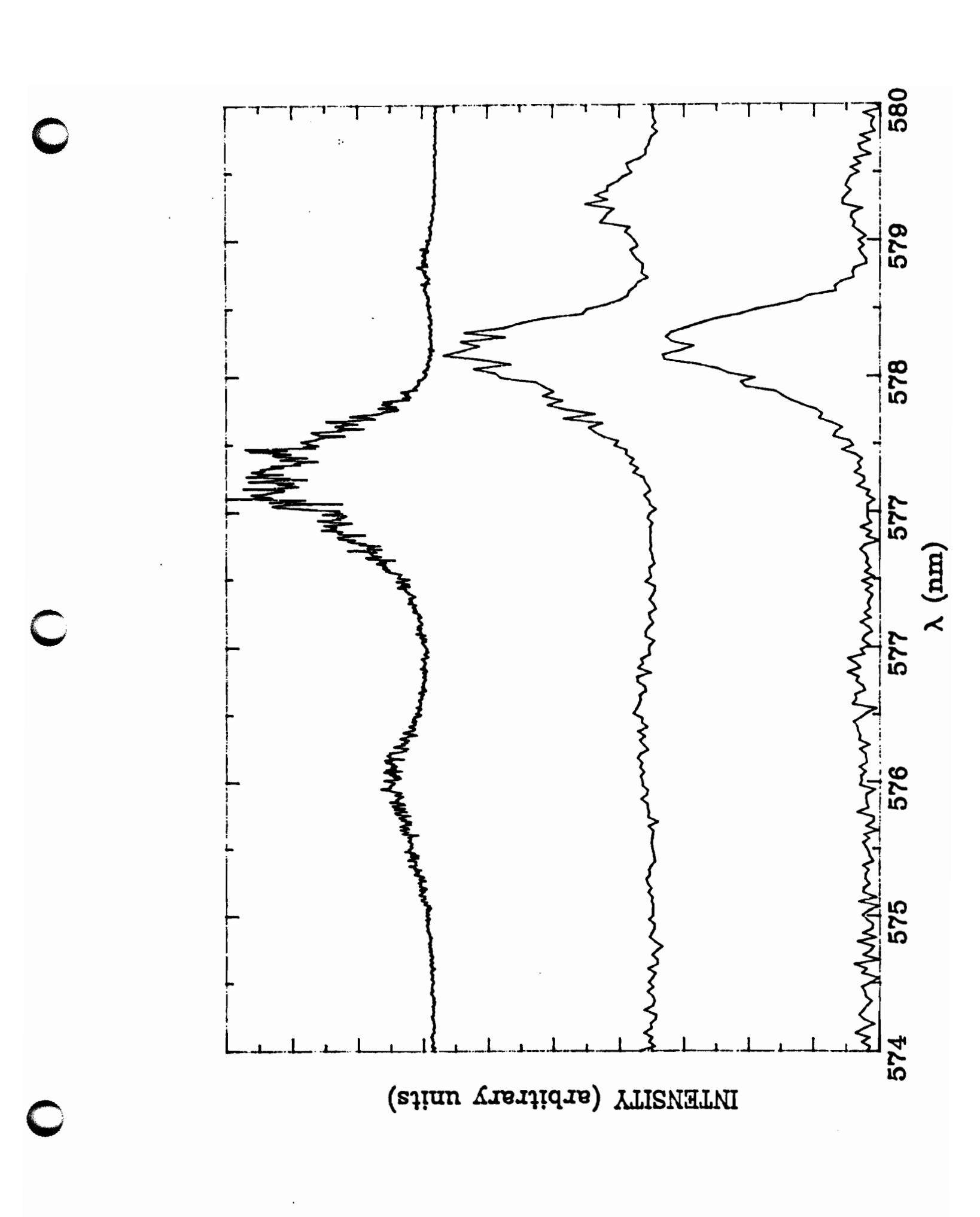
Figure captions

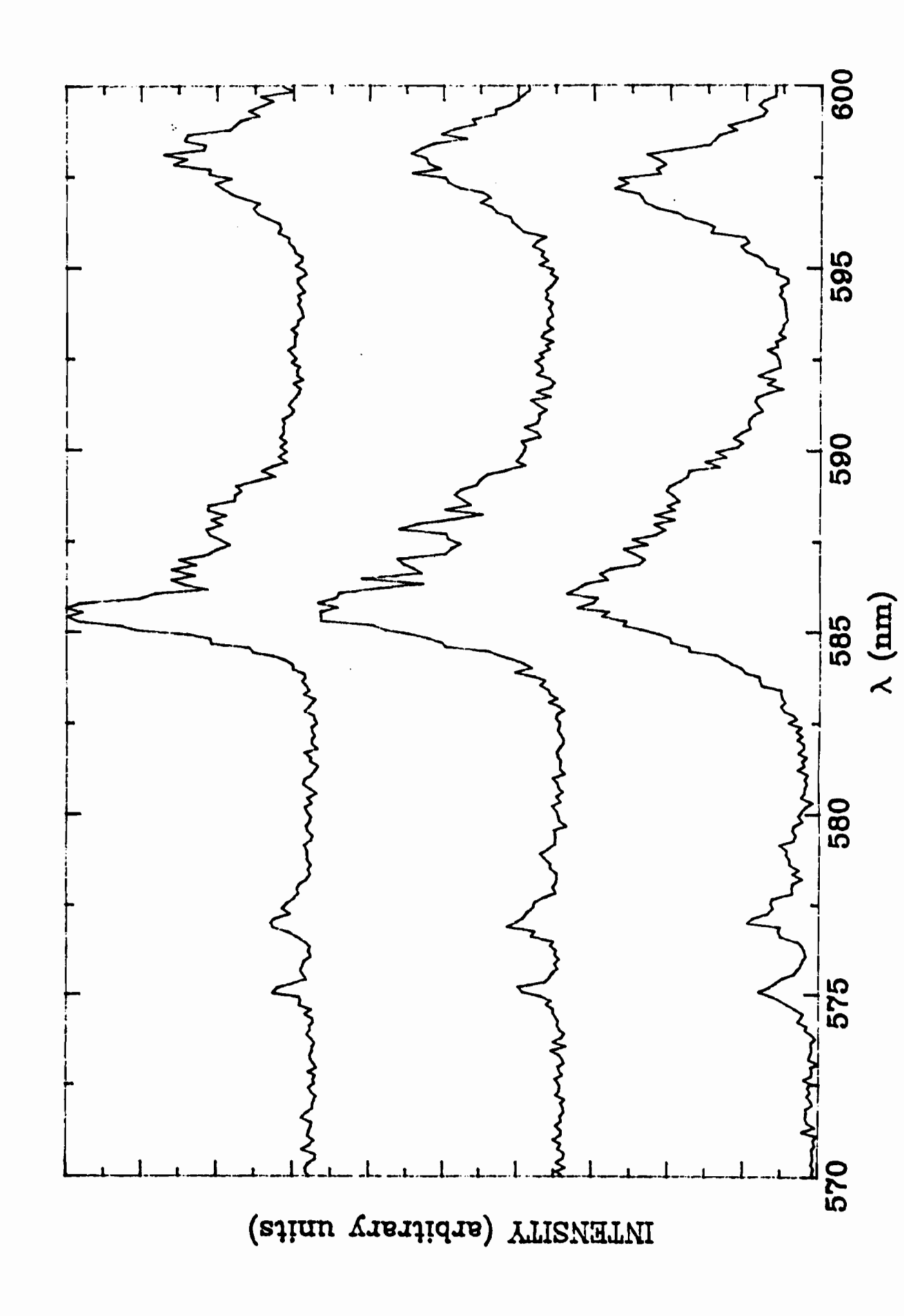
Fig. 1: Excitation spectra at T= 10K in $La_{1-x}Eu_xMgAl_{11}O_{19}$. Emission monitored at λ = 611.5 nm. Top to bottom x=0.1, 0.01, <0.01.

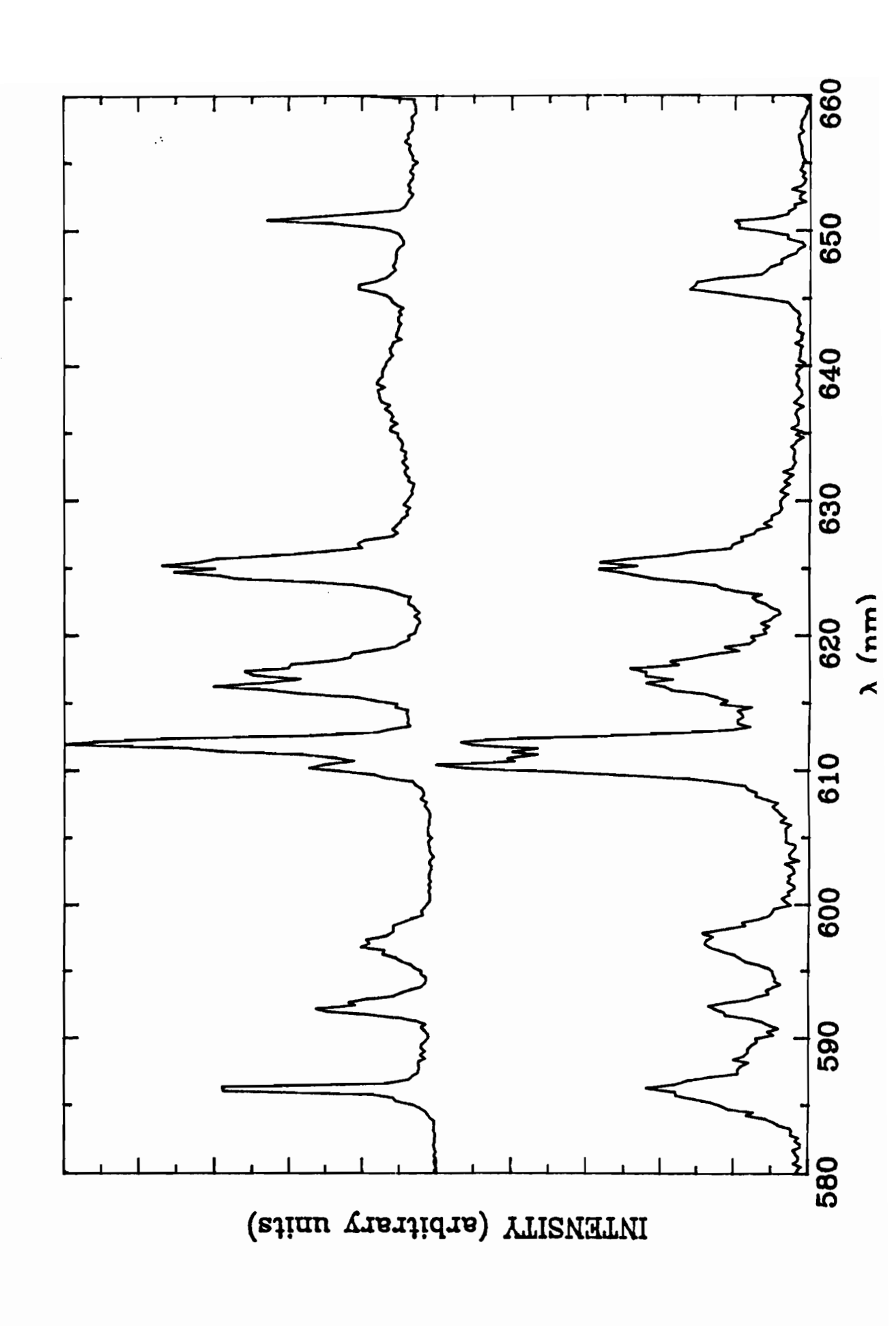
Fig. 2: Eu(III) ${}^5D_0 \longrightarrow {}^7F_{0,1}$ luminescence in La_{1-x}Eu_xMgAl₁₁O₁₉ (x=0.1). Top to bottom T = 10K, 70K, 300K. 7F_0 region 570-580 nm, 7F_1 region: 580-600 nm. $\lambda_{\rm exc}$ = 575.4 nm

Fig. 3: Eu(III) $^5D_0 \longrightarrow ^7F_{1,2,3}$ luminescence in La_{1-x}Eu_xMgAl₁₁O₁₉. x=0.1. Top to bottom 10K and 300K. $\lambda_{\rm exc}$ = 579.2 nm.

Fig. 4: Eu(III) $^5D_0 \longrightarrow ^7F_{1,2,3}$ luminescence in La_{1-x}Eu_xMgAl₁₁O₁₉, x=0.01 at 300K. $\lambda_{exc} = 578.2$ nm.







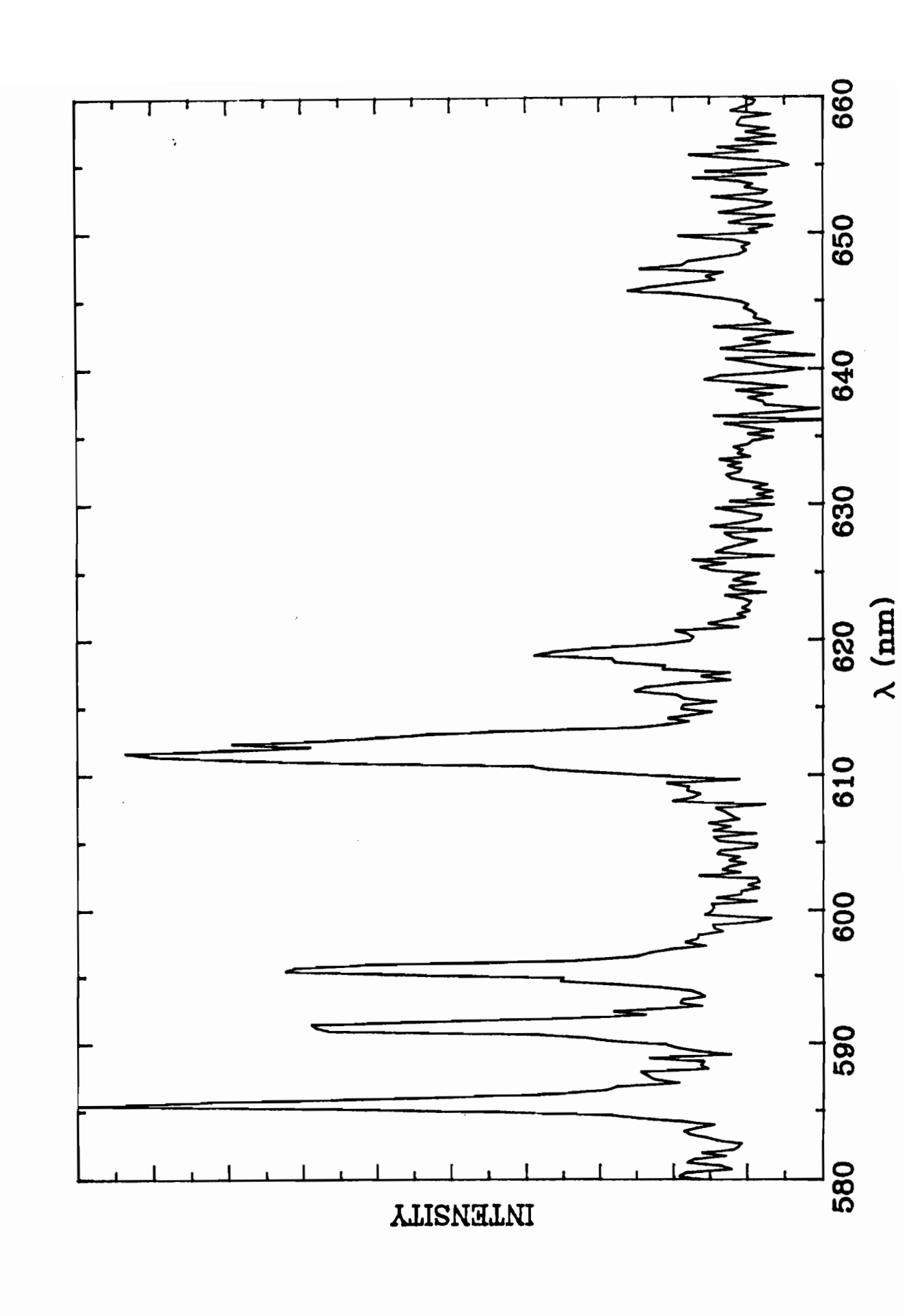


Table I: Positions of the ${}^{7}F_{1}$ levels from the ground state ${}^{7}F_{0}$, for each site.

site 1	site 2	site 3	
$\lambda_{\rm exc} = 575.4 \text{ nm}$	$\lambda_{\rm exc}$ = 577.8 nm	$\lambda_{\rm exc}$ = 579.2 nm	
(cm ⁻¹)	(cm ⁻¹)	(cm ⁻¹)	
306.4	224.7	222.6	
650.0	389.5	398.0	
652.0	539.9	531.0	

Table II: $^7{\rm F_1}$ energy levels in ${\rm D_{3h}}$ and ${\rm C_{2v}}$ symmetries in terms of the crystal field matrix elements.

D _{3h}		C _{2v}	
State 7F ₁ (A' ₂)	Energy H ₀₀	State ⁷ F ₁ (B ₂) or (A ₂)	Energy H _{oo}
⁷ F ₁ (E")	Н ₁₁	⁷ F ₁ (A ₂) or (B ₂) [*] ⁷ F ₁ (B ₁)	H ₁₁ ± H _{1,-1}

:for intermediate site whose main axis z is parallel to c.

References

- [1]. D. Vivien, A-M. Lejus, J. Théry, R. Collongues, J.J. Aubert, R. Moncorgé and F. Auzel, Proceedings of the French Academy of Sciences, 298, 195 (1984).
- [2]. M.M. Nafi, M. Laberge and D.J. Simkin, J. Lumin. 50, 339 (1992).
- [3]. D. Saber, J. Dexpert-Ghys, P. Caro, A-M. Lejus and D. Vivien, J. Chem. Phys. 82, 5648 (1992).
- [4]. M. Buijs and G. Blasse, J. Solid State Chem. 71, 296 (1987).
- [5]. M.M. Nafi, D.J. Simkin and R. Moncorgé, J. Lumin., accepted for publication (1992).
 - [6]. M. Mitsunaga, R. Yano and N. Uesugi, Opt. Lett. 16(23), 1890 (1991).
 - [7]. J.P van Der Ziel and G. van Uittert, Phys. Rev. 180(2), 343 (1969).
- [8]. L.V. Haley, B. Jacquier and A. Köningstein, Can. J. Chem. **59**(16), 2441 (1981).
- [9]. A. Lempicki, H. Samelson and C. Brecher, J. Mol. Spectr., 27, 375 (1968).
- [10]. P. Porcher and P. Caro, J. Lumin., 21, 207 (1980).
- [12]. Y. Salem, C. Linares, B. Jacquier, M.C. Saine, M. Gasperin, A-M Lejus and D. Vivien, J. Chem. Phys. 93, 7076 (1990).

CONCLUSIONS

This work showed that Eu(III) in La_{1-x}Eu_xMgAl₁₁O₁₉ occupies three different distributions of sites. The first one corresponds to the Beevers-Ross crystallographic position (of symmetry D_{3h}). The corresponding ${}^5D_0 \leftarrow {}^7F_0$ transition is found ca. 575 nm. As expected for D_{3h} site symmetry, the luminescence spectrum obtained under laser excitation into this non-degenerate transition shows the following characteristics:

- (i) the forbidden ⁵D₀→⁷F₀ luminescence is very weak,
- (ii) there are only two components in the ${}^5D_0 \longrightarrow {}^7F_1$ region,
- (iii) the weakest peak in the ${}^5D_0 \longrightarrow {}^7F_1$ region which is attributed to the magnetic dipole non-degenerate ${}^5D_0(A_1') \longrightarrow {}^7F_1(E'')$ transition displays the right polarization.

The ${}^5D_0 \leftarrow {}^7F_0$ transition ca. 578 nm is attributed to europium ions located on positions on or very near the mid-oxygen (mO) crystallographic site of symmetry C_{2v} with a principal axis perpendicular to the main crystallographic axis c. This site shows all the characteristic of a C_{2v} or very near C_{2v} symmetry. Furthermore, its luminescence peaks in the ${}^5D_0 \longrightarrow {}^7F_1$ region are easily and unambiguously correlated to the luminescence peaks of the BR site.

The third site distribution displays characteristics which are intermediate between those of the two other distributions. Crystal-field calculations performed on the luminescence data suggest that the "intermediate energy site distribution" is located midway between the two other distributions.

Eu(III) is forced into the Beevers-Ross position as its concentration in the LMA matrix is increased. The position of the maximum of the $^5D_0 \leftarrow ^7F_0$ absorption depends on the concentration of europium. As the latter is

increased, this band shifts to higher energies, for the three site distributions.

There is some evidence of occurrence occurrence of energy transfer processes from the high energy site distribution downwards to the two other distributions. The line width of the luminescence lines do not increase considerably as the temperature is increased, even for the most concentrated samples. For the samples with the lowest concentrations (1% or less) these line widths are very narrow at room-temperature and site selection remains possible up to this temperature. Finally a broad peak ca. is the only luminescence peak with a very short lifetime, it is suggested that it might be due to Cr(III)-Eu(III) ion pair interaction. This peak disappears as the temperature is increased and is most prominent in the samples with the highest Eu content.

1. Contribution to knowledge:

- (a) This work is the first to show evidence for the existence of Eu(III) in or very near the BR crystallographic site.
- (b) It presents the first results of the polarization of Eu(III) laser-induced luminescence in spinel-stacked materials.
- (c) It shows for the first time that such studies can be used in these systems to determine the orientation of the principal axis with respect to the main crystallographic axis c.
- (d) To our knowledge, it is the first example where the correlation between the levels of the least distorted site and those of more distorted sites is established by a polarization study of site-selected luminescence and

not inferred from either crystal-field parameters fitting or any other procedure.

- (e) It gives the first completely rationalized assignments of the ${}^5D_0 \longrightarrow {}^7F_{0,1}$ luminescence and explains that there are inherent theoretical limitations to the ${}^5D_0 \longrightarrow {}^7F_2$ luminescence.
- (f) It proposes an explanation to the variation of the ratio of intensities of the Eu(III) luminescence.

2. Suggestions for further work:

- (a) We believe this fairly well characterized system would be ideal to test the pseudo-multi polar theory of oscillator strength for the ${}^5D_0 \longrightarrow {}^7F_J$ transitions. To be more specific, the determination of the phenomenological $B_{\lambda kq}$ which account for the intensity of the ${}^5D_0 \longrightarrow {}^7F_0$ transition should allow us to answer some fundamental questions concerning the sensitivity of this transition to the local environment of europium.
- (b) The measurement of the temperature dependence of the inhomogeneous line width would provide us with results which could be used to test some recent theoretical models in this "well-behaved" system.
- (c) An Al NMR study (both chemical shifts and relaxation times) might reveal more structural information concerning this system. (*).
- (d) LMA can be used as a structural proto-type for the related β alumina and β "-alumina systems. A comparative study of these materials should be carried out in this perspective. The results presented in this work might help us understand some of the complicated features of the spectroscopic data on (*) We thank Professor D. Gilson for suggesting this work.

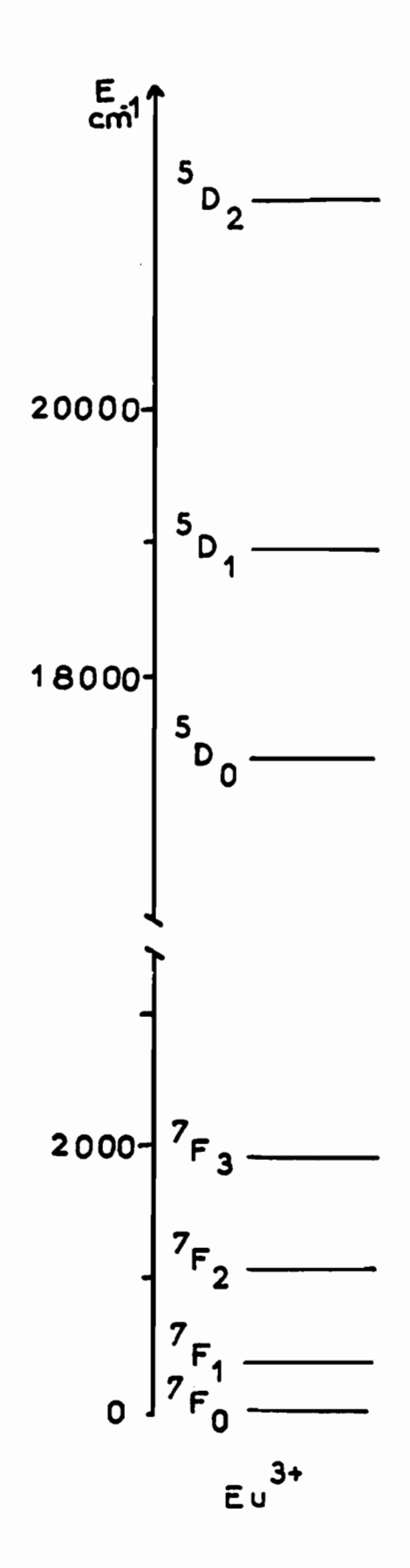
these related systems.

- (e) More work needs to be done to characterize the luminescence attributed to ion pairs. For instance, laser-induced luminescence into regions where only Cr(III) absorbs should be recorded and studied. We recall that the corresponding peaks in our spectra display definite polarization properties. If a reasonable assumption can be made on the nature of these transitions (electrical or magnetic dipole) we might be able to relate these peaks to Cr(III) located on specific sites.
- (f) An extensive theoretical study of the lifetimes should be carried out.

APPENDIX I

Energy level diagramme of the free Eu⁺³ ion.

When Eu(III) is put in a site of a given symmetry, the $|^7F_J\rangle$ degenerate levels split according to the rules described in the second manuscript. It is important to point out that the 5D_0 and the 7F_0 levels do not split under any symmetry. This means that the number of peaks in the $^5D_0 \longrightarrow ^7F_0$ region are directly related to the number of "emitting sites".



APPENDIX II

Comparison between the ${}^5D_0 \longrightarrow {}^7F_{1,2,3}$ luminescence from the three site dirtibutions at 200K and 70K

Wavelength axis scale in Angströms, Intensity axis scale in counts

Fig. 1: High energy site:

 $\lambda_{\rm exc} = 575.4$ nm, T=200K.

Fig. 2: High energy site:

 λ_{exc} = 575.4 nm, T=70K.

Fig. 3: Intermediate energy site: $\lambda_{\text{exc}} = 577.8$ nm, T=200K.

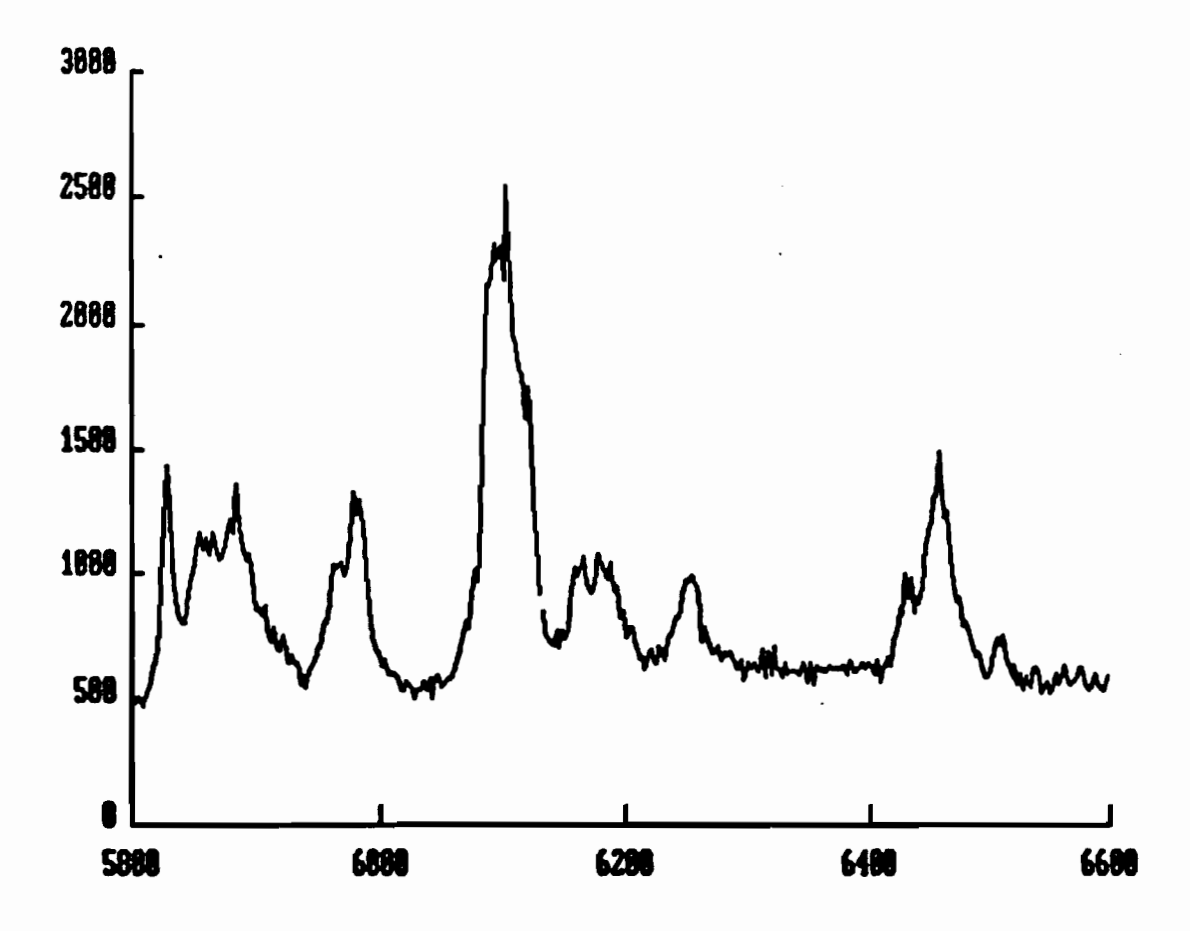
Fig. 4: Intermediate energy site: $\lambda_{\text{exc}} = 577.8 \text{ nm}$, T=70K.

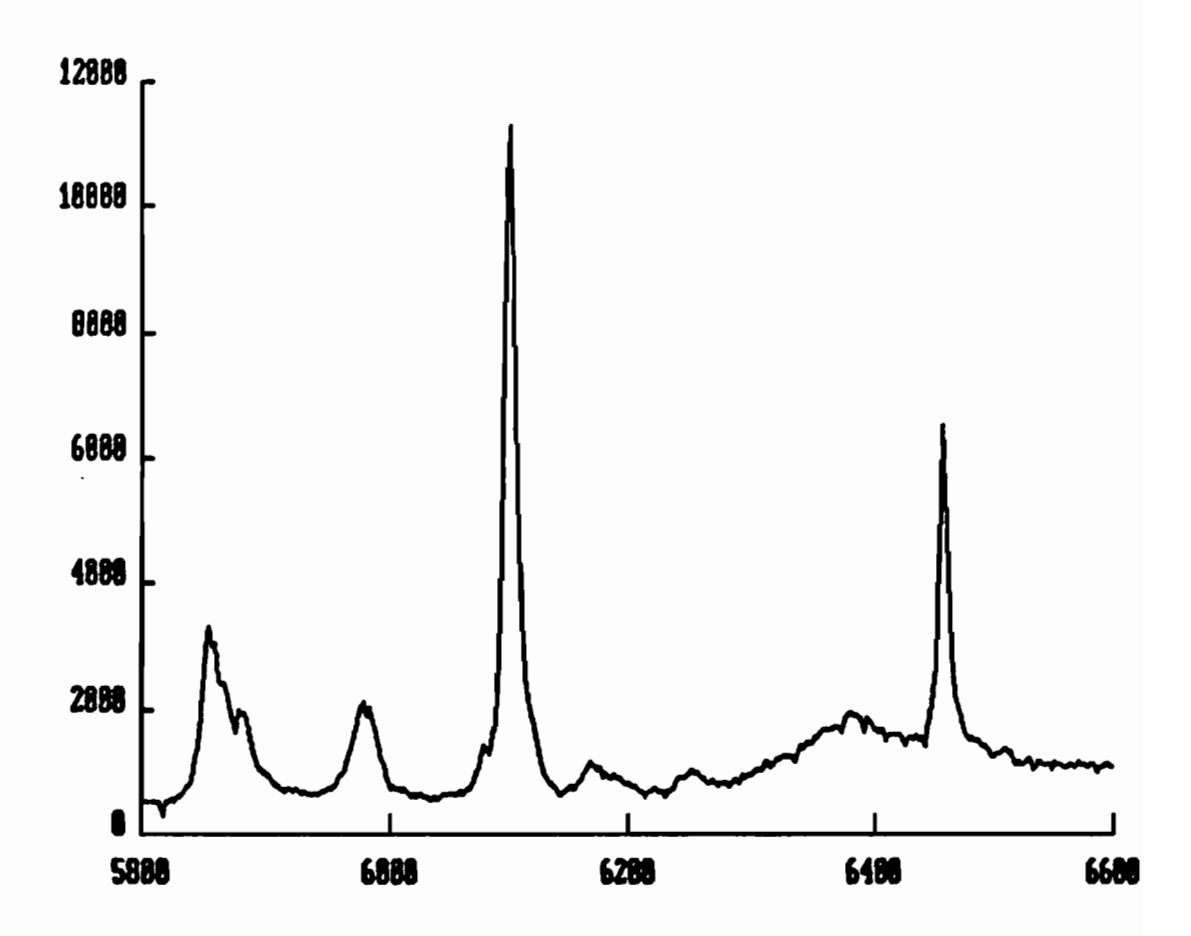
Fig. 5: Low energy site:

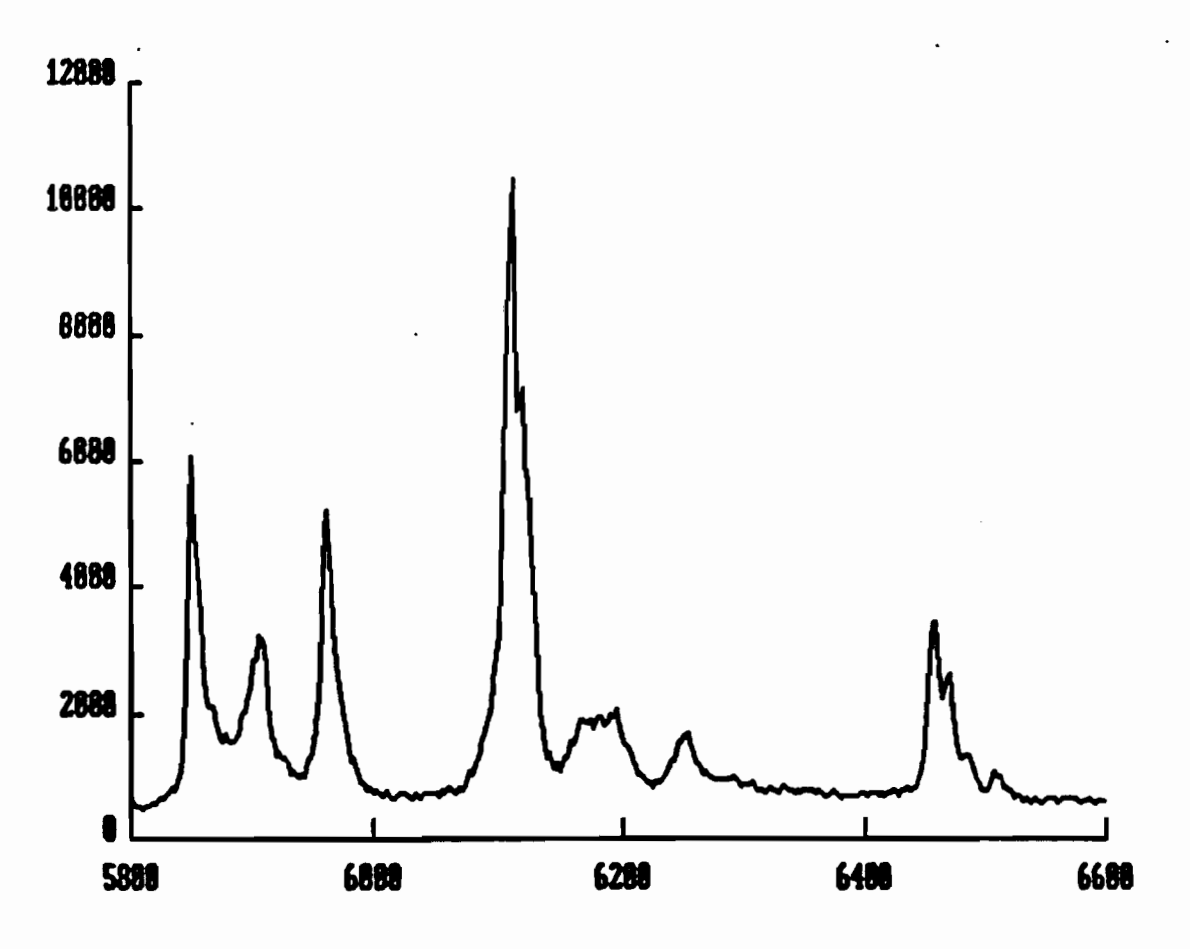
 $\lambda_{\rm exc}$ = 579.2 nm, T=200K.

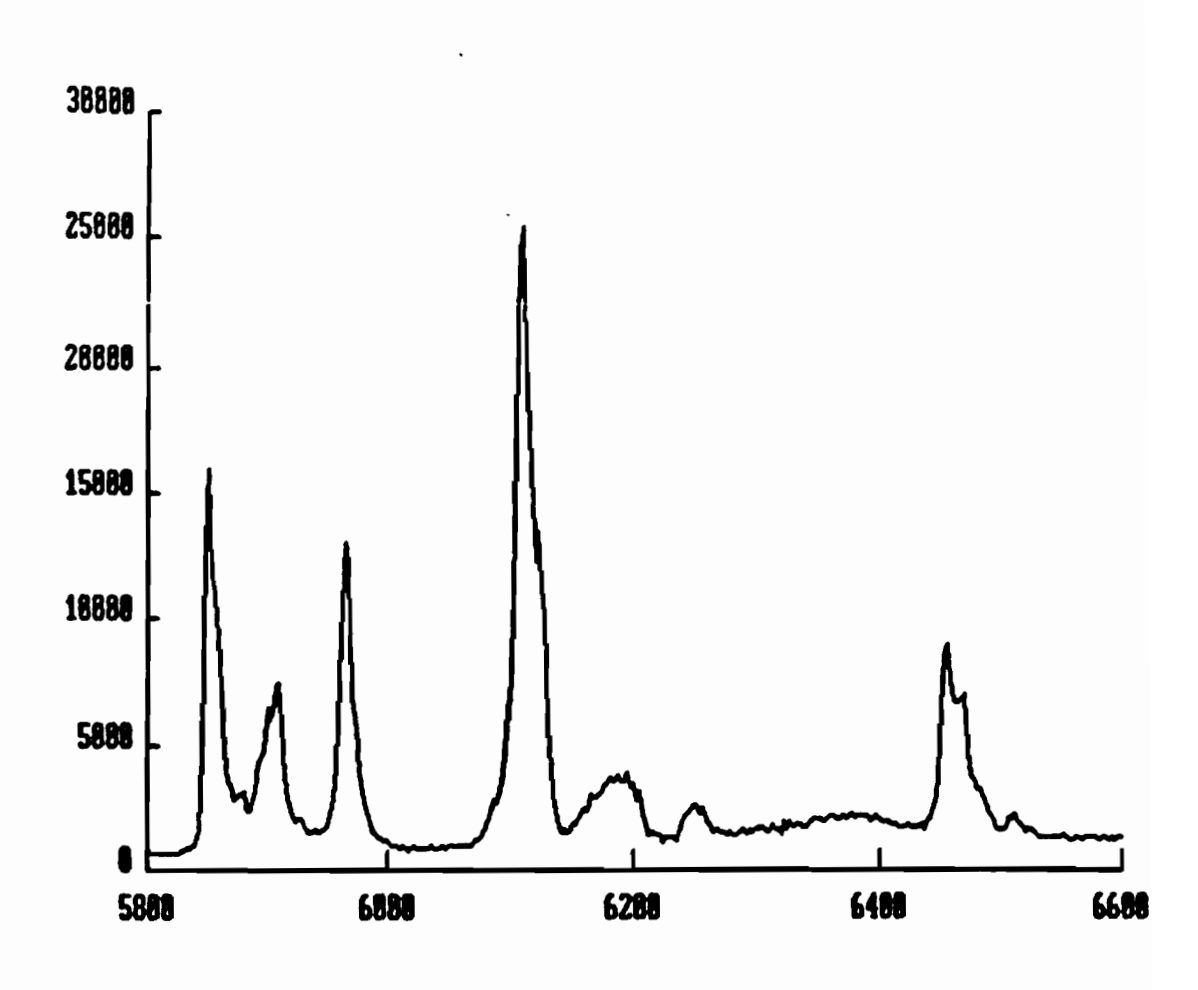
Fig. 6: Low energy site:

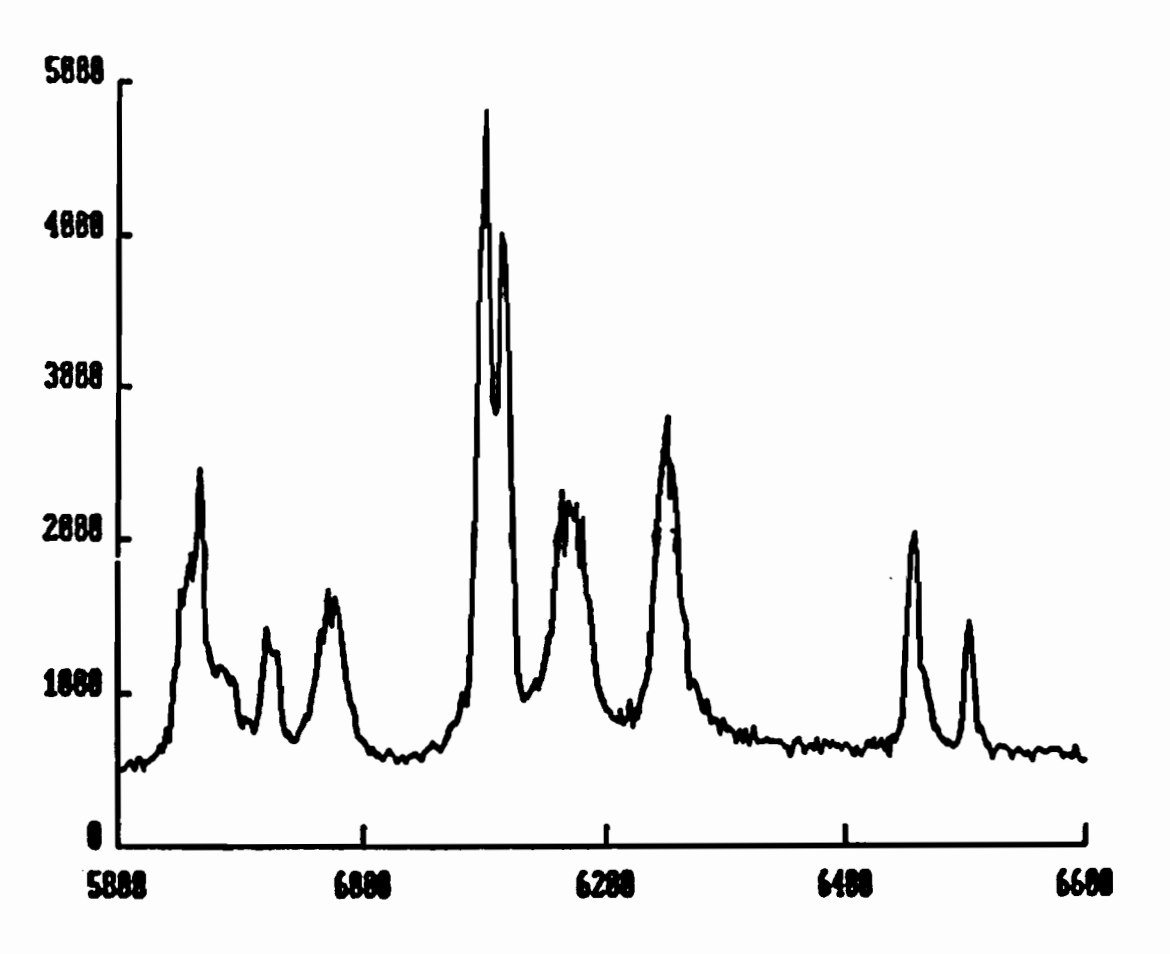
 $\lambda_{\rm exc}$ = 579.2 nm, T=70K.

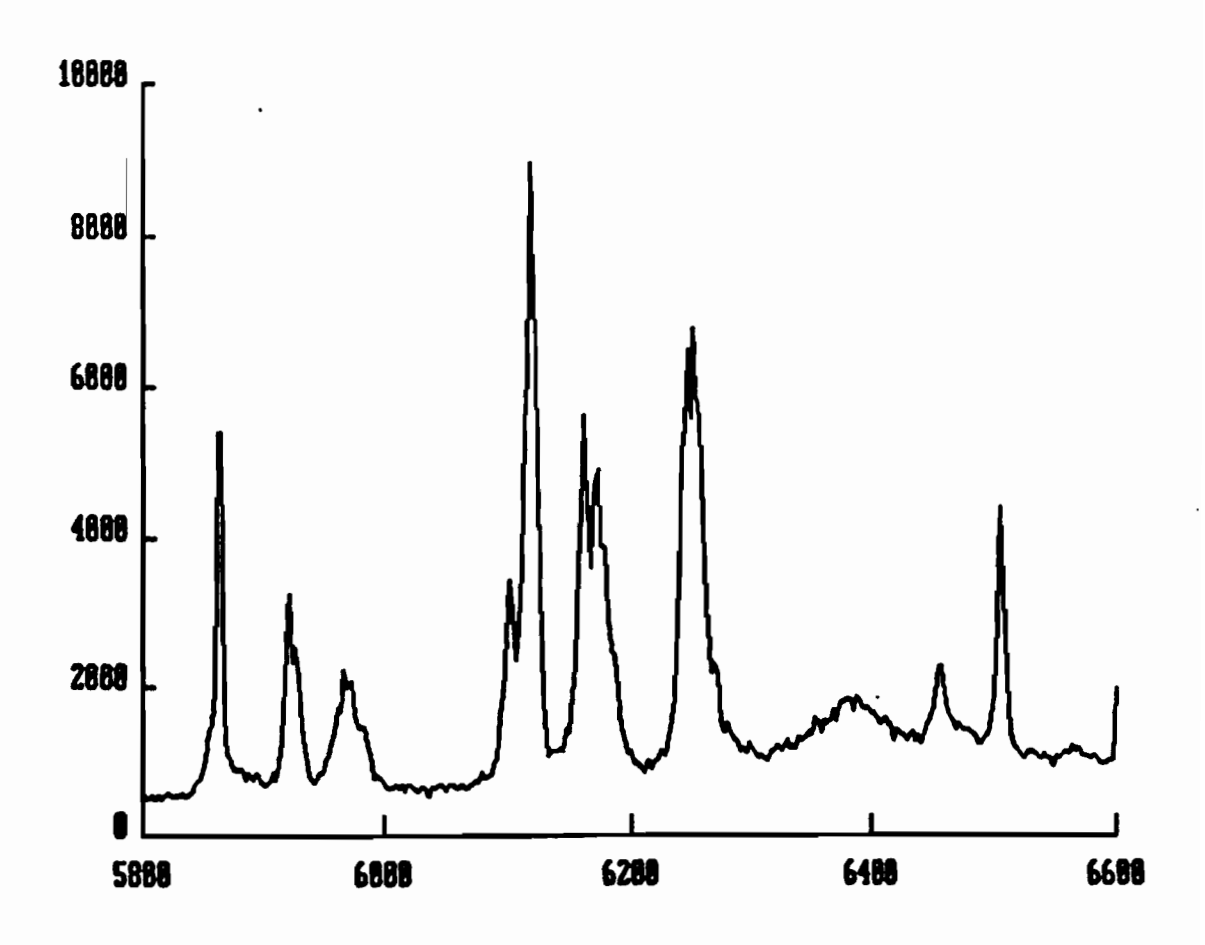










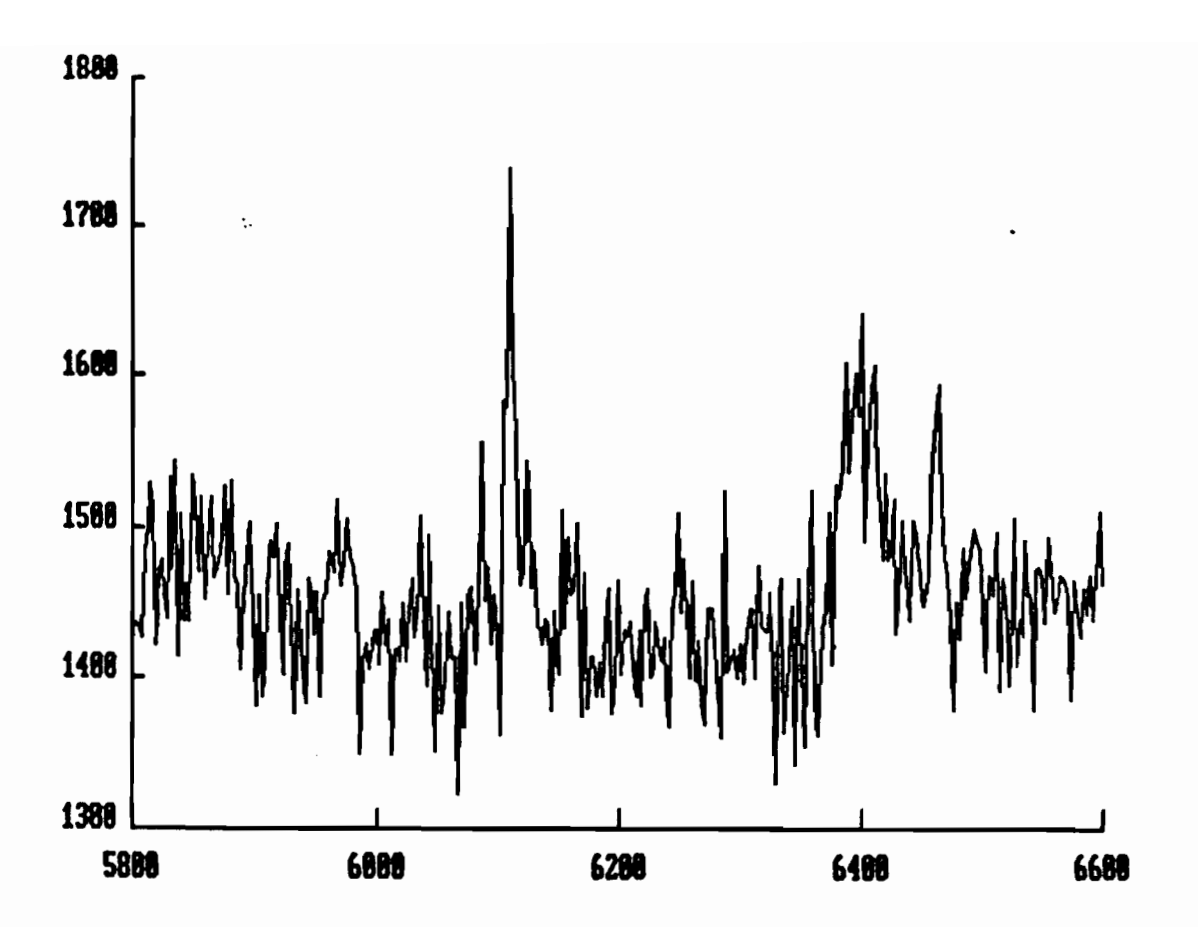


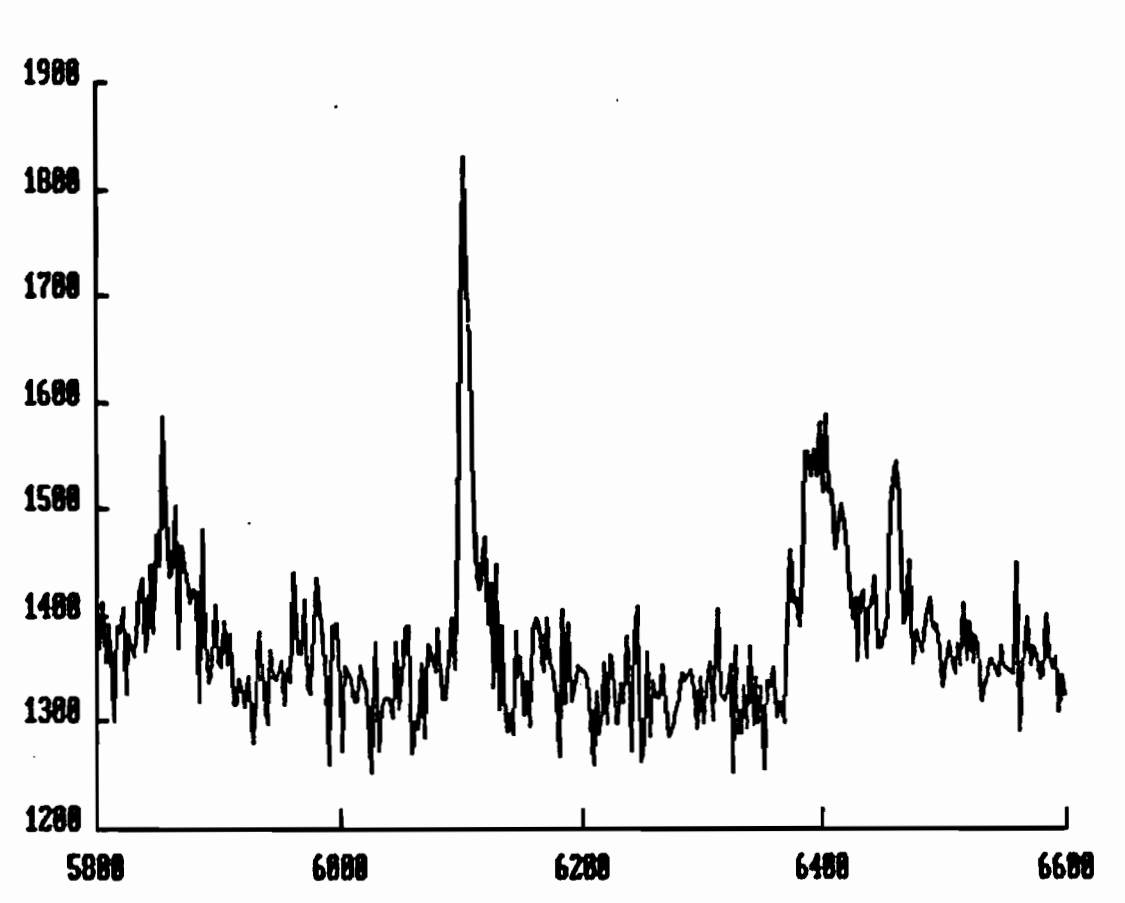
5 .

Wavelength axis scale in Angström, Intensity scale in counts.

Top spectrum: $\lambda_{\text{exc}} = 575.0 \text{ nm}$

Bottom spectrum: $\lambda_{\text{exc}} = 576.0 \text{ nm}$





APPENDIX IV

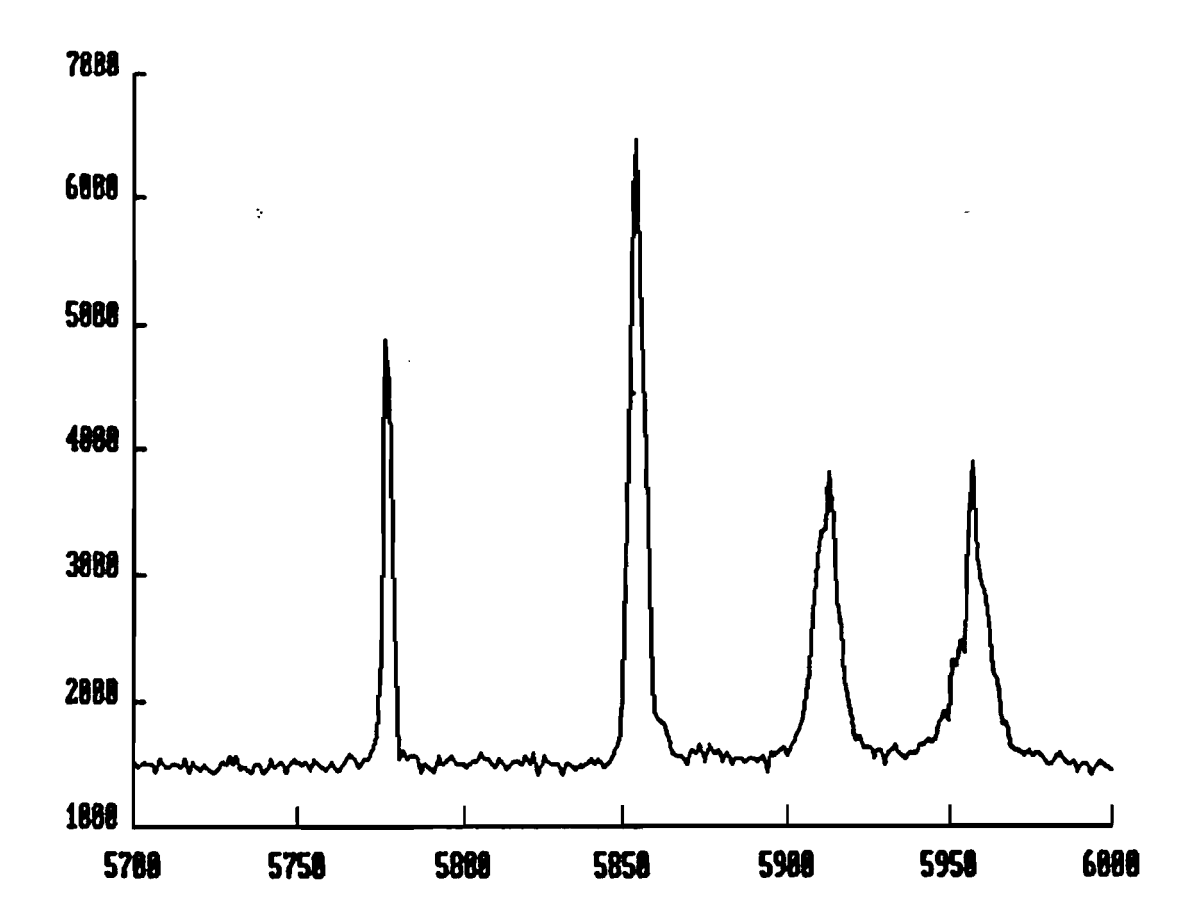
 $^5D_0 \longrightarrow ^7F_{0,1}$ (top spectra) and $^5D_0 \longrightarrow ^7F_{1,2,3}$ (bottom spectra) Eu(III) luminescence from intermediate and low energy sites at 10K and 300K.

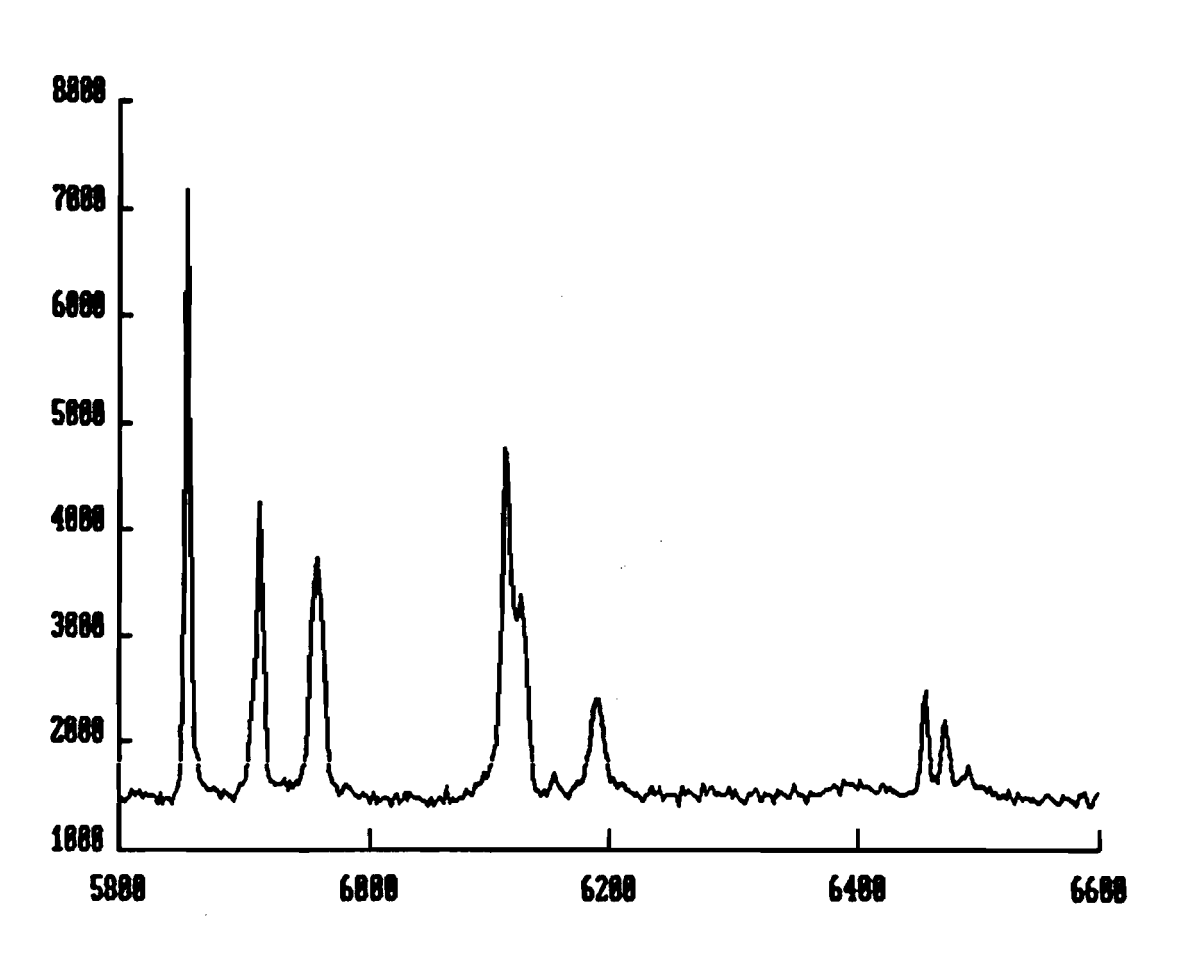
Fig. 1:
$$\lambda_{exc} = 578.4$$
 nm, T=10K

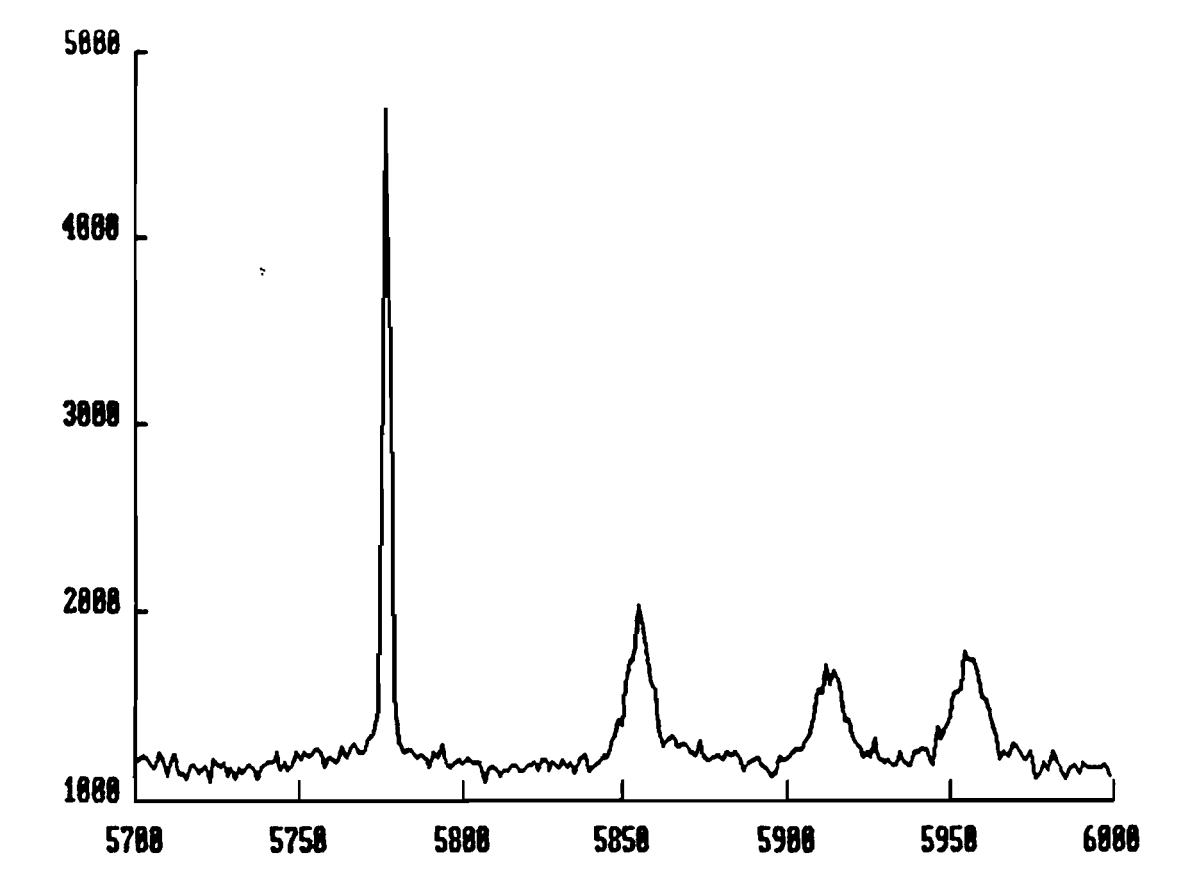
Fig. 2:
$$\lambda_{\rm exc}$$
 = 578.4 nm, T=300K

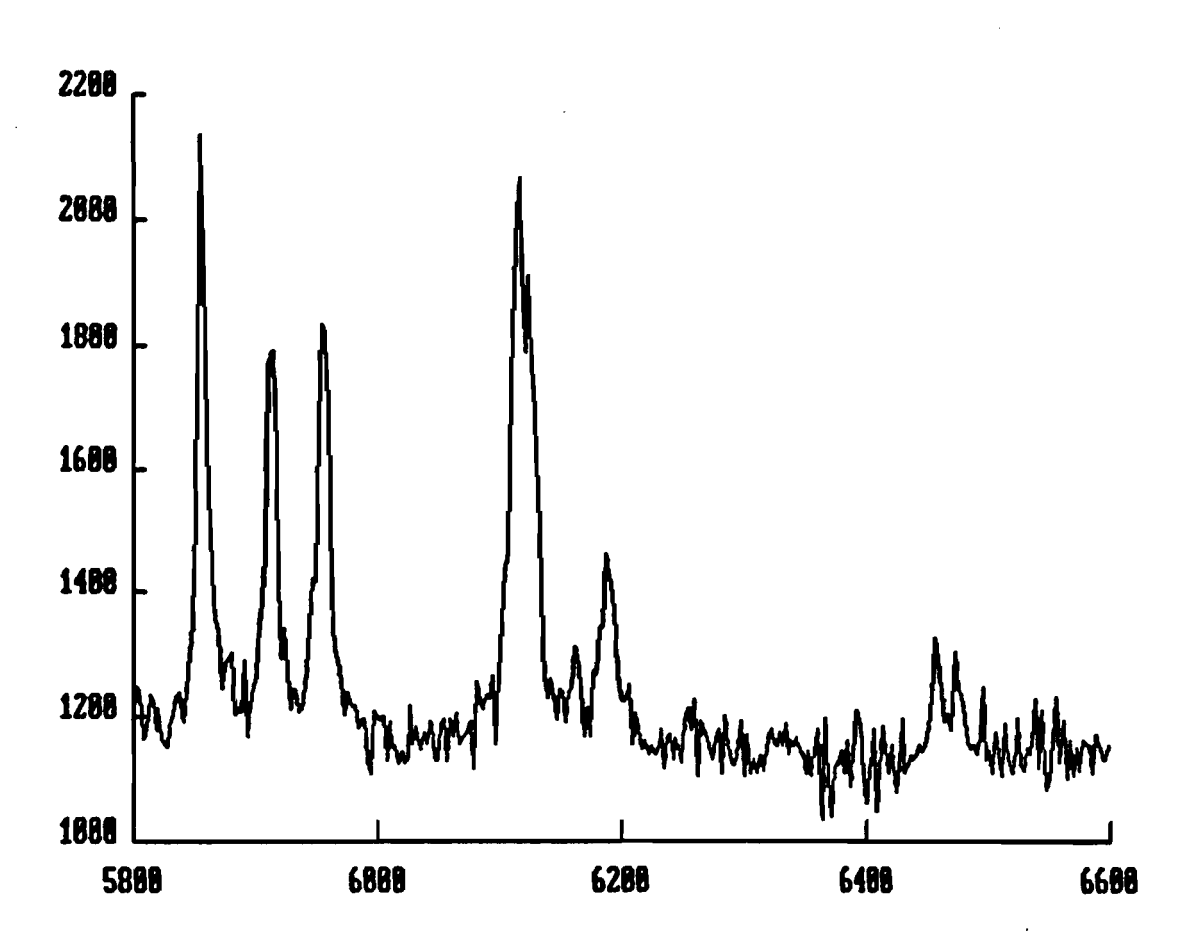
Fig. 3:
$$\lambda_{exc} = 579.4$$
 nm, T=10K

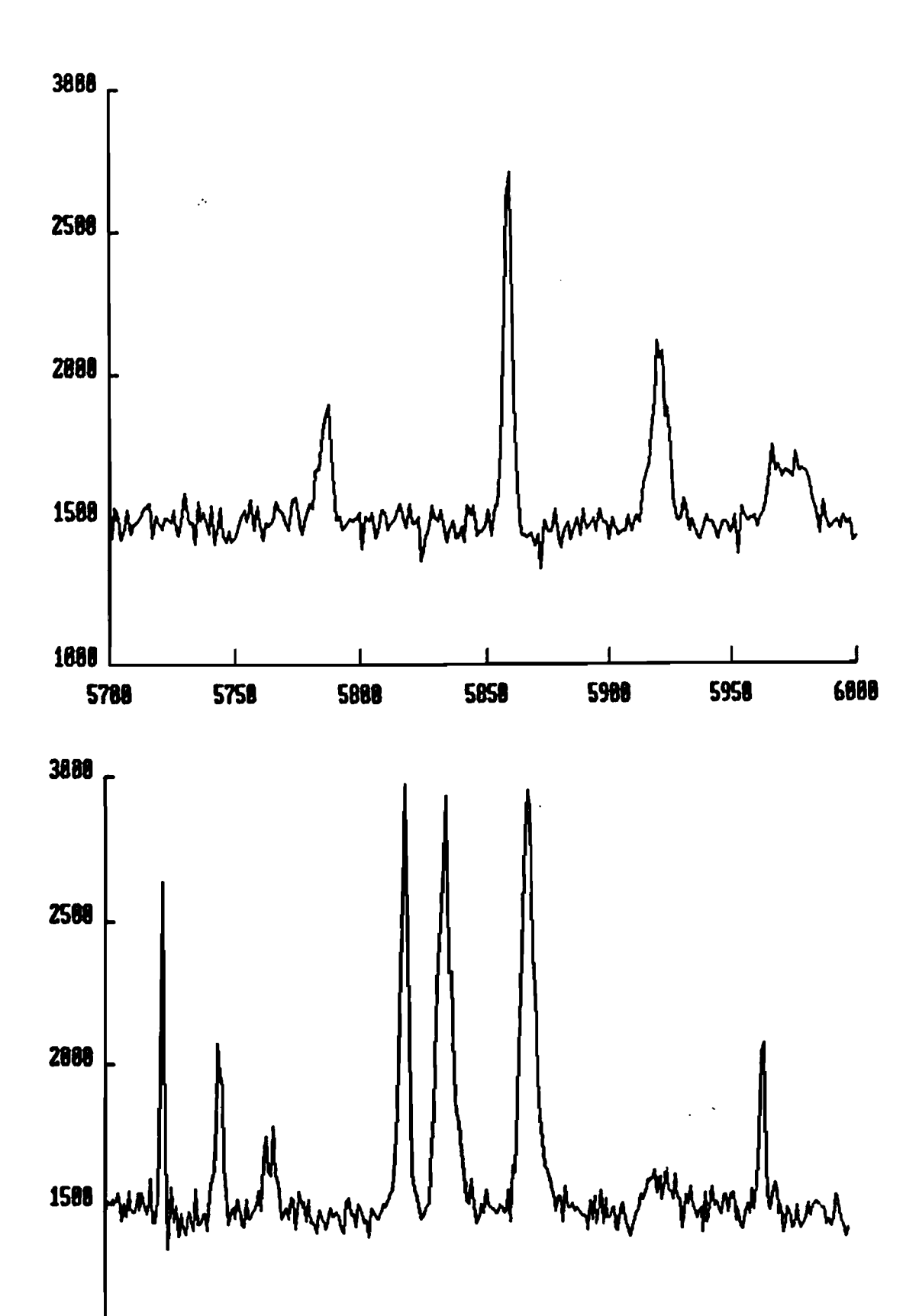
Fig. 4:
$$\lambda_{\text{exc}} = 579.4 \text{ nm}, T=300K$$



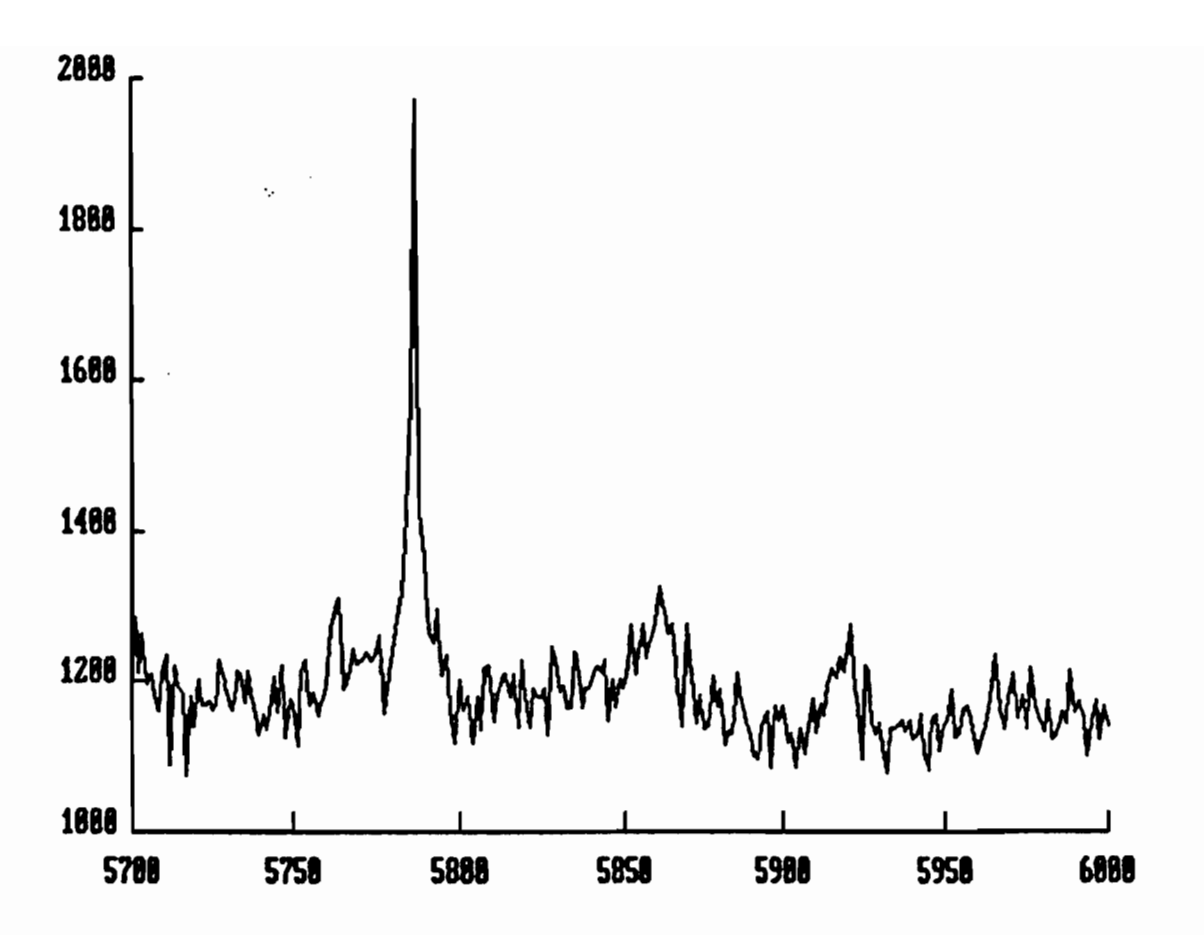


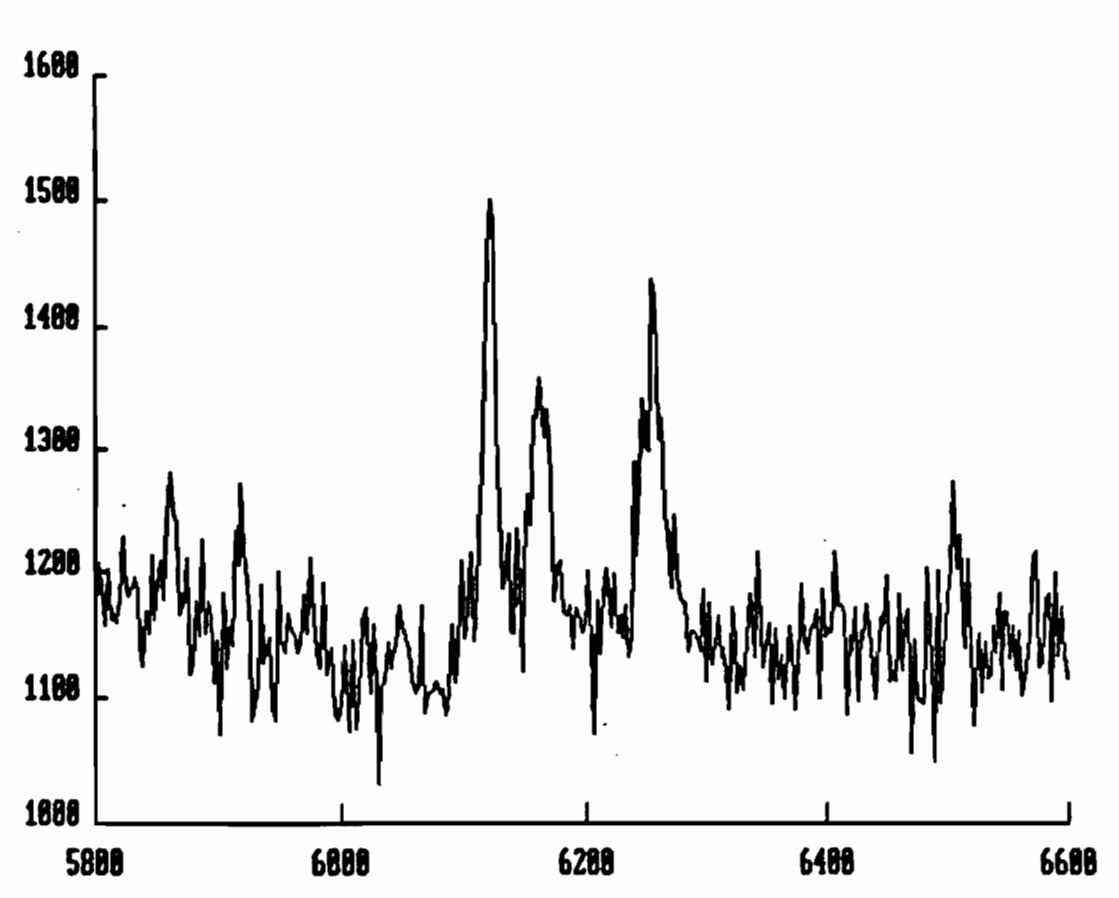






88

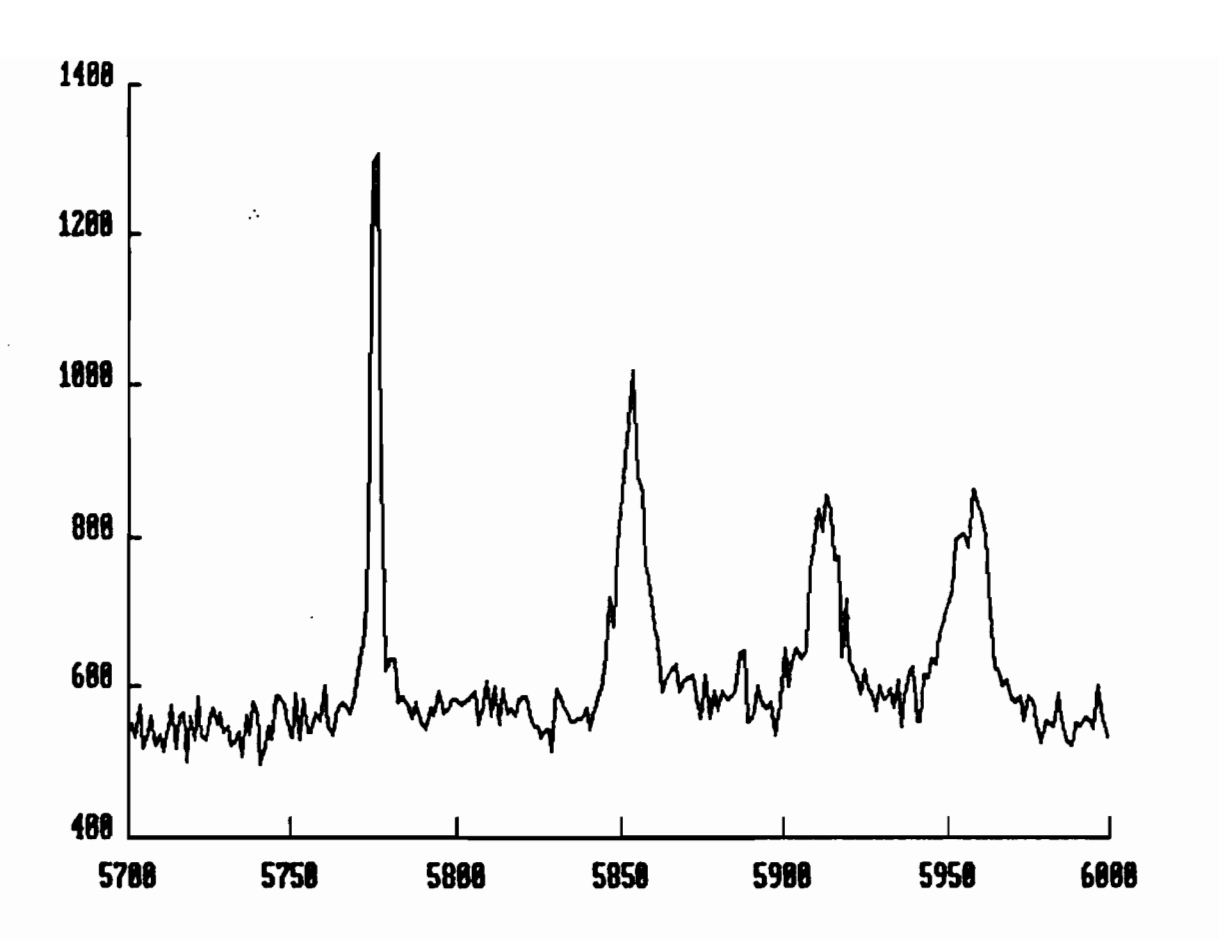


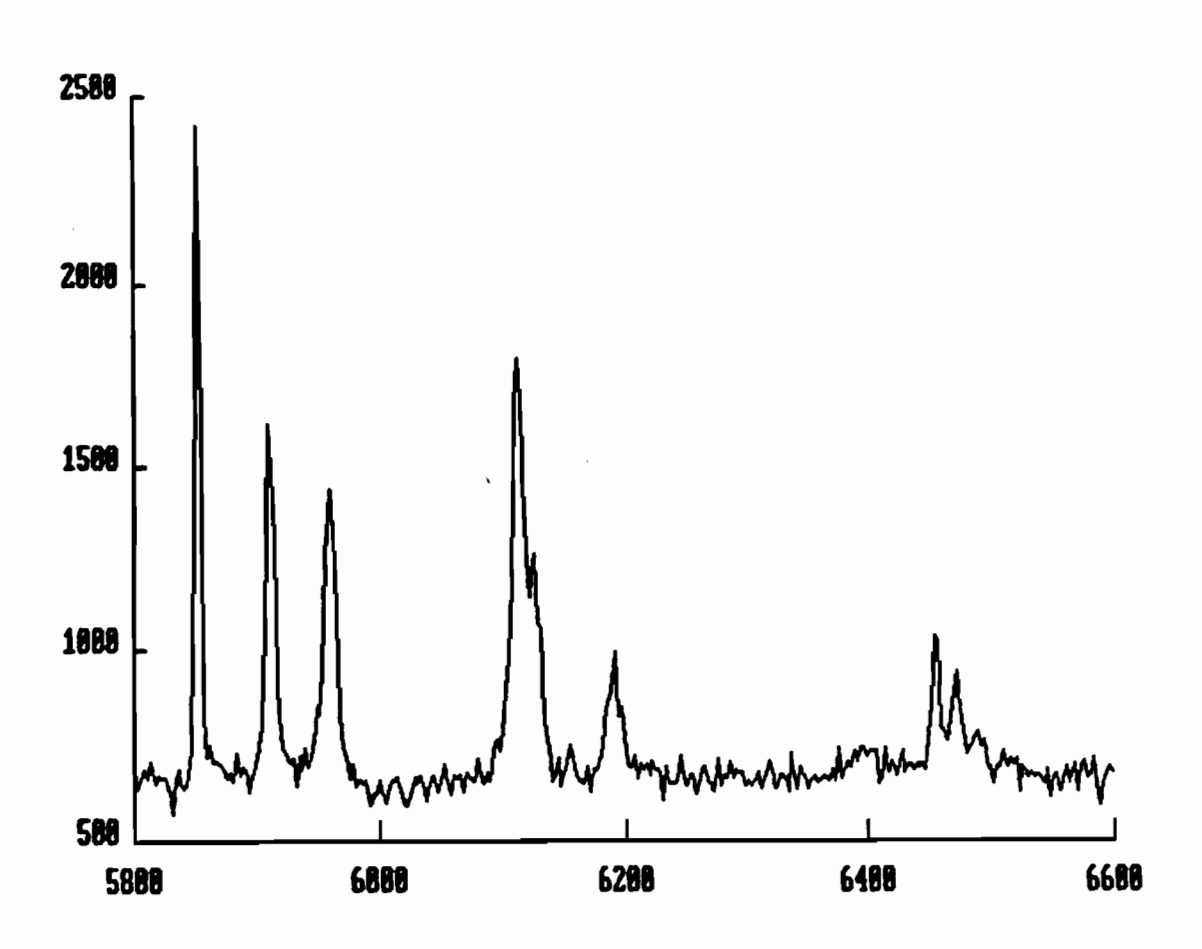


APPENDIX V

 $^5D_0 \longrightarrow ^7F_{0,1}$ (top spectrum) and $^5D_0 \longrightarrow ^7F_{1,2,3}$ (bottom spectrum) Eu(III) luminescence from the intermediate energy site.

$$\lambda_{exc} = 578.4 \text{ nm}$$





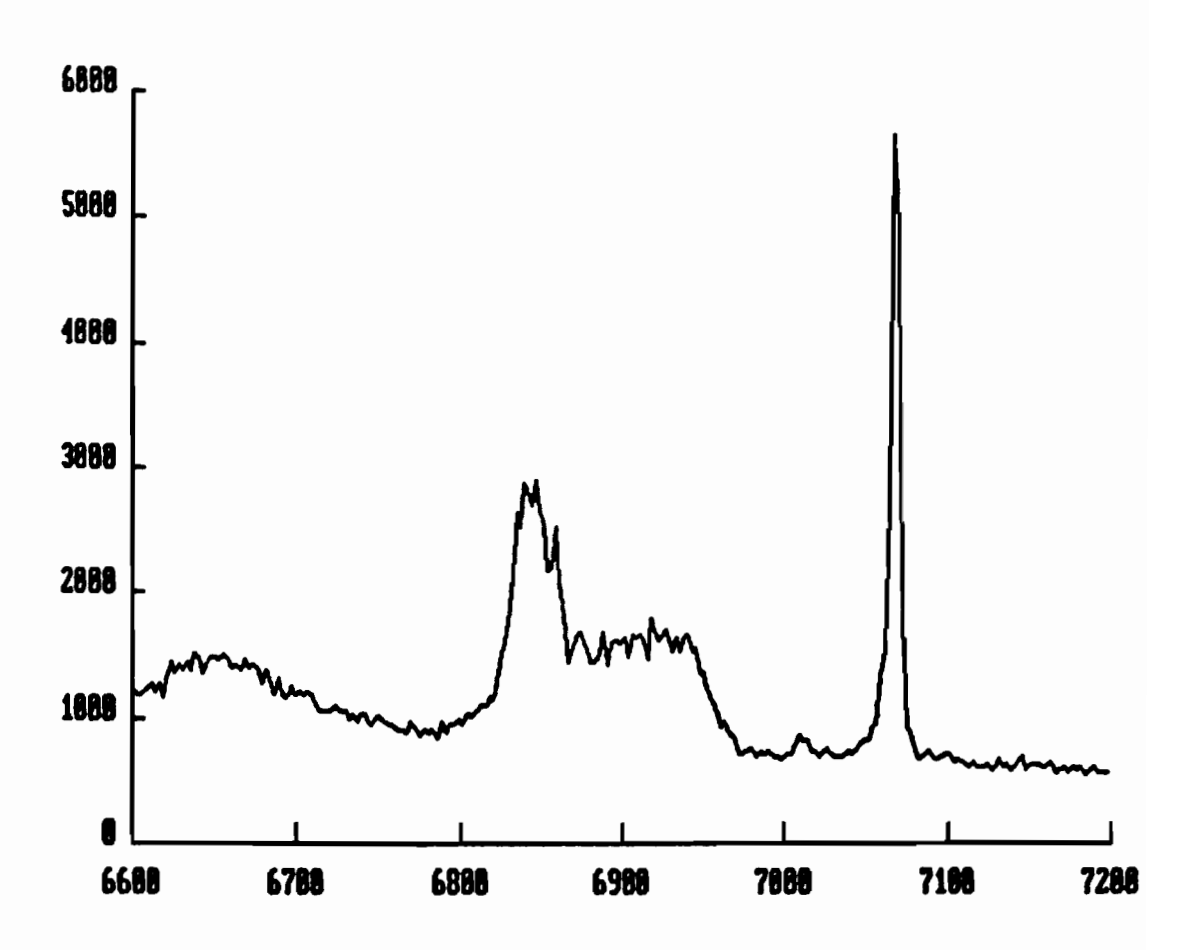
APPENDIX VI

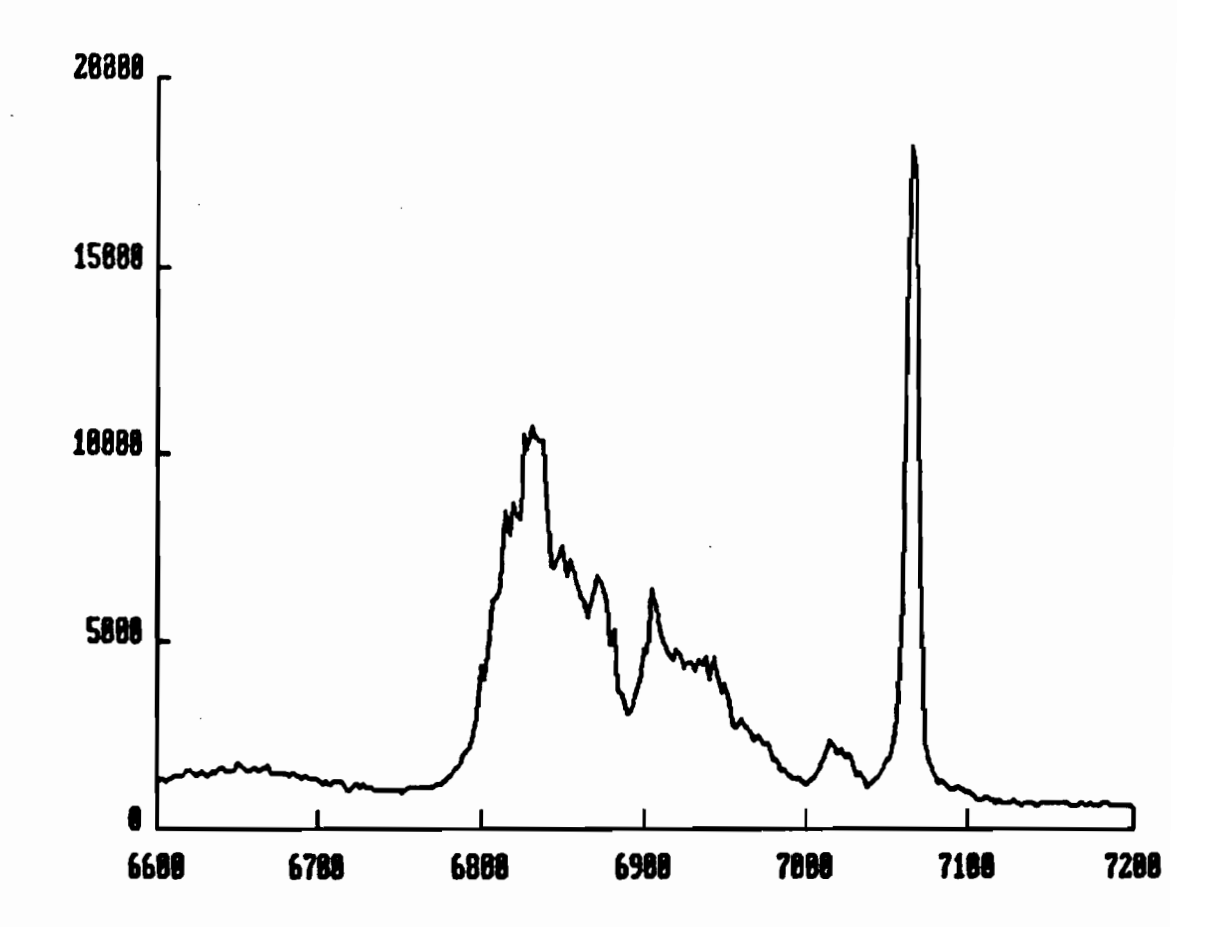
Fig. 1:
$$\lambda_{exc} = 575.4 \text{ nm}$$

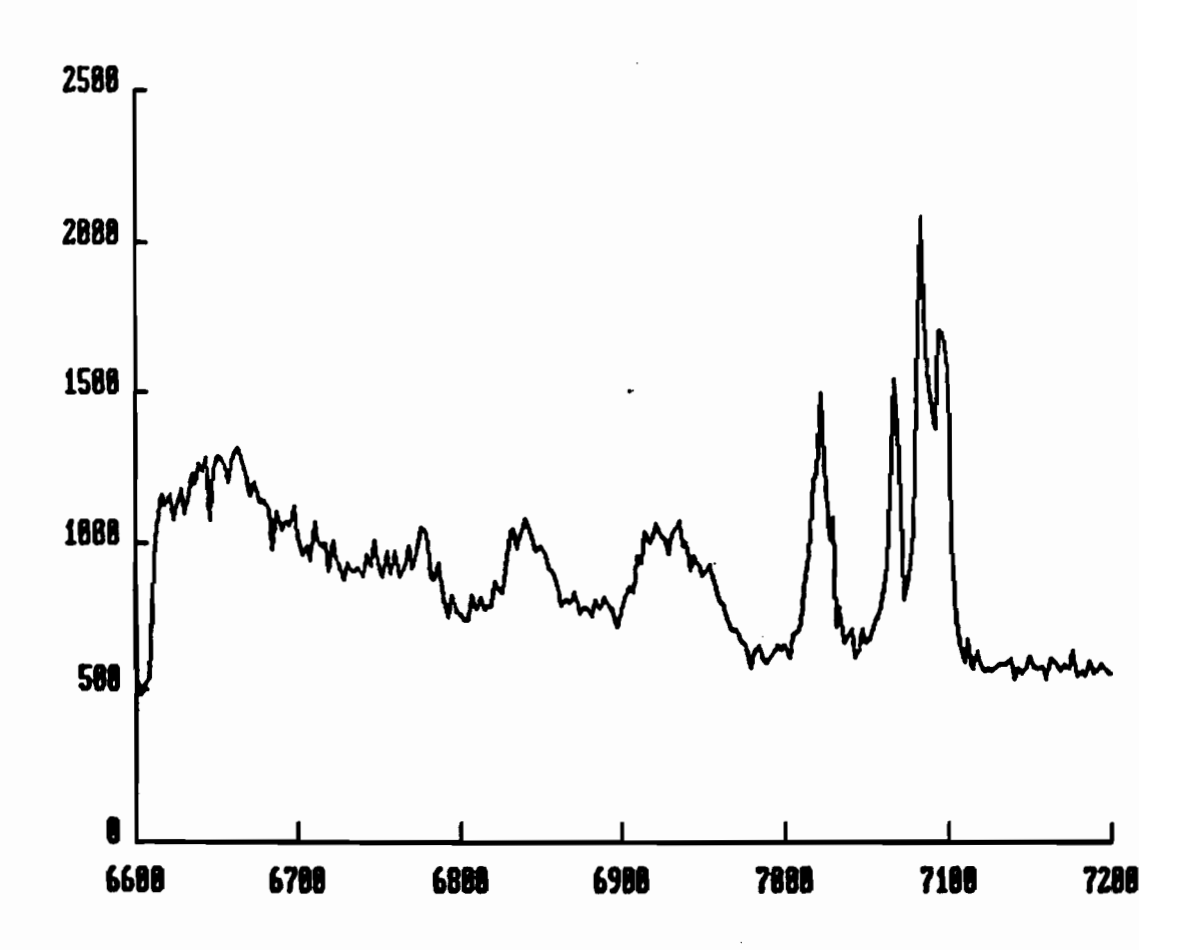
Fig. 2:
$$\lambda_{exc}$$
 = 577.8 nm

Fig. 3:
$$\lambda_{\text{exc}}$$
 = 579.2 nm

Wavelength axis scale in Angströms, Intensity in counts







APPENDIX VII

Comparison between the excitation spectra of the 640 nm luminescence(top spectrum) and the 610 nm luminescence (bottom).

